

AD-A084 663

OHIO STATE UNIV COLUMBUS ELECTROSCIENCE LAB
BROADBAND METALLIC RADOME.(U)

F/6 9/5

SEP 79 J S ERNST

F33615-76-C-1024

UNCLASSIFIED

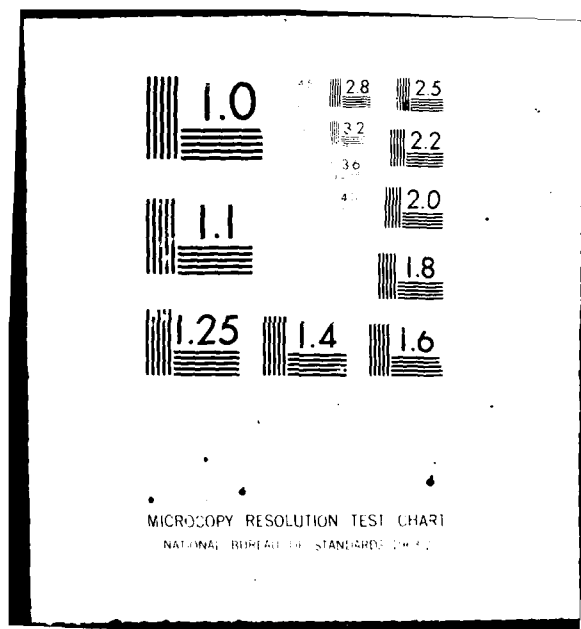
ESL-784346-11

AFAL-TR-79-1142

NL

1 of 2
AD-A084663





ADA 084663

AFAL-TR-79-1142

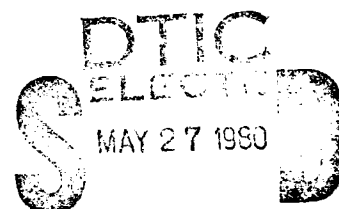


BROADBAND METALLIC RADOME

THE OHIO STATE UNIVERSITY
ELECTROSCIENCE LABORATORY
DEPARTMENT OF ELECTRICAL ENGINEERING
COLUMBUS, OHIO 43212

SEPTEMBER 1979

TECHNICAL REPORT AFAL-TR-79-1142
Interim Report for January 1976 to September 1979



Approved for public release; distribution unlimited.

AIR FORCE AVIONICS LABORATORY
AIR FORCE WRIGHT AERONAUTICAL LABORATORIES
AIR FORCE SYSTEMS COMMAND
WRIGHT-PATTERSON AIR FORCE BASE, OHIO 45433

THIS DOCUMENT IS BEST QUALITY PRACTICABLE.
THE COPY FURNISHED TO DDC CONTAINED A
SIGNIFICANT NUMBER OF PAGES WHICH DO NOT
REPRODUCE LEGIBLY.

DDC FILE COPY

80 5 27 • 058

NOTICE

When Government drawings, specifications, or other data are used for any purpose other than in connection with a definitely related Government procurement operation, the United States government thereby incurs no responsibility nor any obligation whatsoever; and the fact that the government may have formulated, furnished, or in any way supplied the said drawings, specifications, or other data, is not to be regarded by implication or otherwise as in any manner licensing the holder or any other person or corporation, or conveying any rights or permission to manufacture, use, or sell any patented invention that may in any way be related thereto.

This report has been reviewed by the Information Office (OI), and is releasable to the National Technical Information Service (NTIS). At NTIS, it will be available to the general public, including foreign nations.

This technical report has been reviewed and is approved for publication.

Carl A. Mentzer
Carl A. Mentzer
Project Engineer

William F. Bahret
William F. Bahret, Chief
Passive ECM Br, EW Division
Avionics Laboratory

FOR THE COMMANDER

Joseph H. Jacobs
Joseph H. Jacobs, Colonel, USAF
Chief, Electronic Warfare Division
Avionics Laboratory

*"If your address has changed, if you wish to be removed from our mailing list,
or if the addressee is no longer employed by your organization please notify
AFWAL/AAWP, W-PAFB, OH 45433 to help us maintain a current mailing list".*

*Copies of this report should not be returned unless return is required by se-
curity considerations, contractual obligations, or notice on a specific document.*

DISCLAIMER NOTICE

**THIS DOCUMENT IS BEST QUALITY
PRACTICABLE. THE COPY FURNISHED
TO DTIC CONTAINED A SIGNIFICANT
NUMBER OF PAGES WHICH DO NOT
REPRODUCE LEGIBLY.**

DD FORM 1473 EDITION OF 1 NOV 65 IS OBSOLETE

SECURITY CLASSIFICATION OF THIS PAGE (When Data Entered)

20.

The method of design involves an iterative procedure carried out through computer calculations. This procedure produces good results.

The final design makes use of a cosinusoidal voltage distribution along the slot when in the non-transmitting (scattering) mode. This should increase the accuracy between measured and calculated transmission curves at the upper portion of the frequency band. A sinusoidal voltage distribution was previously used.

The final design for the metallic radome results in a 1 dB bandwidth for angles of incidence from 0° to 60° of approximately 43 percent. For angles of incidence up to 75° , the bandwidth is somewhat reduced. This is the largest and most constant bandwidth to date.

This work is important to the Air Force in that it will allow metallic radomes with large constant bandwidths to be designed.

ACKNOWLEDGMENTS

The author wishes to express his gratitude to the individuals at the ElectroScience Laboratory who assisted in work involved in this thesis. A special thanks goes to Dr. Benedikt Munk for his counsel in all phases of the investigation and to Prof. Leon Peters for his review of this thesis.

The work reported in this thesis was supported in part by Contract F33615-76-C-1024 between Air Force Avionics Laboratory, Wright-Patterson Air Force Base, Ohio and The Ohio State University Research Foundation.

Approved for P.R.	
b	c
d	e
f	g
h	i
j	k
l	m
n	o
p	q
r	s
t	u
v	w
x	y
z	

A 23
HP

TABLE OF CONTENTS

Section	Page
I INTRODUCTION	1
II DEVELOPMENT OF THE THEORY	5
A. Determination of the induced currents $I_{S,in}$ and $I_{a,in}$	6
B. Determination of $V_{S,2}(\ell)$ and $V_{a,2}(\ell)$	9
C. The Transmitted Field	18
III DEVELOPMENT OF DATA AND RESULTS	19
IV CONCLUSIONS	41
 Appendix	
A LIST OF ADMITTANCES FOR GIVEN STRUCTURE	42
B T-FACTOR FOR THE STRUCTURE OF FIGURE 1	44
C THE PLANE OF INCIDENCE AND THE PLANES OF SCATTERING	46
D REFLECTION COEFFICIENTS FOR THE H-FIELD	47
E MUTUAL ADMITTANCE (y_{as} AND y_{sa}) BETWEEN SYMMETRIC AND ASYMMETRIC MODES	49
F PATTERN FACTORS IN THE YZ-PLANE FOR INTERLACE STRUCTURE	52
G COMPUTER LISTING FOR BIPLANAR SLOT ARRAY OF THREE-LEGGED ELEMENTS IN A STRATIFIED DIELECTRIC MEDIUM	56
REFERENCES	109

LIST OF FIGURES

Figure		Page
1	Biplanar slot arrays of three-legged elements imbedded in three dielectric slabs.	3
2	Three-legged slot array geometry. L. A. denotes Leg Angle.	4
3	Generalized three legged element showing critical parameters.	5
4	The voltage modes on a generalized three legged element.	6
5	Coordinate system for incident fields	7
6	Structure used to define certain variables needed to determine the admittances in slab m bounded by the planes $y=b_m$ and $y=b_{m+1}$.	8
7	Showing excited modes in YZ SCAN PLANE.	14
8	Transmission curves for orthogonal incident and orthogonal transmitted H-field with $\alpha=0^\circ$ using the voltage distributions of Equations (11) and (12). (Data set TS9)	22
9	Transmission curves for parallel incident and parallel transmitted H-field with $\alpha=0^\circ$ using the voltage distributions of Equations (11) and (12). (Data set TS9).	23
10	Transmission curves for orthogonal incident and orthogonal transmitted H-field with $\alpha= 90^\circ$ using the voltage distributions of Equations (11) and (12). (Data set TS9)	24
11	Transmission curves for parallel incident and parallel transmitted H-field with $\alpha= 90^\circ$ using the voltage distributions of Equations (11) and (12). (Data set TS9)	25
12	Comparison of calculated and measured transmission curves for orthogonal polarization for a mono-planar slot array using sinusoidal voltage distribution of Equation (29) or the sinusoidal voltage distribution of Equation (12).	26

13	Comparison of calculated and measured transmission curves for parallel polarization for a mono-planar slot array using the voltage distributions of Figure 12.	27
14	Transmission curves for orthogonal incident and orthogonal transmitted H-field with $\alpha=0^\circ$ using the voltage distributions of Equations (11) and (29). (Data set TD9A)	29
15	Transmission curves for parallel incident and parallel transmitted H-field with $\alpha=0^\circ$ using the voltage distributions of Equations (11) and (29). (Data set TS9A)	30
16	Transmission curves for orthogonal incident and orthogonal transmitted H-field with $\alpha=90^\circ$ using the voltage distributions of Equations (11) and (29) (Data set TS9A)	31
17	Transmission curves for parallel incident and parallel transmitted H-field with $\alpha=90^\circ$ using the voltage distributions of Equations (11) and (29). (Data set TS9A)	32
18	Transmission curves for orthogonal incident and orthogonal transmitted H-field for the various cases used in discussing the slight gain that occurs when using the voltage distributions of Equations (11) and (29). (Data set TS9A except where noted.)	34
19	Transmission curves for orthogonal incident and orthogonal transmitted H-field for the various cases used in discussing the slight gain that occurs when using the voltage distributions of Equations (11) and (29). (Data set TS9A except where noted.)	35
20	Transmission curves for orthogonal incident and orthogonal transmitted H-field for the various cases used in discussing the slight gain that occurs when using the voltage distributions of Equations (11) and (29). (Data set TS9A except where noted.)	36
21	Transmission curves for parallel incident and parallel transmitted H-field for the various cases used in discussing the slight gain that occurs when using the voltage distributions of Equations (11) and (29). (Data set TS9A except where noted.).	37

22	Transmission curves for parallel incident and parallel transmitted H-field for the various cases used in discussing the slight gain that occurs when using the voltage distributions of Equations (11) and (29). (Data set TS9A except where noted.)	38
23	Transmission curves for parallel incident and parallel transmitted H-field for the various cases used in discussing the slight gain that occurs when using the voltage distributions of Equations (11) and (29). (Data set TS9A except where noted.)	39
D1	Incident wave on a dielectric boundary.	47
G1	Program structure.	58
G2	Defining the physical structure.	59

SECTION I INTRODUCTION

In many applications it is necessary to place a protective cover over an antenna. Such a cover is commonly referred to as a radome and the conventional approach has been to use solid or laminated dielectric materials for these covers. Recently, substantial effort has been directed to a study of metallic radomes.

Metallic radomes possess many inherent advantages over conventional dielectric radomes. Some of these are

- 1) Elimination of the precipitation static (p-static) noise, which may cause certain radars and electronic equipment to malfunction,
- 2) Inherent lightning protection,
- 3) Reflection from a thermonuclear flash,
- 4) Better shielding against low frequency EM-pulses since a metallic radome in general can be regarded as a bandpass filter with high attenuation for low frequencies,
- 5) Potentially better laser hardening, and
- 6) Potentially higher mechanical strength.

Periodic surfaces are employed in the design of metallic radomes. Previous designs of periodic surfaces have been used for band rejection of an incident signal by utilizing dipole arrays and they have been used as narrow bandpass filters by utilizing slot arrays. The objective of this study is, through the use of planar periodic slot arrays, to design a passband filter with the largest bandwidth to date. The bandwidth is considered to be that range of frequencies in which the field transmitted through the structure has a loss of less than 1 dB. In some applications a typical constraint is given as 3 dB but this would mean 50% of the energy is lost. This lost energy is not necessarily absorbed but can be reflected in directions different from that on the main beam. This could have the undesirable effect of increasing the side lobe level of the antenna.

The type of metallic radome to achieve the objective is found to be an extension of previous results. From the results in [1], it is determined that the type of element in the planar periodic slot array be a generalized three-legged element. This type of element allows for a closer packing of the elements and also allows the elements to be unloaded. From the results in [2], it is determined that a skewed grid (i.e., interlace design) should improve the bandwidth. From the results in [3], it is determined that two planar periodic slot arrays placed in parallel results in an increase in bandwidth with more control of the shape of the transmission curve. This results in a flat response in the pass-band region and greater attenuation outside the pass-band region.

There must be a dielectric structure to be used to separate and to support the two arrays. From the results in [4] it is determined that dielectric layers are needed. These layers are used to provide a constant bandwidth for the varying angles of incidence. From the results in [5], it is determined that three dielectric layers should be used. The dielectric layers serve the dual function of physical support as well as stabilizing the bandwidth. The outer dielectric layers produce a constant bandwidth and the middle dielectric layer provides the proper coupling between the arrays.

All of this leads to the structure of Figures 1 and 2, that being a biplanar slot array of generalized three-legged elements imbedded in three dielectric slabs. The slabs have relative permittivity, ϵ_{rm} , and thickness, d_m , where m refers to the dielectric media. The theory is described in the next chapter and the actual transmission curves and input variables are determined in Chapter III. The conclusions are presented in Chapter IV.

The approach used in this report is to use the previous solutions as a guide and to apply them with a view toward obtaining as large a bandwidth as possible. Since much of the theory is contained in detail in these prior studies by other authors, it is not repeated here. Only the final equations are presented so that the casual reader can observe what is being achieved. This also allows the achievements to be presented with a minimum of clutter. The serious reader will, of course, refer to these original and rather elaborate reports.

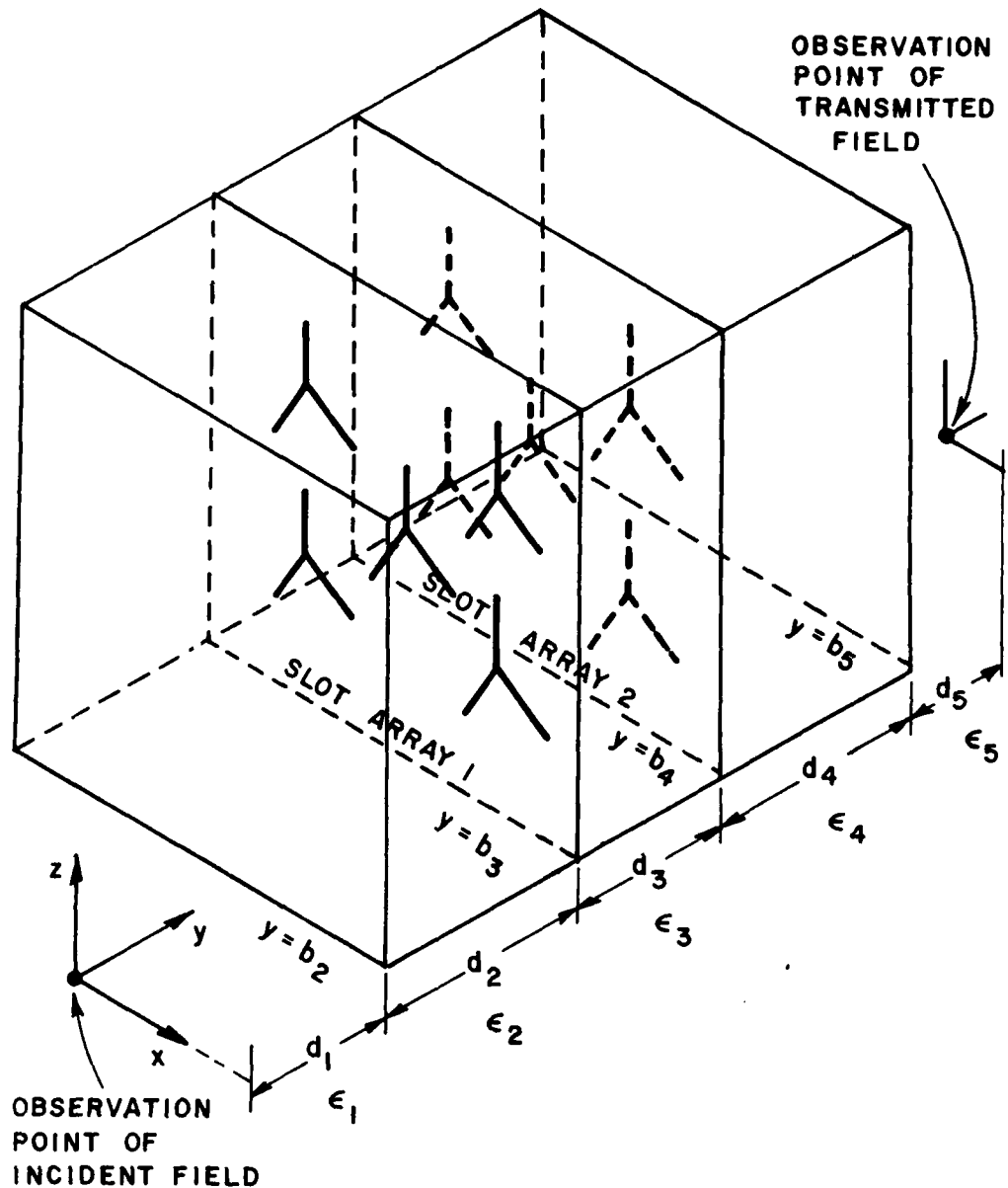


Figure 1. Biplanar slot arrays of three-legged elements imbedded in three dielectric slabs.

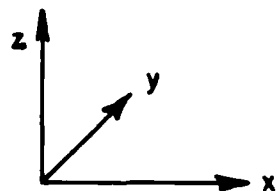
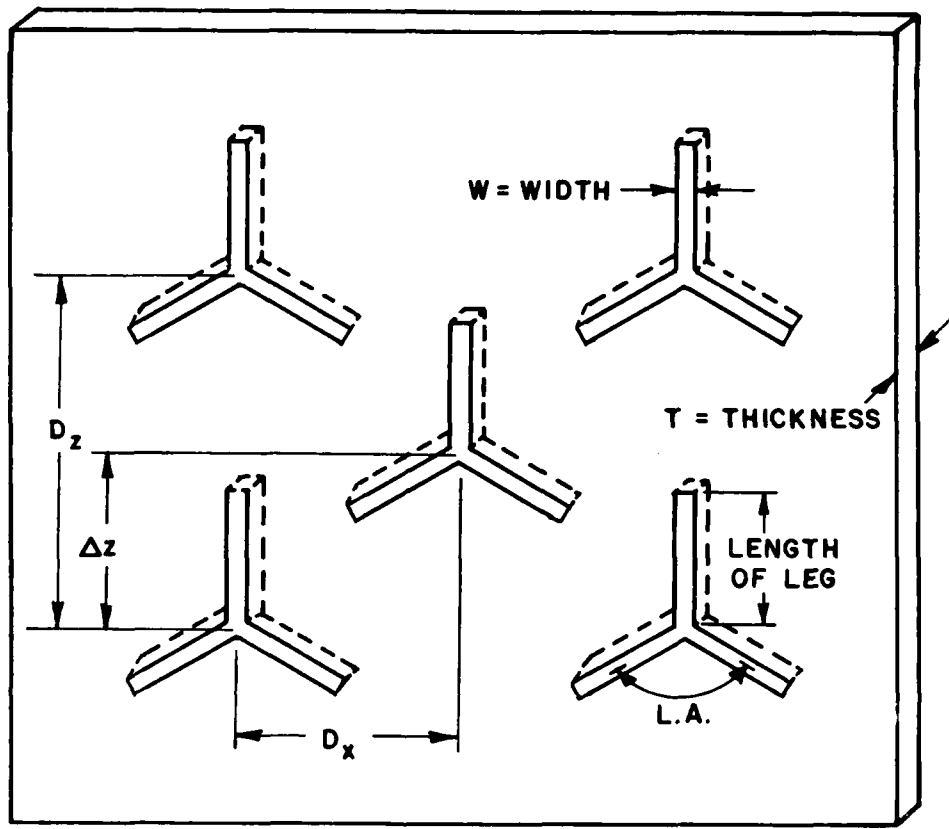


Figure 2. Three-legged slot array geometry.
L. A. denotes Leg Angle.

SECTION II
DEVELOPMENT OF THE THEORY

Generalized three legged elements consist of three monopoles connected together at a single point each of arbitrary length and direction. The lengths being $\ell_{1,i}$, $\ell_{2,i}$, $\ell_{3,i}$ and the directions being unit vectors $\hat{p}_{1,i}$, $\hat{p}_{2,i}$, $\hat{p}_{3,i}$ where the superscripts refer to the leg number and array index, respectively*. The parameters of the generalized three legged element are illustrated in Figure 3. The lengths and unit vectors will remain fixed in each array but may differ between arrays for the remainder of this report. It has been shown in earlier work[6] that the voltage distribution along the reference slot in array i is the sum of two modes:

- 1) the symmetric mode, $v_{s,i}(\ell)$ $i = 1,2$
- 2) the asymmetric mode $v_{a,i}(\ell)$

as shown in Figure 4.

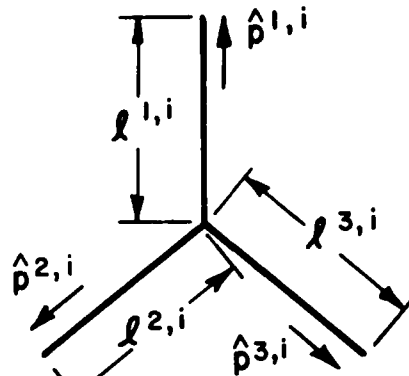


Figure 3. Generalized three legged element showing critical parameters.

* Note: The superscript is sometimes enclosed with a parenthesis so that it is not confused with the power of a variable (i.e., $\hat{p}^{(2)}$ is not \hat{p} squared).

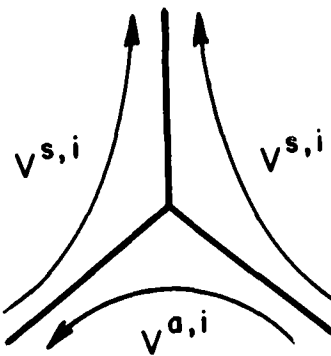


Figure 4. The voltage modes on a generalized three legged element.

To determine the transmission through this structure, the procedure is similar to that of an earlier report[7]. This consists of the following three parts:

- A. determination of the symmetric current, $I^{s,in}$, and the asymmetric current, $I^{a,in}$ induced by the incident H-field,
- B. determination of the symmetric and asymmetric voltage modes, $V^{s,2}(\ell)$ and $V^{a,2}(\ell)$ respectively, where the superscript 2 refers to the second array,
- C. determination of the transmitted H-field reradiated by the two voltage modes above of the second array.

A. Determination of the induced currents $I^{s,in}$ and $I^{a,in}$

Let the configuration shown in Figure 1 be exposed to the incident plane wave whose magnetic field is given by

$$\bar{H}_1^{\text{inc}}(\bar{R}) = \bar{H}_1^{\text{inc}} e^{-j\beta_1 \bar{R} \cdot \hat{s}_1}$$

where

\hat{s}_1 is the direction of the incident plane wave signal in medium 1 (as shown in Figure 5),

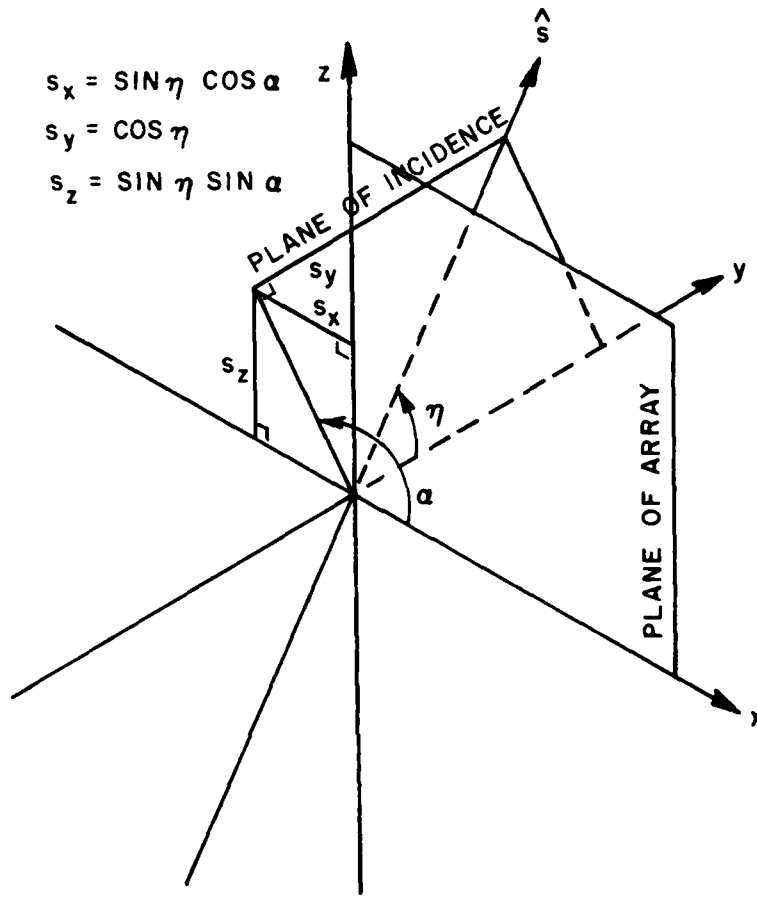


Figure 5. Coordinate system for incident fields.

β_1 is the propagation constant of medium 1,

\bar{R} is the position vector for the point of observation for the incident field (as shown in Figure 6).

A slot can be considered as a magnetic element mounted directly in front of an electrically perfectly-conducting ground plane[8]. Because of this electric screen effect, the incident plane wave will only induce $I_{s,in}$ and $I_{a,in}$ in array 1. Also the induced currents, $I_{s,in}$ and $I_{a,in}$, are independent of whatever exists behind array 1.* Thus

* The effect of the structure behind array 1 is contained in the mutual coupling terms between the two arrays.

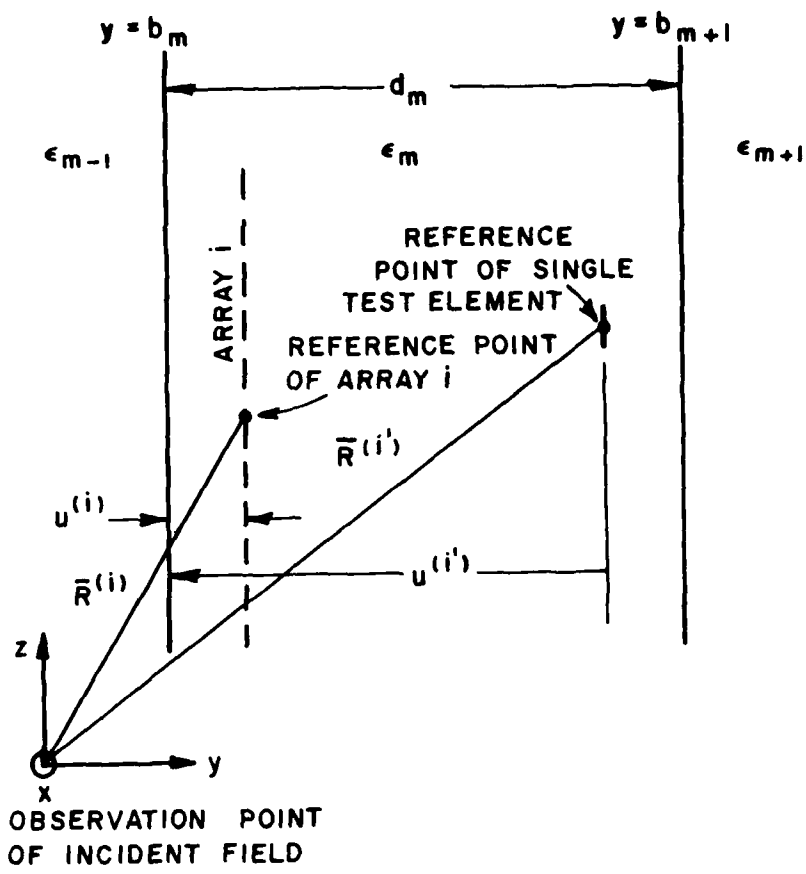


Figure 6. Structure used to define certain variables needed to determine the admittances in slab m bounded by the planes $y=b_m$ and $y=b_{m+1}$.

the induced currents are of the same form as Equations (11) and (12) in [9]. The symmetric and asymmetric current are:

$$I^{s,in} = [\bar{H}_1^{inc}(\bar{R}) \cdot \downarrow \hat{n}_1 \downarrow p^{sxt} \downarrow T_{2/1}(0,0) + \bar{H}_1^{inc}(\bar{R}) \cdot \parallel \hat{n}_1 \parallel p^{sxt} \parallel T_{2/1}(0,0)] e^{-j\beta_2(\bar{R}^{(1)} - \bar{R}) \cdot \hat{s}_2} \quad (1)$$

$$I^{a,in} = [\bar{H}_1^{inc}(\bar{R}) \cdot \downarrow \hat{n}_1 \downarrow p^{alt} \downarrow T_{2/1}(0,0) + \bar{H}_1^{inc}(\bar{R}) \cdot \parallel \hat{n}_1 \parallel p^{alt} \parallel T_{2/1}(0,0)] e^{-j\beta_2(\bar{R}^{(1)} - \bar{R}) \cdot \hat{s}_2} \quad (2)$$

where

\hat{n}_1 is a unit vector orthogonal to the plane of incidence in medium 1 (see Appendix C),

" \hat{n}_1 is a unit vector parallel to the plane of incidence and orthogonal to the direction of propagation in medium 1 (see Appendix C),

$\bar{R}^{(1)}$ is the position vector for the reference point of the reference element in array 1 (see Figure 6),

$\{\frac{1}{\parallel}\}^{psit}$ is the composite symmetric transmitting pattern factor for array 1 in medium 1, orthogonal and parallel components.

$\{\frac{1}{\parallel}\}^{alt}$ is the composite asymmetric transmitting pattern factor for array 1 in medium 1, orthogonal and parallel components,

$\{\frac{1}{\parallel}\}^T_{2/1}(0,0)$ is the transformation function for dielectric media 2 normalized to media 1. (normalized T-factor).

The pattern factors are the far field patterns due to a voltage distribution on an element of the array. They represent the relative magnitude of the plane waves propagating in certain directions. See section B2, The Pattern Factors, for defining equations.

The transformation function represents the transformation of the field as a result of the dielectric interfaces. The plane waves will be partly reflected and partly transmitted at each interface. The transformation function sums up this effect of multiple reflections of the waves and transforms the field from one dielectric media to another. see section B3, The Transformation Functions, for defining equations.

B. Determination of $V^{s,2}(\ell)$ and $V^{a,2}(\ell)$

Certain quantities needed for the evaluation of $V^{s,2}(\ell)$ and $V^{a,2}(\ell)$ are evaluated in the following sections.

B1. Determination of Admittances

As developed in [10], the impedances for dipole arrays was defined as

$$z^{i',i} = - \frac{\text{Voltage induced in the single test element } i'}{\text{Terminal current of the reference element of the array } i^*}$$

*This does not imply that the currents in the remaining slots are zero. In fact they are related to the reference element by Floquet's theorem.

Through use of duality (i.e., the induced voltage becomes the induced current and the terminal current becomes the terminal voltage), the admittance for slot arrays is defined as

$$\gamma^{i',i} = - \frac{\text{Current induced in the single test element } i'}{\text{Terminal voltage of the reference element of the array } i}$$

Now each voltage mode, $v^{si}(z)$ and $v^{ai}(z)$ of each array induces a symmetric current in the reference element of each array. Hence there is a total of sixteen admittances.

Using the dual of Equation (44) in [11] with some change of notation and generalizing to the medium m results in

$$\begin{aligned} \gamma^{Ai',Bi} &= \frac{\gamma_m}{2D_x D_z} \sum_{k=-\infty}^{\infty} \sum_{n=-\infty}^{\infty} \frac{e^{-j\beta_m(\bar{R}(i') - \bar{R}(i)) \cdot \hat{r}_m}}{r_{my}} \\ &[{}_1 P_m^{Ai'x} {}_1 P_m^{Bi} {}_1 T_m(u(i), d_m - u(i')) + {}_n P_m^{Ai'x} {}_n P_m^{Bi} {}_n T_m(u(i), d_m - u(i'))] \end{aligned} \quad (3)$$

where

A, B are dummy superscripts that refer to the symmetric or asymmetric composite pattern factors,

$\{{}_1\} P_m^{Ai'x}, \{{}_n\} P_m^{Bi}$ are defined in the section on Pattern Factors,

γ_m is the characteristic admittance of dielectric media m ,

D_x, D_z are the interelement spacings between adjacent slots measured in the \hat{x} and \hat{z} direction respectively,

β_m is the propagation constant of media m ,

$u(i), u(i')$ are defined in Figure 6,

$\bar{R}(i')$ is the position vector of the single test element reference point,

$\bar{R}(i)$ is the position vector of the reference point of the reference element of array i ,

$\{{}_1\} T_m(u(i), d_m - u(i'))$ is defined in section B3, Transmission Function.

The unit vector, \hat{r}_m , indicates the directions in which the bundle of plane, inhomogeneous waves are being scattered by the array. Using Equations (D2) and (D3) in [12] together with results developed in [13], \hat{r}_m for a skewed array is found to be

$$\hat{r}_m = \hat{x} \left(s_{mx} + \frac{k\lambda_m}{D_x} - \frac{n\Delta z \lambda_m}{D_x D_z} \right) + \hat{y} r_{my} + \hat{z} \left(s_{mz} + \frac{n\lambda_m}{D_z} \right) \quad (4)$$

where

$$r_{my} = \pm \left(1 - \left(s_{mx} + \frac{k\lambda_m}{D_x} - \frac{n\Delta z \lambda_m}{D_x D_z} \right)^2 - \left(s_{mz} + \frac{n\lambda_m}{D_z} \right)^2 \right)^{1/2} \quad (5)$$

and

Δz is the interlace spacing in the z direction, and is defined as the distance between two slots that are adjacent in the x direction (see Figure 2),

λ_m is the wavelength in media m .

It can be shown that results obtained interlacing in the x direction are equal to those obtained from the analysis for interlacing in the z direction. Also the solution for geometries interlaced in both directions at once can be evaluated by redefining D_x and D_z to new values.

Now r_{my} may either be real or imaginary. When it is real, r_{my} represents a wave propagating away from the array, hence the plus sign must be used. When it is imaginary, r_{my} represents a wave which attenuates as it moves away from the array, hence the negative sign must be used. For $k=n=0$, the equation for \hat{r}_m reduces to \hat{s}_m (and the specular direction).

The self admittance is closely approximated by the mutual coupling between the single test element located $w/4$ (w is the width of the slot) away from the reference element of the array [14]. Assuming that the x components and the z components of $\bar{R}(i')$ and $\bar{R}(i)$ are equal.

$$(\bar{R}(i') - \bar{R}(i)) \cdot \hat{r}_m = \frac{w}{4} r_{my} \quad (6)$$

For mutual admittances, the single test element is assumed to be an element of the other array. Using the given structure with the same assumptions as before, results in

$$(\bar{R}^{(i')}-\bar{R}^{(i)}) \cdot \hat{r}_m = d_3 r_{3y} . \quad (\text{Note: } R_{x,z}^{(i)}=R_{x,z}^{(i')}) \quad (7)$$

Using Equations (6) and (7) will assist in determination of the self and mutual admittances. Appendix A contains a complete list of all the admittances for the structure in Figure 1.

B2. The Pattern Factors

The transmitting and non-transmitting pattern factor for each leg is found through the application of duality to Equations (D14) and (40) in [15] to give

$$P^{vit}(g) = \frac{1}{V^{vit}(0)} \int_0^{\ell(g)} V^{vit}(\ell) e^{-j\beta\ell(g)i_p g, i \cdot \hat{r}} d\ell \quad (8)$$

and

$$P^{vi}(g) = \frac{1}{V^{vi}(0)} \int_0^{\ell(g)} V^{vi}(\ell) e^{j\beta\ell(g)i_p g, i \cdot \hat{r}} d\ell \quad (9)$$

respectively, where g is the leg number and i again refers to the array index.

There is a symmetric pattern and an asymmetric pattern corresponding to the symmetric and asymmetric voltage modes respectively. Hence the dummy superscript 'v' for variable becomes an 's' for the symmetric voltage mode and becomes an ' a^T ' for the asymmetric voltage mode.

Note that it is not necessary to specify the media for β and \hat{r} since it was assumed that the arrays are planar (i.e., $\hat{p}(g)$ contains no y component). Using Equations (B1) and (B2) in [16] it can be shown that

$$\beta_m \hat{p}^{(g)} i \cdot \hat{r}_m = \beta_q \hat{p}^{(g)} i \cdot \hat{r}_q \quad (\text{for planar elements only}) \quad (10)$$

where m and q refer to the dielectric media. Hence the media subscripts, m and q , can be eliminated.

The form of $V^{vit}(\ell)$ and $V^{vi}(\ell)$ is usually assumed to be [17]

$$V^{vit}(\ell) = V^{vit}(0) \sin \theta_{ef}^{(g)} i - \ell^{(g)} i \quad (11)$$

and

$$V^{Vi}(\ell) = V^{Vi}(0) \sin \beta_d (\ell^{g,i} - \ell^{g,i})^* \quad (12)$$

where

β_d is the effective dielectric propagation constant
(Equation (C-2) in [18]),

ℓ_{ef} is the effective length of the leg due to the
inductance at the ends of each leg.

This inductance effectively increases the length of the legs.
 $V^{vit}(0)$ and $V^{Vi}(0)$ are the magnitudes of the voltages for each mode
at the terminals (i.e., point where legs join). It must be noted that
only the form of the voltages $V^{vit}(\ell)$ and $V^{Vi}(\ell)$ is used to calculate
the patterns since the magnitude at the terminals divides out. The
magnitude of each voltage for the second array will be determined
later. It is needed to calculate the transmitted H-field. (Part C).

There is a generalized composite pattern factor for the trans-
mitting and non-transmitting (scattering) case for each voltage mode.
By inspection of Figure 7b and the use of Equation (42) in [19] the
generalized composite pattern factors for the generalized three-leg-
ged elements are

$$\left\{ \begin{smallmatrix} \downarrow \\ \| \end{smallmatrix} \right\} P_m^{sit} = (2\hat{p}^{(1)} i_p s1t - \hat{p}^{(2)} i_p s2t - \hat{p}^{(3)} i_p s3t) \cdot \left\{ \begin{smallmatrix} \downarrow \\ \| \end{smallmatrix} \right\} \hat{n}_m \quad (13)$$

$$\left\{ \begin{smallmatrix} \downarrow \\ \| \end{smallmatrix} \right\} P_m^{ait} = (\hat{p}^{(2)} i_p a2t - \hat{p}^{(3)} i_p a3t) \cdot \left\{ \begin{smallmatrix} \downarrow \\ \| \end{smallmatrix} \right\} \hat{n}_m \quad (14)$$

$$\left\{ \begin{smallmatrix} \downarrow \\ \| \end{smallmatrix} \right\} P_m^{psi} = (2\hat{p}^{(1)} i_p s1 - \hat{p}^{(2)} i_p s2 - \hat{p}^{(3)} i_p s3) \cdot \left\{ \begin{smallmatrix} \downarrow \\ \| \end{smallmatrix} \right\} \hat{n}_m \quad (15)$$

$$\left\{ \begin{smallmatrix} \downarrow \\ \| \end{smallmatrix} \right\} P_m^{ai} = (\hat{p}^{(2)} i_p a2 - \hat{p}^{(3)} i_p a3) \cdot \left\{ \begin{smallmatrix} \downarrow \\ \| \end{smallmatrix} \right\} \hat{n}_m \quad (16)$$

*An alternate form for $V^{Vi}(\ell)$ will be presented in section III, Development
of Data and Results. The reasons for this change are discussed in
that section.

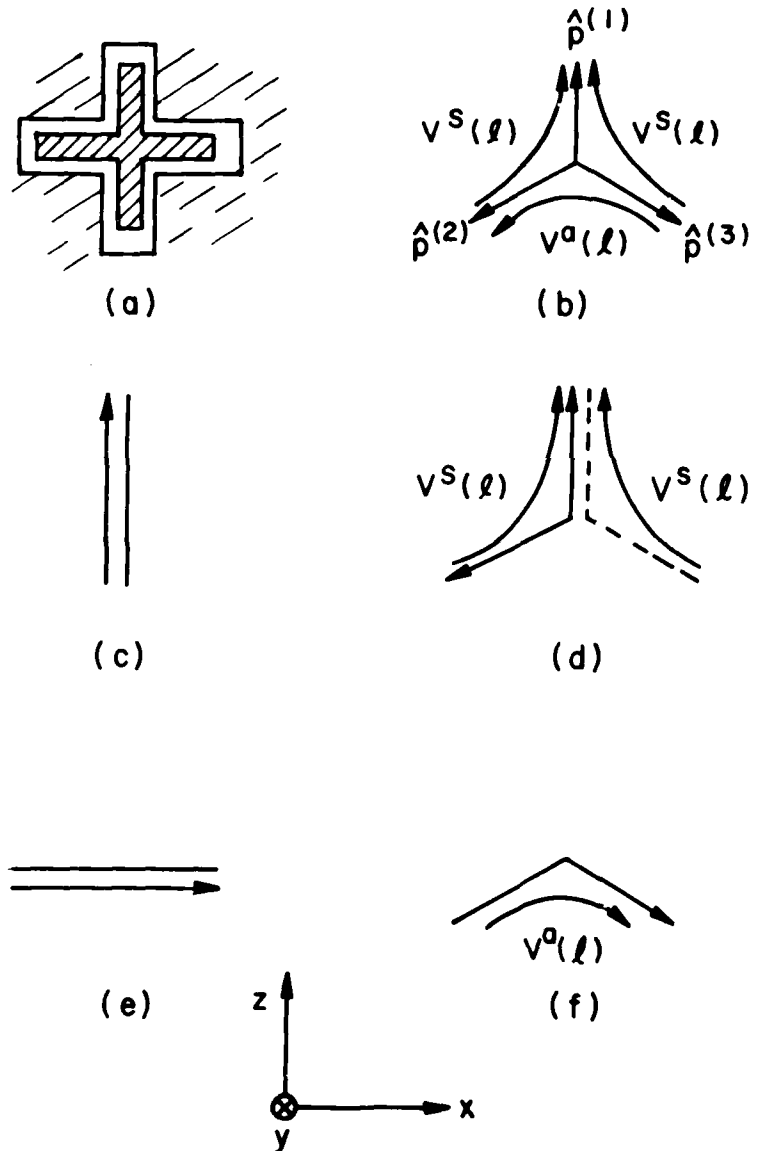


Figure 7. Showing excited modes in YZ SCAN PLANE

- (a) Loaded straight slot (L.S.S.)
- (b) Three legged direction vectors and voltages defined
- (c) L.S.S. for parallel incident polarization
- (d) Three legged parallel incident polarization
- (e) L.S.S. for orthogonal incident polarization
- (f) Three legged orthogonal incident polarization.

The factor of 2 comes from the fact that $V^S(\ell)$ is being counted twice on leg $\ell(1)$. The negative signs appear because the vector 'magnetic current' is going in the opposite direction of the unit vectors of leg directions as shown in Figure 7b. All patterns have now been specified.

B3. The Transformation Functions

The transformation functions (T factor) needed in admittance calculations are found from Equation (29) in [20] by changing from reflection coefficients for the electric field to reflection coefficients for the magnetic field and generalizing the results to layer m

$$\begin{aligned} \left\{ \frac{\downarrow}{\uparrow} \right\} T_m(u^{(i)}, d_m - u^{(i')}) = & \left[\left(1 + \left\{ \frac{\downarrow}{\uparrow} \right\} R_{m,m-1} e^{-j2\beta_m u^{(i)} r_{my}} \right) \right. \\ & \times \left. \left(1 + \left\{ \frac{\downarrow}{\uparrow} \right\} R_{m,m+1} e^{-j2\beta_m (d_m - u^{(i')}) r_{my}} \right) \right] / \\ & \left(1 - \left\{ \frac{\downarrow}{\uparrow} \right\} R_{m,m-1} \left\{ \frac{\downarrow}{\uparrow} \right\} R_{m,m+1} e^{-j\beta_m d_m r_{my}} \right) \end{aligned} \quad (17)$$

This is the generalized non-normalized T-factor for slot arrays such that the array and the single test element are separated by at most only one dielectric layer for $u^{(i)} > u^{(i')}$. For $u^{(i)} < u^{(i')}$ see remarks at the end of this section. For the given structure, $\left\{ \frac{\downarrow}{\uparrow} \right\}_{m,m-1}$ and $\left\{ \frac{\downarrow}{\uparrow} \right\}_{m,m+1}$ are the reflection coefficients between two dielectric media whose equations are listed in Appendix D. The T-factors used in admittance calculations can now be computed. See Appendix B.

It was found that expressing the induced currents and the transmitted H-field in a normalized form results in conceptually simpler equations. The T-factors used in these equations are hence normalized. Modification of Equation (33) in [21] in the same manner Equation (29) was modified in [22] gives

$$\begin{aligned} \left\{\frac{1}{n}\right\}_{m/q}^T(u^{(i)}, d_m - u^{(i')}) &= \left(\frac{1 - \left\{\frac{1}{n}\right\}_{m,q}}{1 + \left\{\frac{1}{n}\right\}_{m,q}} \right) \\ &\quad \left(1 + \left\{\frac{1}{n}\right\}_{m,m-1}^r e^{-j2\beta_m u^{(i)} r_{my}} \right) \left(1 + \left\{\frac{1}{n}\right\}_{m,m+1}^r e^{-j2\beta_m (d_m - u^{(i')}) r_{my}} \right) \\ &\quad \frac{1 - \left\{\frac{1}{n}\right\}_{m,m-1}^r \left\{\frac{1}{n}\right\}_{m,m+1}^r e^{-j2\beta_m d_m r_{my}}}{(18)} \end{aligned} \quad (18)$$

This is the generalized normalized T-factor with $u^{(i')} > u^{(i)}$ and where $q = m \pm 1$ depending on whether calculation of induced currents or transmitted field is involved. For $u^{(i)} > u^{(i')}$ again see the remarks at the end of this section.

The following sign changes must be made for the case $u^{(i)} > u^{(i')}$ as is shown in Appendix D in [23]

change from to

subscript +	subscript -
subscript -	subscript +

Determination of $v^{s,i}$ and $v^{a,i}$ $i=1,2$

The form of $v^{s,i}(z)$ and $v^{a,i}(z)$ has been assumed previously (see Equation (12)) in order to calculate the patterns. The magnitude of $v^{s,i}(0)$ and $v^{a,i}(0)$ is now calculated. Denote the load admittances for the symmetric and asymmetric mode by y_L^{si} and y_L^{ai} , respectively. Hence, from Kirchoff's current law (i.e., the sum of all currents entering a node must equal 0), the load admittance multiplied by the unknown voltage will equal the sum of induced currents.

$$y_L^{si} v^{s,i}(0) = I^{s,in} + I^{s1s1} + I^{s1a1} + I^{s1s2} + I^{s1a2} \quad (19)$$

$$y_L^{ai} v^{a,i}(0) = I^{a,in} + I^{als1} + I^{ala1} + I^{als2} + I^{ala2} \quad (20)$$

$$y_L^{s2} v^{s,2}(0) = 0 + I^{s2a2} + I^{s2a2} + I^{s2s1} + I^{s2a1} \quad (21)$$

$$\gamma_L^{a2} \gamma^{a,2}(0) = 0 + I^{a2s2} + I^{a2a2} + I^{a2s1} + I^{a2a1} \quad (22)$$

Using the equations for admittances developed in the preceding section results in:

$$\begin{bmatrix} I_{s,in} \\ I_{a,in} \\ 0 \\ 0 \end{bmatrix} = [Y] \begin{bmatrix} \gamma_{s,1} \\ \gamma_{a,1} \\ \gamma_{s,2} \\ \gamma_{a,2} \end{bmatrix} \quad (23)$$

where $[Y]$ is defined as the admittance matrix

$$[Y] = \begin{bmatrix} \gamma_{s1s1} + \gamma_L^{s1} & \gamma_{s1a1} & \gamma_{s1s2} & \gamma_{s1a2} \\ \gamma_{als1} & \gamma_{ala1} + \gamma_L^{a1} & \gamma_{als2} & \gamma_{ala2} \\ \gamma_{s2s1} & \gamma_{s2a1} & \gamma_{s2s2} + \gamma_L^{s2} & \gamma_{s2a2} \\ \gamma_{a2s1} & \gamma_{a2a1} & \gamma_{a2s2} & \gamma_{a2a2} + \gamma_L^{a2} \end{bmatrix} \quad (24)$$

All symmetric and asymmetric voltages for each array can now be found. Since the transmitted H-field into the semi-infinite space, $y>d_4$, is desired, only the node voltages from the second array, $\gamma^{s,2}(0)$ and $\gamma^{a,2}(0)$, need be found. Using Cramer's rule with the determinant of the admittance matrix,

$$D = |Y|, \quad (25)$$

gives

$$\gamma^{s,2}(0) = \frac{1}{D} \begin{vmatrix} \gamma_{s1s1} + \gamma_L^{s1} & \gamma_{s1a1} & I_{s,in} & \gamma_{s1a2} \\ \gamma_{als1} & \gamma_{ala1} + \gamma_L^{a1} & I_{a,in} & \gamma_{ala2} \\ \gamma_{s2s1} & \gamma_{s2a1} & 0 & \gamma_{s2a2} \\ \gamma_{a2s1} & \gamma_{a2a1} & 0 & \gamma_{a2a2} + \gamma_L^{a2} \end{vmatrix} \quad (26)$$

and

$$V^{a,2}(0) = \frac{1}{D} \begin{vmatrix} \gamma_{s1s1} + \gamma_L^{s1} & \gamma_{s1a1} & \gamma_{s1s2} & I^{s,in} \\ \gamma_{a1s1} & \gamma_{a1a1} + \gamma_L^{a1} & \gamma_{a1s2} & I^{a,in} \\ \gamma_{s2s1} & \gamma_{s2a1} & \gamma_{a2s2} + \gamma_L^{s2} & 0 \\ \gamma_{a2a1} & \gamma_{a2a1} & \gamma_{a2s2} & 0 \end{vmatrix} \quad (27)$$

This completely determines the magnitudes $V^{s,2}(0)$ and $V^{a,2}(0)$ since all the quantities on the right side of Equations (26) and (27) have been previously determined.

Note that the physical implementation of the load impedance is not important and in fact are assumed to be zero in the computer program. They were included here in order to keep the theory as general as possible.

C. The Transmitted Field

After having determined the two voltages $V^{s,2}(0)$ and $V^{a,2}(0)$ of the second array, the transmitted field into the semi-infinite space, $y > d_4$, can now be found. No radiation takes place from the first array because of the shielding effect of the second array so by a slight change in notation of Equation (43) in [24], the total transmitted H-field re-radiated by $V^{s,2}(0)$ and $V^{a,2}(0)$ is

$$\begin{aligned} \hat{H}_5^{\text{tot}} = & \frac{Y_5}{2D_x D_z} \sum_{k=-\infty}^{\infty} \sum_{n=-\infty}^{\infty} \frac{e^{-j\beta_5(\bar{R}-yb_4) \cdot \hat{r}_5} e^{-j\beta_4(yb_4 - \bar{R}^{(2)}) \cdot \hat{r}_4}}{r_5 y} \\ & [\hat{n}_5 (\downarrow P_s V^{s,2}(0) + \downarrow P_a V^{a,2}(0)) T_{4/5}(0,0) \\ & + \hat{n}_5 (\parallel P_s V^{s,2}(0) + \parallel P_a V^{a,2}(0)) T_{4/5}(0,0)] \end{aligned} \quad (28)$$

where Y_5 is the characteristic admittance in the semi-space $y > b_5$ of Figure 1 and where all other quantities have been previously defined.

Since the total transmitted H-field is desired in the far-field, all evanescent modes have disappeared. So only the $k=n=0$ term is of importance provided no grating lobes exist. For most practical applications grating lobes are avoided as is the case for this report. They are avoided since a null usually occurs near the frequency at which the grating lobe appears.

From [25] or simply from conservation of energy, it is known that the cross polarized component of the transmitted field should be as small as possible in order to have unit transmission coefficient.

SECTION III DEVELOPMENT OF DATA AND RESULTS

The introduction explained qualitatively the analysis of the structure of Figures 1 and 2. Quantitative values are to be obtained in order to calculate the transmitted field through the structure and hence the bandwidth. To do so, the following observations are useful. Refer to Figure 7 for additional insight.

Assume the incident field is in the YZ-plane ($\alpha=90^\circ$). For an incident field orthogonal to the plane of incidence only the asymmetric mode will be excited ($I_{in}=0$). The analysis is reduced to that of an array of bent 'straight' slots shown in Figure 7f. For an incident field parallel to the plane of incidence only the symmetric mode will be excited ($I_{in}=0$). This results again in an array of bent 'straight' slots as shown in Figure 7d. Hence for at least the YZ scan plane the structure of Figure 1 is similar to that of the structure in [26]. It is therefore reasonable to use one of the data sets provided in [27] as a basis for the starting data in order to calculate transmission curves. As the leg angle L.A. is decreased from 180° to 120° the above starting data are not necessarily optimum.

From [28] it was demonstrated that a symmetric configuration for a monoplanar structure led to the largest bandwidth of transmission curves for orthogonal and parallel polarizations. Using this for the biplanar structure requires that:

$$d_2 = d_4$$

$$\epsilon_2 = \epsilon_4$$

$$\epsilon_1 = \epsilon_5$$

Data set P27 given in [29] is then used as the initial data for the structure of Figure 1. For development of the data to this point refer to that reference. Kornbau found that for an equilateral triangular grid ($\Delta z = D_z/2$) a leg angle L.A. of 120° yielded the best performance with respect to low cross polarization. Hence this case is assumed in the data. All initial parameters are now known and computer calculations of the transmission curves can now be produced. It should be noted that although the theory and computer program have been developed to allow for any interlace spacing, leg angle L.A., and dielectric constants, they remain fixed throughout. See Data (TS9) for values, Table 1.

Since a direct synthesis is not feasible at this time, a systematic computer solution approach to increase the bandwidth of the transmission curves was used. This approach is to change one variable and recalculate the curves and keep repeating the process. This is possible because the effect of each variable of the data set is qualitatively known. This allows for prudent choices concerning changes to be made to improve bandwidth.

The important variables that were changed as part of the iterative procedure to improve bandwidth were the slot dimensions, the interelement spacing, the interlace spacing and the width of the middle dielectric layer. The nature of the changes follows.

The length of each leg of the slot was increased in order to lower the resonance frequency. This increased the bandwidth by moving the lower frequency end down in frequency while the change in the upper end was slight. The interelement spacing and interlace spacing were reduced in order to move the upper frequency end up in frequency. The width of the middle dielectric layer determines the mutual coupling between the arrays. Since it was found by inspection of Reference [3] that an increase in the coupling was needed, the width was decreased. Note that these changes were repeated several times.

Each variable is not completely independent of all the other variables so practical limits do exist. As an example, suppose the inter-element spacing is reduced while holding the leg length constant. Eventually, the individual slots in each array would overlap. Hence, the results would no longer be correct.

Figures 8 to 11 are the resulting transmission curves for data set TS9 using the voltage distribution given by Equations (11) and (12). Notice that the bandwidth is approaching an octave for both orthogonal and parallel polarizations* in each principle plane ($\alpha=0, 90^\circ$) for angles of incidence up to 75° from normal. The transmission curves are in fact very similar which is the desired result. The cross polarizations, transmitted polarizations orthogonal to polarizations of the incident field, have been calculated and are found to be -20 dB or less. The cross polarizations, are indeed small as desired to provide for unity transmission.

After completion of the above transmission curves some developments occurred concerning similar slot elements. Measurements on a mono-planar slot array imbedded in an asymmetric dielectric configuration, A-sandwich, showed disagreement with calculated transmission curves for frequencies above the first resonance.** (Figures 12 and 13.)*** It should be noted that below that frequency, the curves agree.

* This is in reference to the H-field and plane of incidence.

** Resonance is the frequency at which the transmission curve has no loss, i.e., unity gain.

***Figures 12 and 13 were extracted from [30]. For further study see that reference.

Table 1

```

1 DECIDE ON V DSTR FOR NT PATTERN =1(SINUSOIDAL), =2(COSINUSOIDAL)
2
3 IF SYMMETRIC CONFIGURATION SET NEXT LINE TO 1
4
5 DECIDE ON PRINTED OUTPUT
6
7 FREQL = 1.0000 LOWEST FREQ USED IN CALCULATIONS IN GHZ
8 FREQH = 18.0000 HIGHEST FREQ USED IN GHZ
9 FINCRM = 0.5000 FREQ INCREMENT IN GHZ
10 D1 = 0.0 DISTANCE FROM ORIGIN
11 D2 = 1.10 THICKNESS OF DIELECTRIC LAYERS IN CM
12 D3 = 0.50
13 D4 = 1.10
14 D5 = 0.0 DISTANCE TO OBSERVATION PT FROM MEDIA 4
15 READ NUMBER OF INCIDENT ANGLES DESIRED
16 10
17 ANGLES ALPHA,ETA OF INCIDENT FIELD IN DEGREES
18 0.0,1.0,0.0,30.0,0.0,60.0,0.0,70.0,0.0,75.0
19 90.0,1.0,90.0,30.0,90.0,60.0,90.0,70.0,90.0,75.0
20 ER1 = 1.0 RELATIVE PERMITTIVITY OF DIELECTRIC LAYERS
21 ER2 = 1.30
22 ER3 = 1.9
22 ER4 = 1.30
24 ER5 = 1.0
25 DX = 0.75
26 DZ = 0.867
27 DELTZ = 0.4335
28 RL = 0.75
29 WIDTH = 0.120
30 THIK = 0.0071
31 ANGLE BETWEEN LEG 2 & LEG 3 OF ARRAY 1 IN DEGREES
32 120
33 ANGLE BETWEEN LEG 2 & LEG 3 OF ARRAY 2 IN DEGREES
34 120
35 ----- END OF INPUT FILE -----

```

DATA SET: TS9: (change line two to a 2 to get DATA SET TS9A).

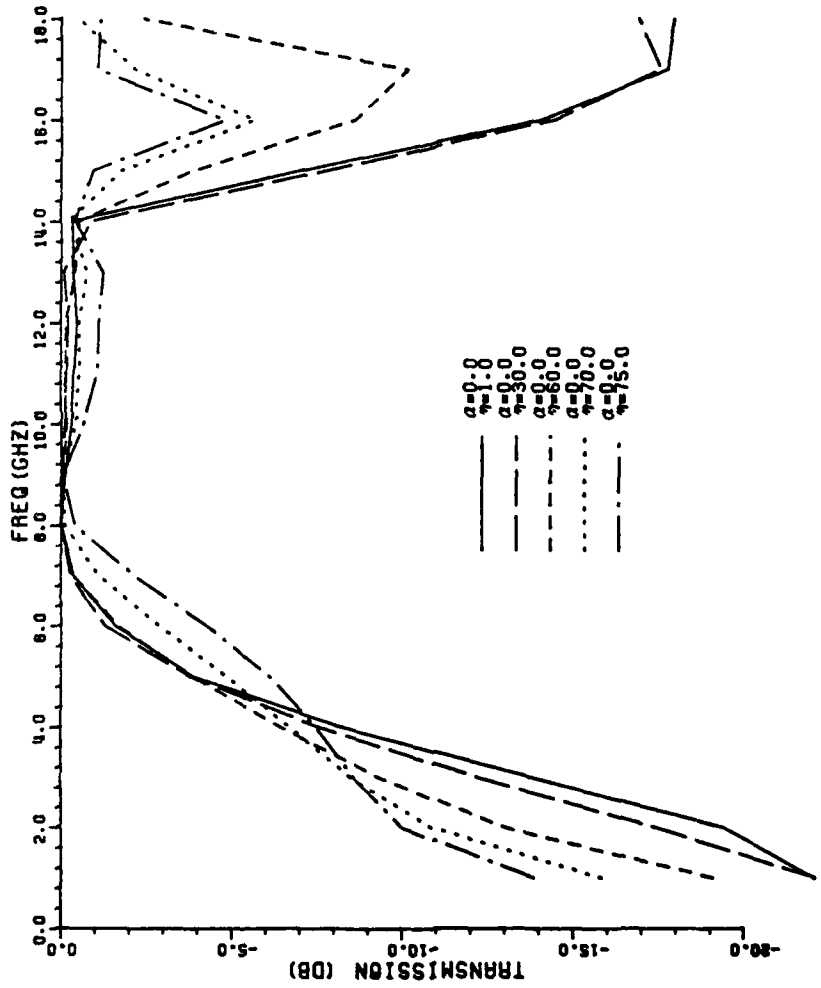


Figure 8. Transmission curves for orthogonal incident and orthogonal transmitted H-field with $\alpha=0^\circ$ using the voltage distributions of Equations (11) and (12). (Data set TS9)

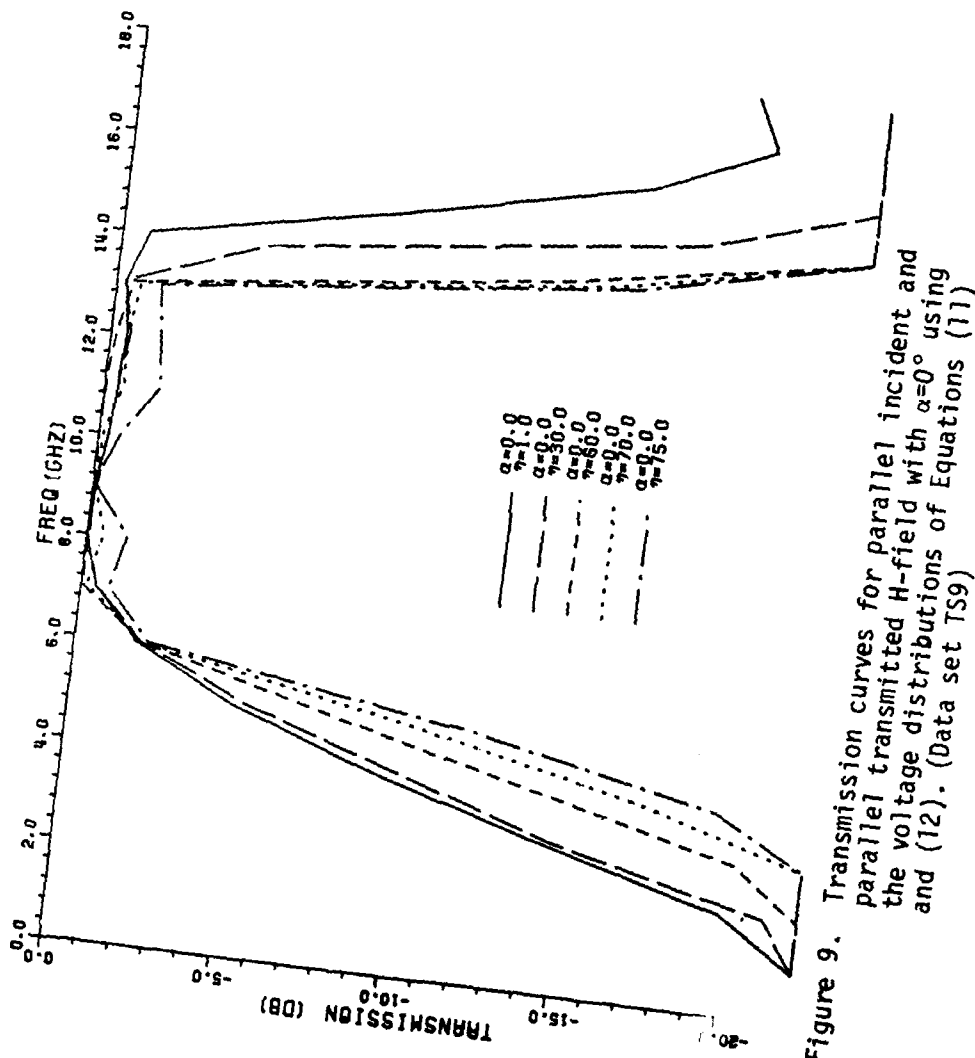


Figure 9. Transmission curves for parallel transmitted H-field with $\alpha=0^\circ$ and the voltage distributions (12) and (11). (Data set TSG9)

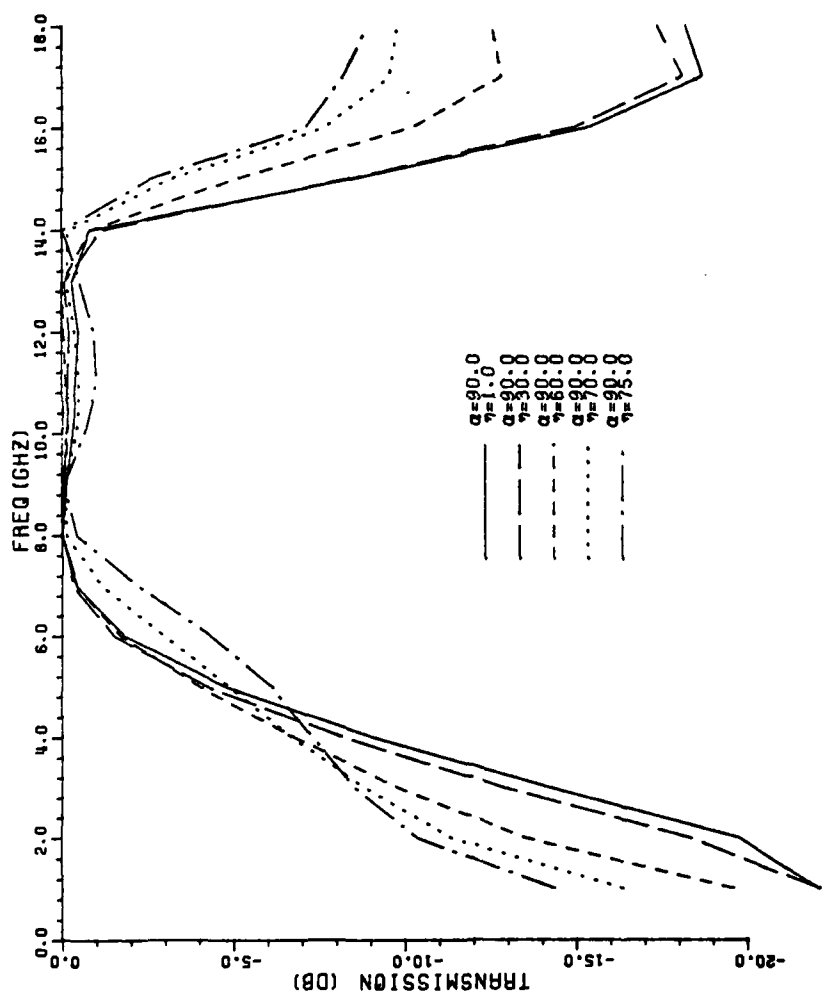


Figure 10. Transmission curves for orthogonal incident and orthogonal transmitted H-field with $\alpha=90^\circ$ using the voltage distributions of Equations (11) and (12). (Data set TS9)

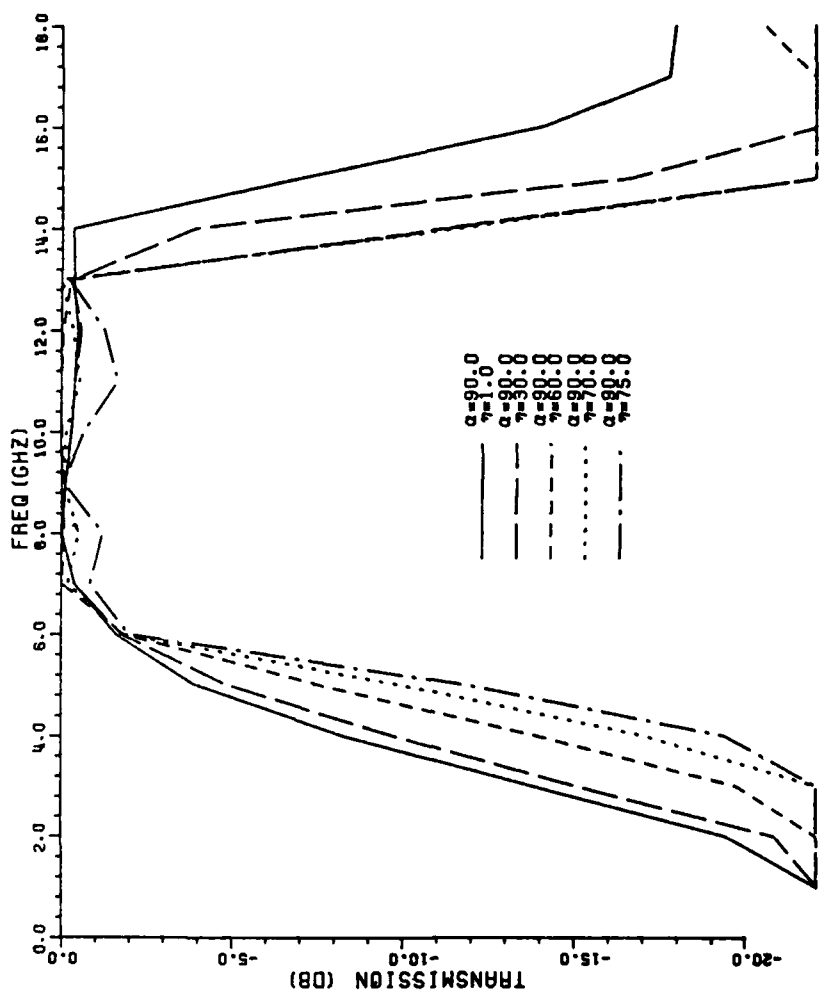


Figure 11. Transmission curves for parallel incident and parallel transmitted H-field with $\alpha=90^\circ$ using the voltage distributions of Equations (11) and (12). (Data set TS9)

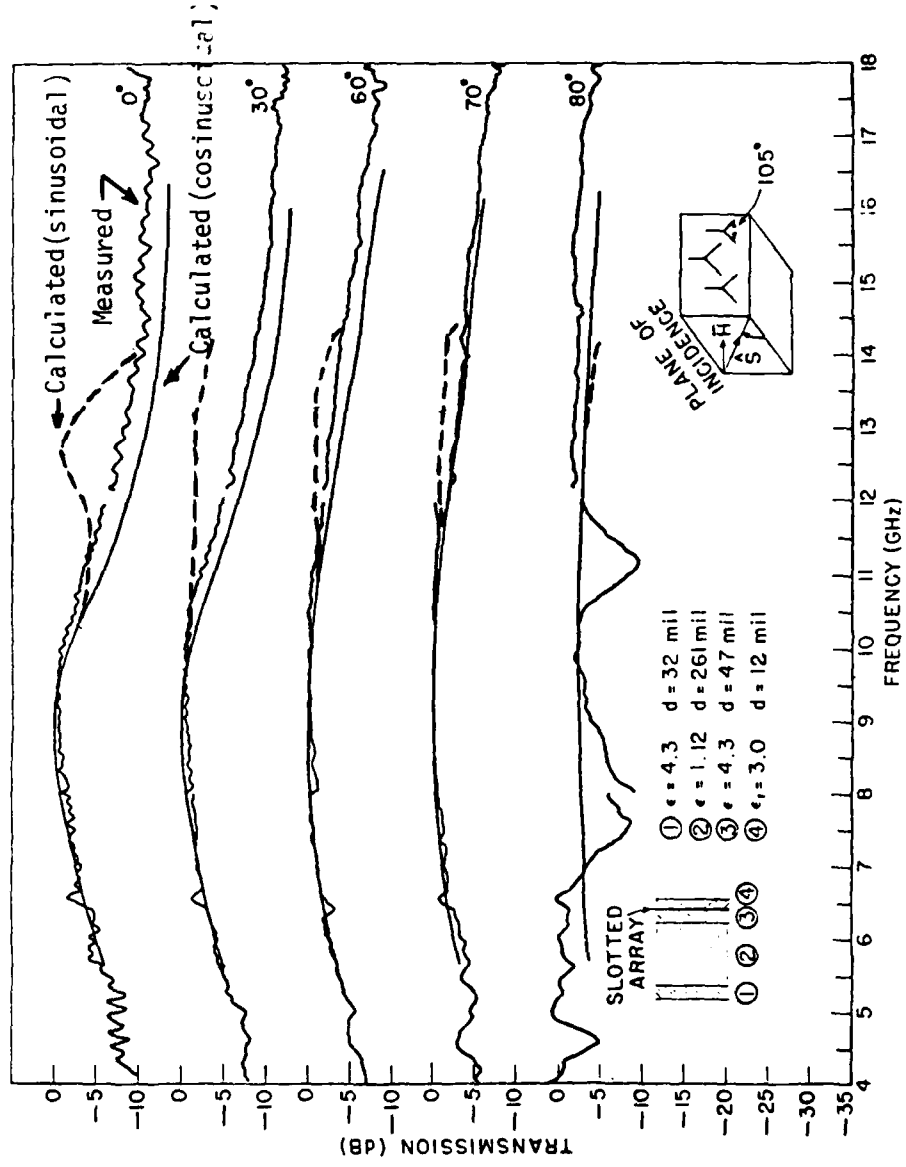


Figure 12. Comparison of calculated and measured transmission curves for orthogonal polarization for a mono-planar slot array using sinusoidal voltage distribution of Equation (29) or the sinusoidal voltage distribution of Equation (12).

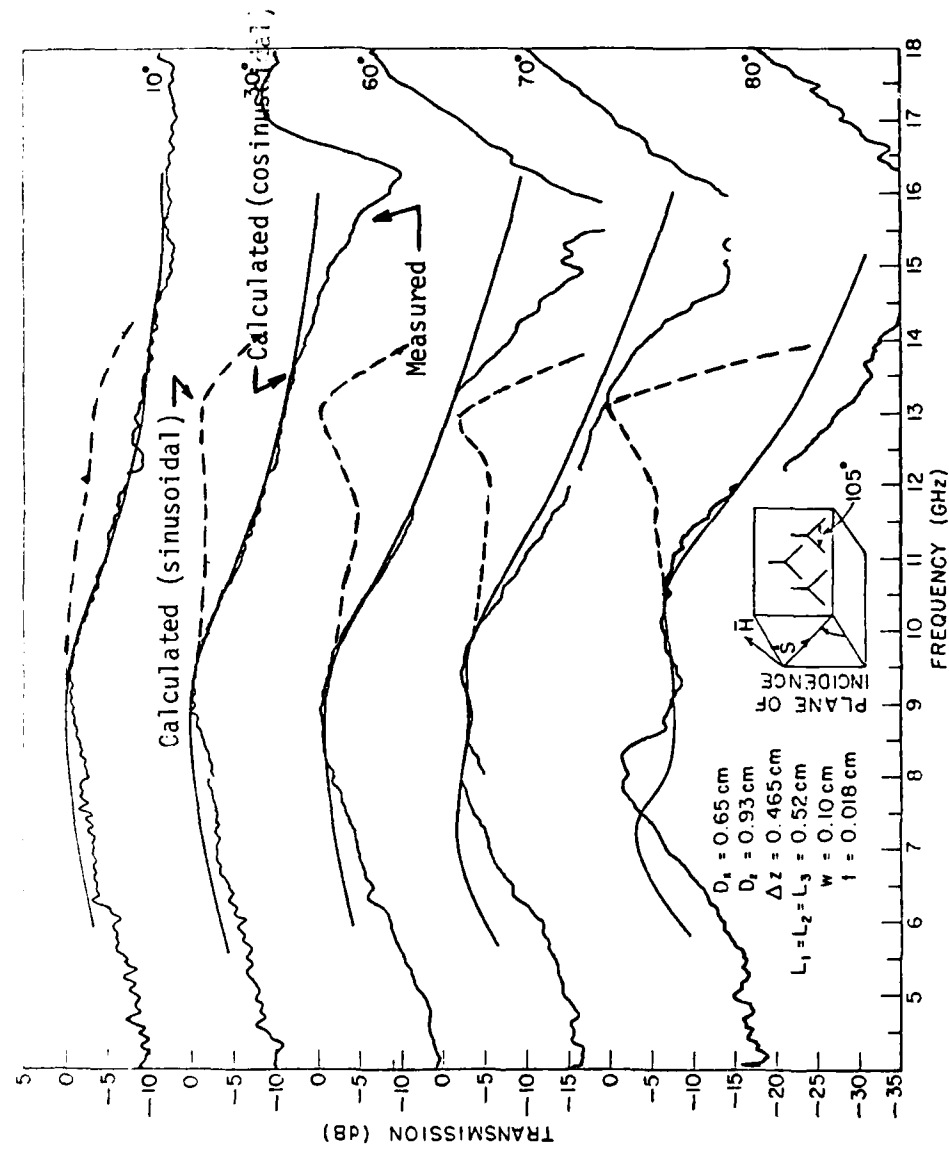


Figure 13. Comparison of calculated and measured transmission curves for parallel polarization for a mono-planar slot array using the voltage distributions of Figure 12.

The measured transmission curves did not contain a second resonance but continued to have greater loss as the frequency increased above resonance. For the structure of Figure 1 no measured results are available. However, the same agreement below resonance and the same general disagreement above resonance would occur.

To achieve closer agreement, a new voltage distribution along the slot elements when in the non-transmitting (scattering) mode is assumed. The new assumed distribution will more closely represent the actual voltage distribution. According to [3] the assumed voltage distribution for an unloaded receiving antenna is of a cosinusoidal form,

$$V^{Vi}(\ell) = \frac{\cos\beta_d\ell - \cos\beta_d\ell_{ef}}{1 - \cos\beta_d\ell_{ef}} \quad (29)$$

instead of the assumed form given by Equation (12).

For frequencies below the first resonance the different forms are approximately the same. The transmitted curves below this frequency should be approximately the same. When using Equation (29) in a previously developed program for the mono-planar slot case, the resulting calculated curves agreed with the measured ones for all range of frequencies (Figures 12 and 13). This cosinusoidal equation was then incorporated into the computer program developed for the structure of this report as the voltage distribution for the non-transmitting mode. For the transmitting mode the voltage distribution is the same as before, sinusoidal. At this point, the transmission curves were recalculated. The same iterative procedure used before was not redone. The data previously developed was reused to calculate the new transmission curves. The following Figures 14 to 17 give the new computed transmission curves. It can be seen that the bandwidth is no longer as constant with different incident polarizations. The bandwidth in fact has been reduced. A slight gain also is observed. We have not been able to explain the reason for this gain although the transmission curves are expected to be more accurate than for the sinusoidal case above. It should be possible to slightly improve the bandwidth so that it is nearly constant for the varying angles of incidence and different polarizations. This could possibly be done by decreasing the interelement spacings and the interlace spacing. This would raise the upper frequency end of the transmission curves. Since the interelement spacings and interlace spacing are almost decreased to a point where the slots overlap, not much improvement is expected. However, this has not been attempted at this time.

A slight discrepancy has arisen when using Equation (29) as the voltage distribution of the slot elements in the receiving mode. For this passive structure, a small gain (~ 0.3 dB or less) has occurred for certain incident angles and certain polarizations. See Figure 16. This, of course, is physically impossible.

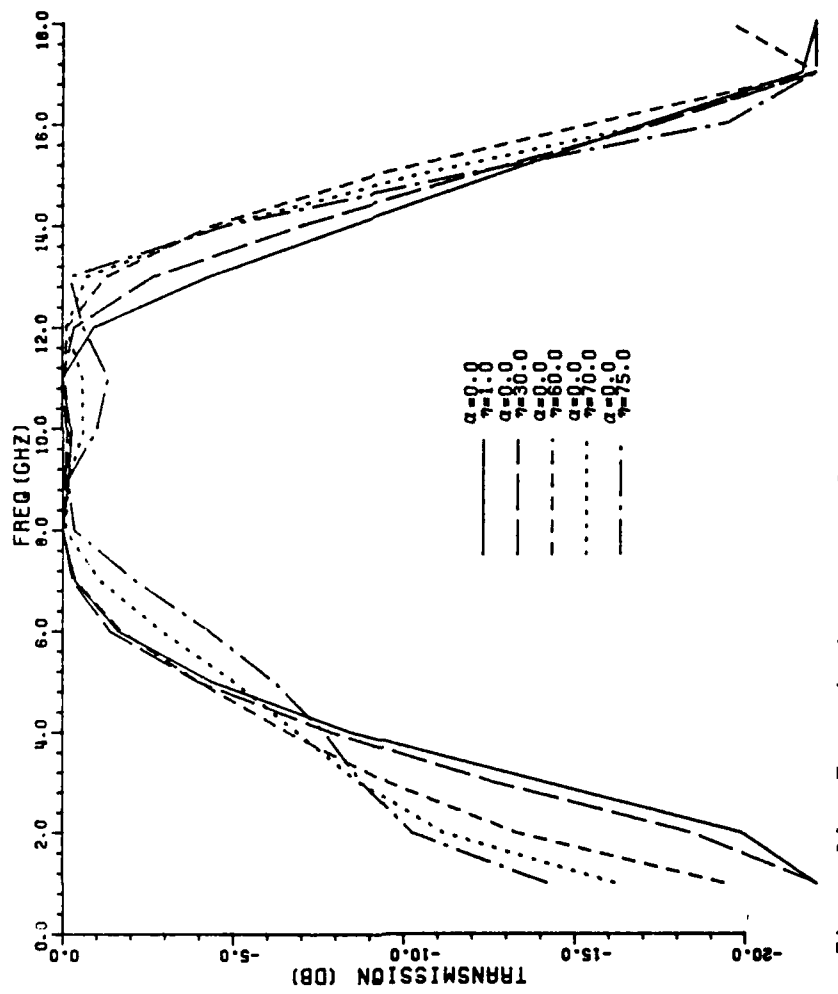


Figure 14. Transmission curves for orthogonal incident and orthogonal transmitted H-field with $\alpha=0^\circ$ using the voltage distributions of Equations (11) and (29). (Data set TS9A)

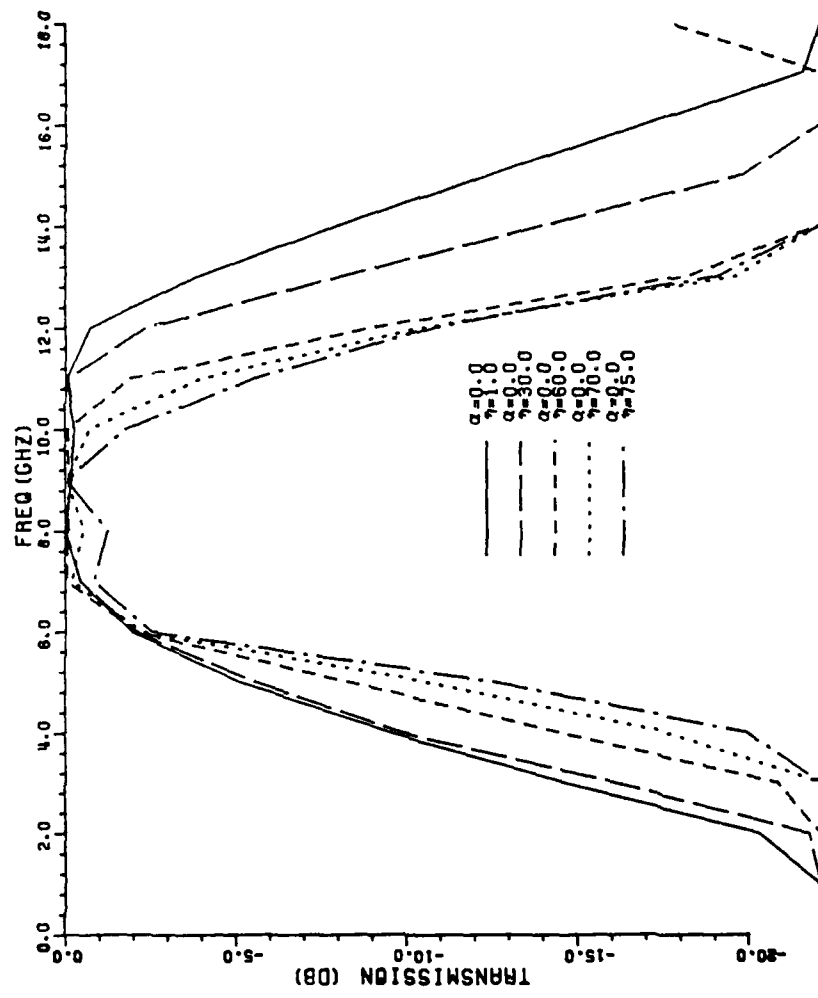


Figure 15. Transmission curves for parallel incident and parallel transmitted H-field with $\alpha=0^\circ$ using the voltage distributions of Equations (11) and (29). (Data set TS9A)

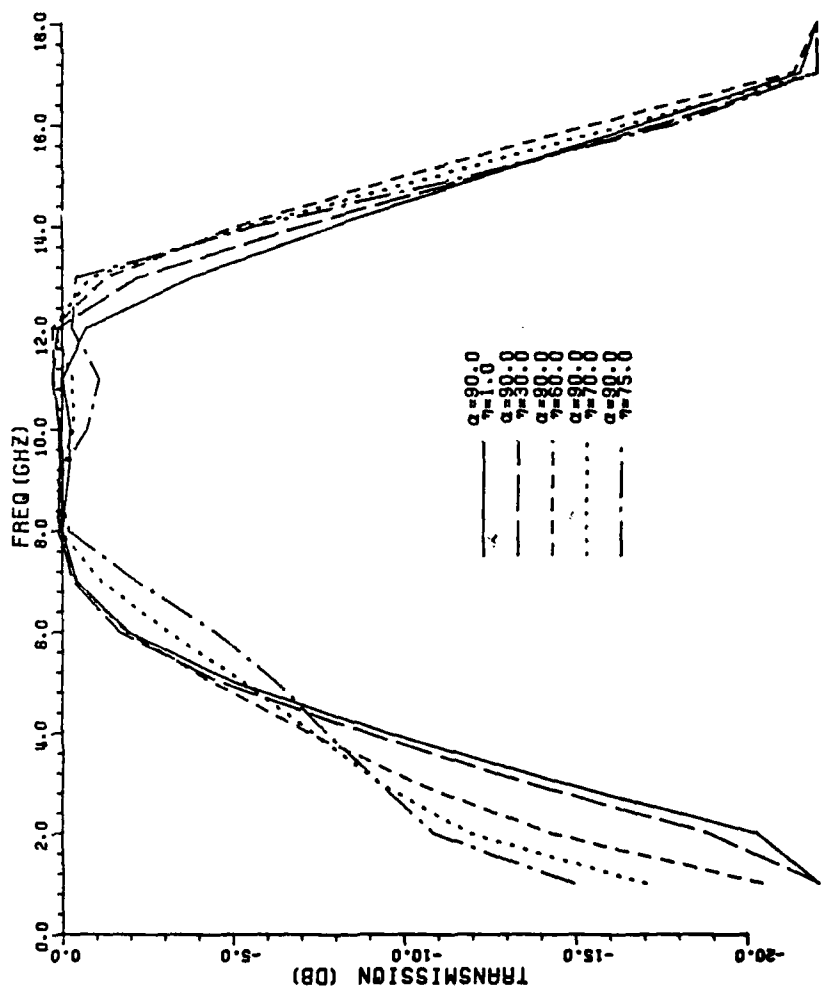


Figure 16. Transmission curves for orthogonal incident and orthogonal transmitted H-field with $\alpha=90^\circ$ using the voltage distributions of Equations (11) and (29). (Data set TS9A)

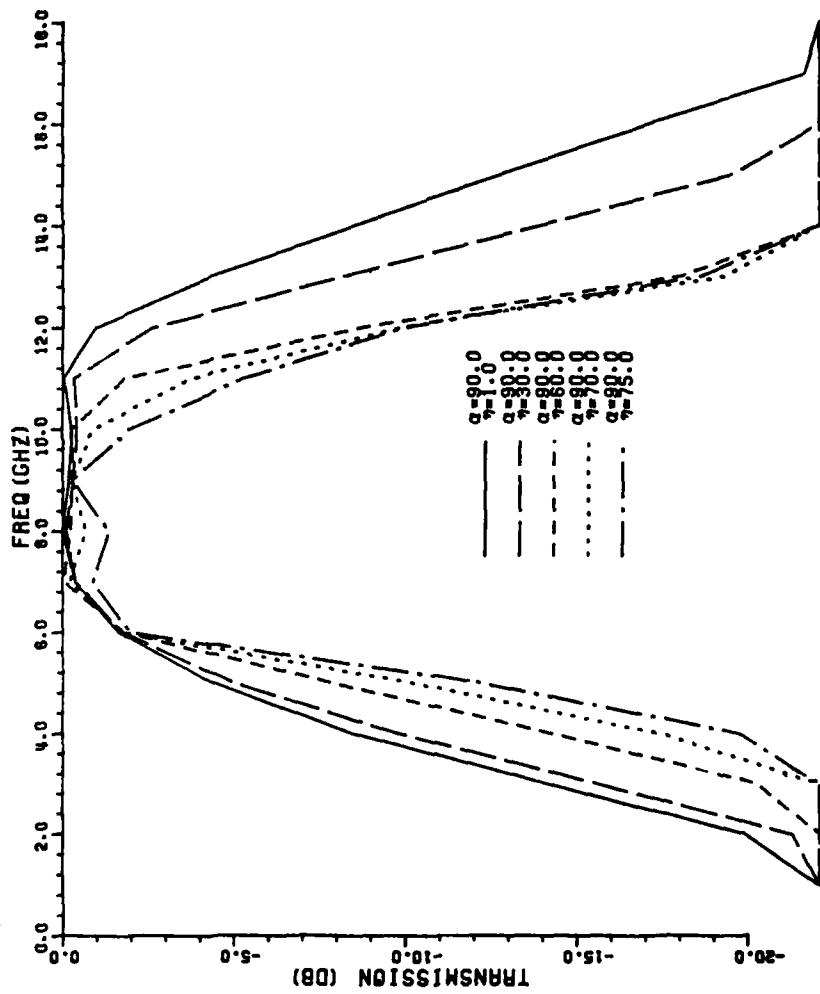


Figure 17. Transmission curves for parallel incident and parallel transmitted H-field with $\alpha=90^\circ$ using the voltage distributions of Equations (11) and (29). (Data set TS9A)

The source of this gain has not yet been located although attempts were made to resolve the problem. The computer program was re-examined with no apparent discrepancy between theory and program found. The method of performing the infinite sums through use of the convergence numbers was tested without any changes resulting in the gain.* Certain roundoff errors were considered but to no avail.

Next the slight gain was considered to be caused by the method of handling the end effects of the slots in the manner of an effective length. Ignoring the end effects by setting the effective length equal to the physical length of each leg, reduced the gain slightly (gain ~0.25 dB or less).

Re-examining the voltage distribution being used shows that it was developed for infinitely thin slots. The cause of the gain was then thought to be caused by using slots of finite width. The width of the slots was then reduced by an arbitrarily chosen factor of 4. An effective length was reinstated. The gain was reduced (~0.15 dB or less). Again neglecting the end effects results in even less gain (~0.06 dB or less). Figures 18 to 23 show the critical portions of the transmission curves for each of the above cases. Although each step offered improvement through reduced gain, a gain still existed. Lack of time has limited further search for the cause of the gain. However, the effective length does not seem to be the cause since end effects cannot physically be ignored. If the slots were made even thinner the gain would most likely reduce. Since the effective length was small, the final transmission curves were calculated making use of it.

Note that the achieved bandwidth varies from approximately 2 GHz to 6 GHz depending on the angle of incidence and polarization. This is still the largest and most constant bandwidth to date. For angles of incidence from normal (0°) to 60° the bandwidth has a range of 6.5 GHz to 10 GHz.

Interlace Anomaly

Examining the transmission curves given in [32] for the biplanar straight slot case imbedded in three dielectrics results in the following observations. When the plane of incidence is the $\alpha=0$ plane (ϕ -plane), with polarization orthogonal to the plane, zero transmission occurs at several frequencies. The 'zero' of interest is that one which limits the highest frequency that passes through the filter with little (~1 dB) attenuation. This 'zero' will limit the bandwidth in that plane.

The cause for this is that the structure anticipates the onset of a trapped grating lobe in the middle dielectric.** When this occurs the

*The convergence number was decreased from 10^{-3} to 10^{-5} to allow more terms in the summation to be used.

**Since the middle dielectric has a higher permittivity, the grating lobe will occur there at a lower frequency than in the other dielectric layers.

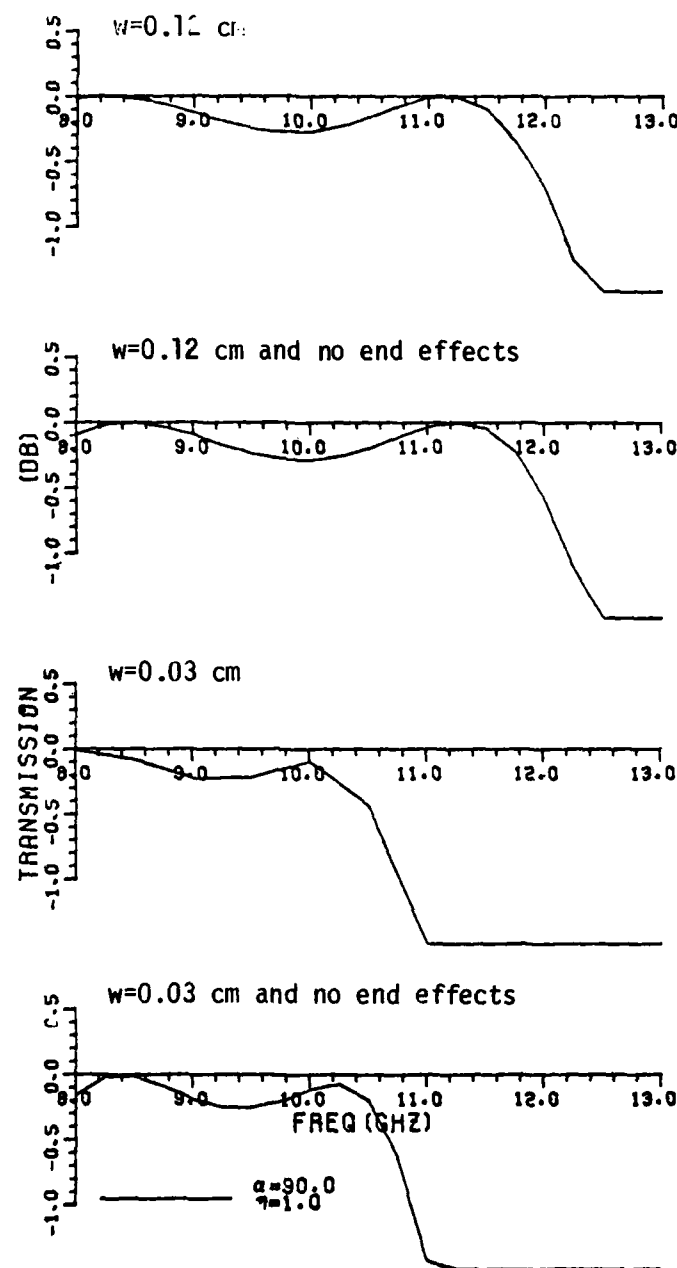


Figure 18. Transmission curves for orthogonal incident and orthogonal transmitted H-field for the various cases used in discussing the slight gain that occurs when using the voltage distributions of Equations (11) and (29). (Data set TS9A except where noted.)

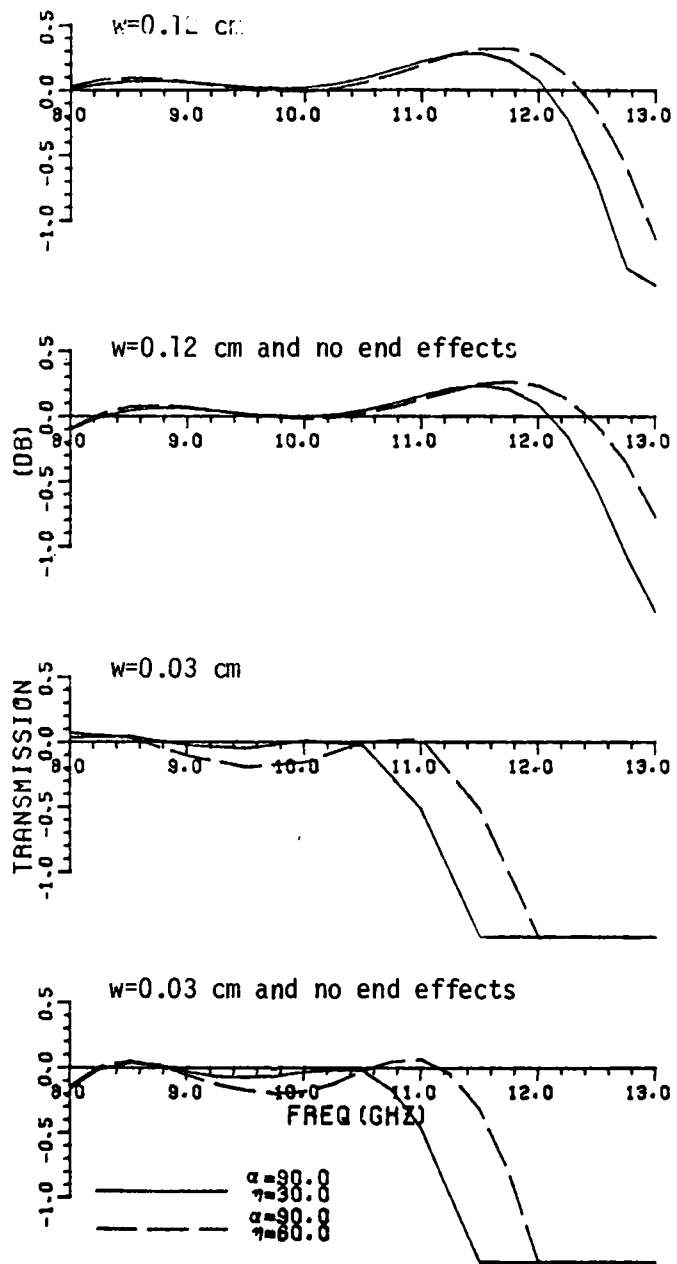


Figure 19. Transmission curves for orthogonal incident and orthogonal transmitted H-field for the various cases used in discussing the slight gain that occurs when using the voltage distributions of Equations (11) and (29). (Data set TS9A except where noted.).

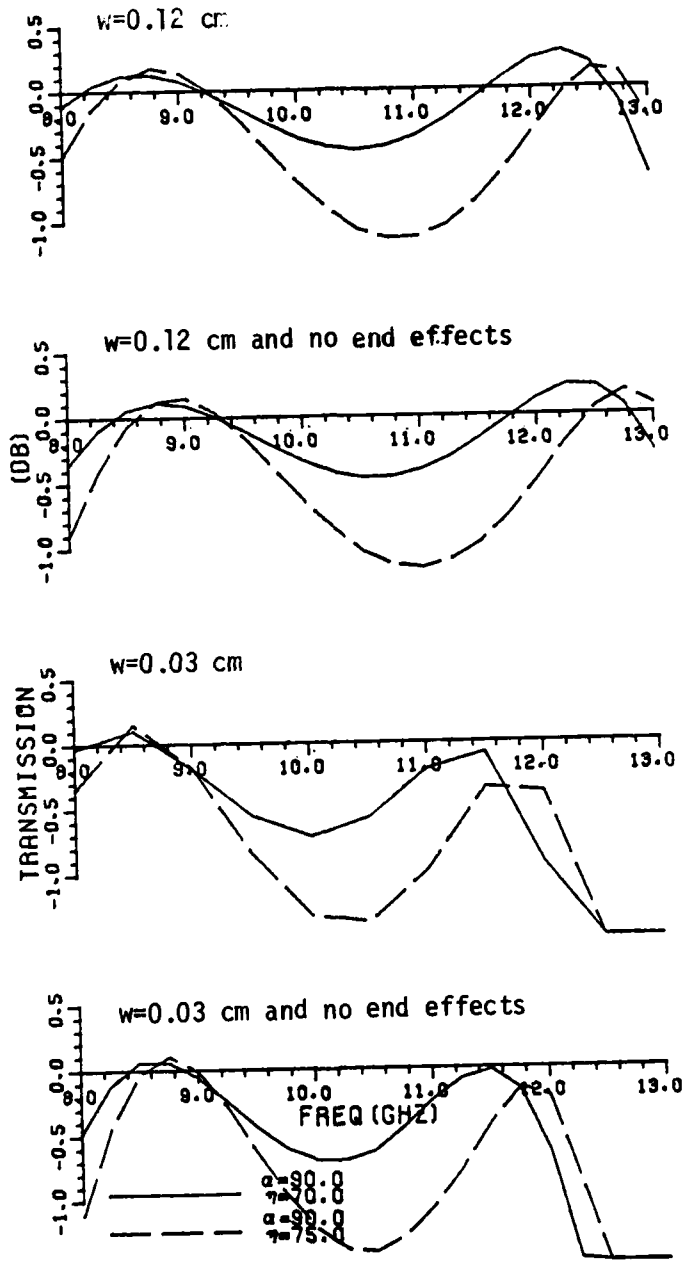


Figure 20. Transmission curves for orthogonal incident and orthogonal transmitted H-field for the various cases used in discussing the slight gain that occurs when using the voltage distributions of Equations (11) and (29). (Data set TS9A except where noted.)

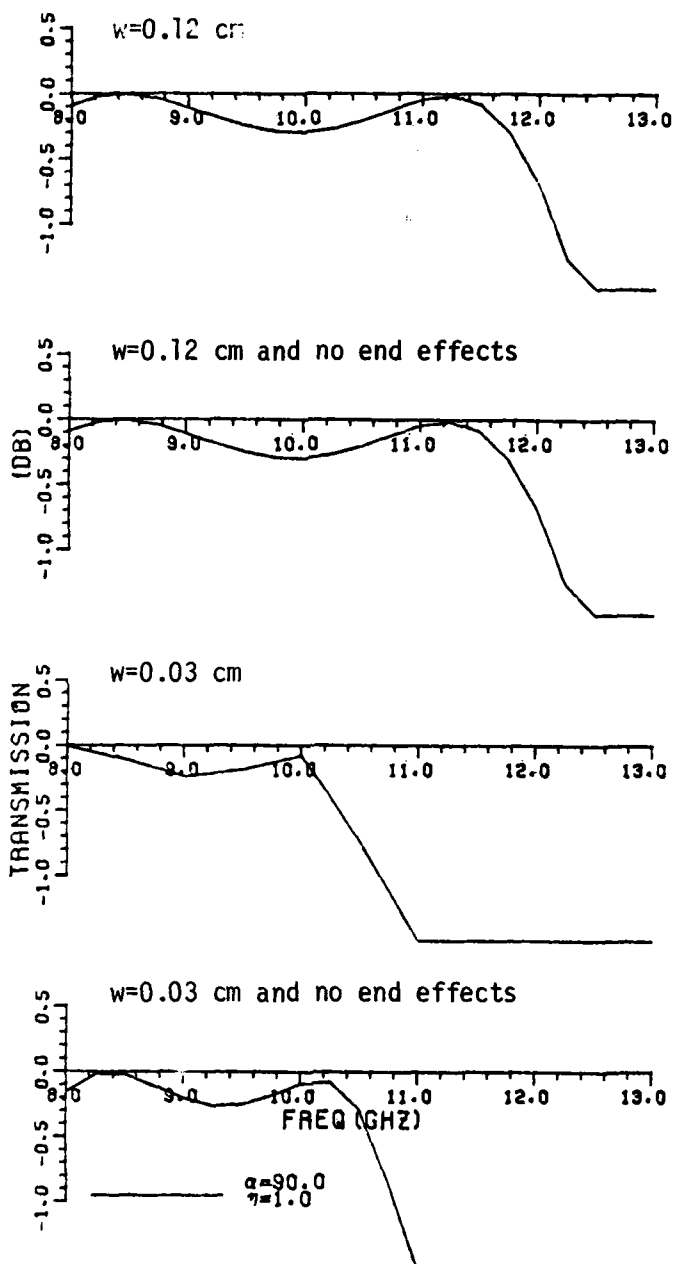


Figure 21. Transmission curves for parallel incident and parallel transmitted H-field for the various cases used in discussing the slight gain that occurs when using the voltage distributions of Equations (11) and (29). (Data set TS9A except where noted.)

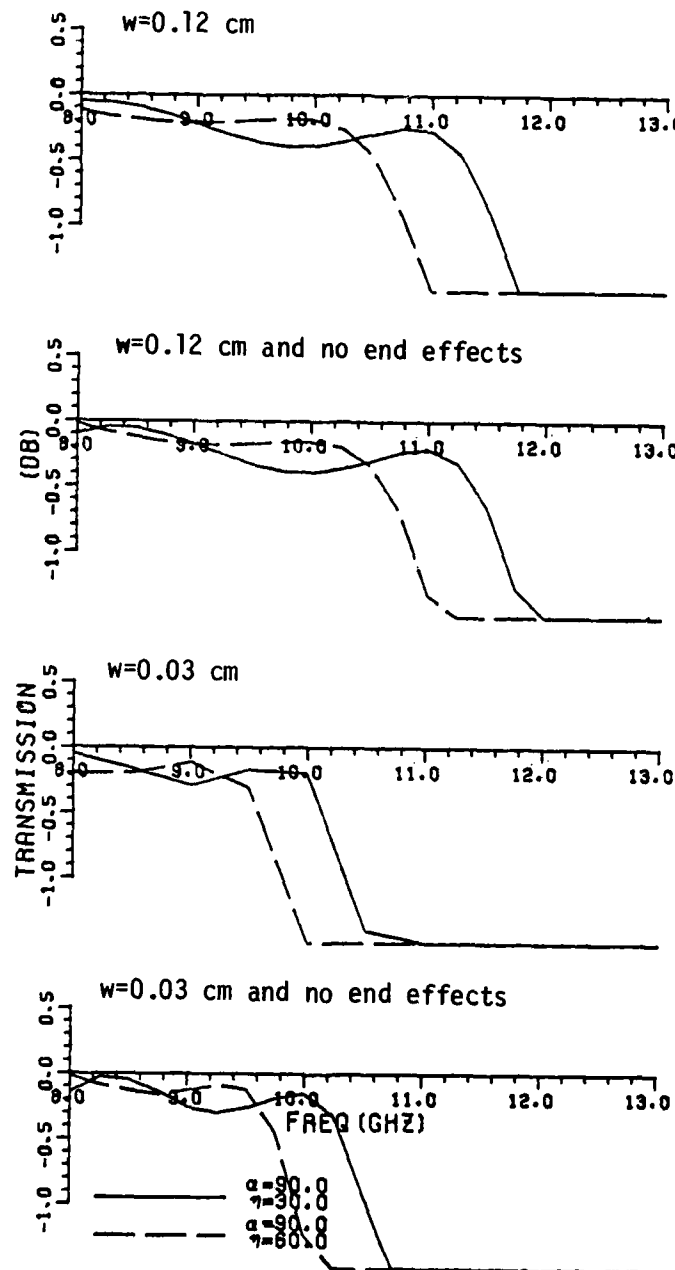


Figure 22. Transmission curves for parallel incident and parallel transmitted H-field for the various cases used in discussing the slight gain that occurs when using the voltage distributions of Equations (11) and (29). (Data set TS9A except where noted.)

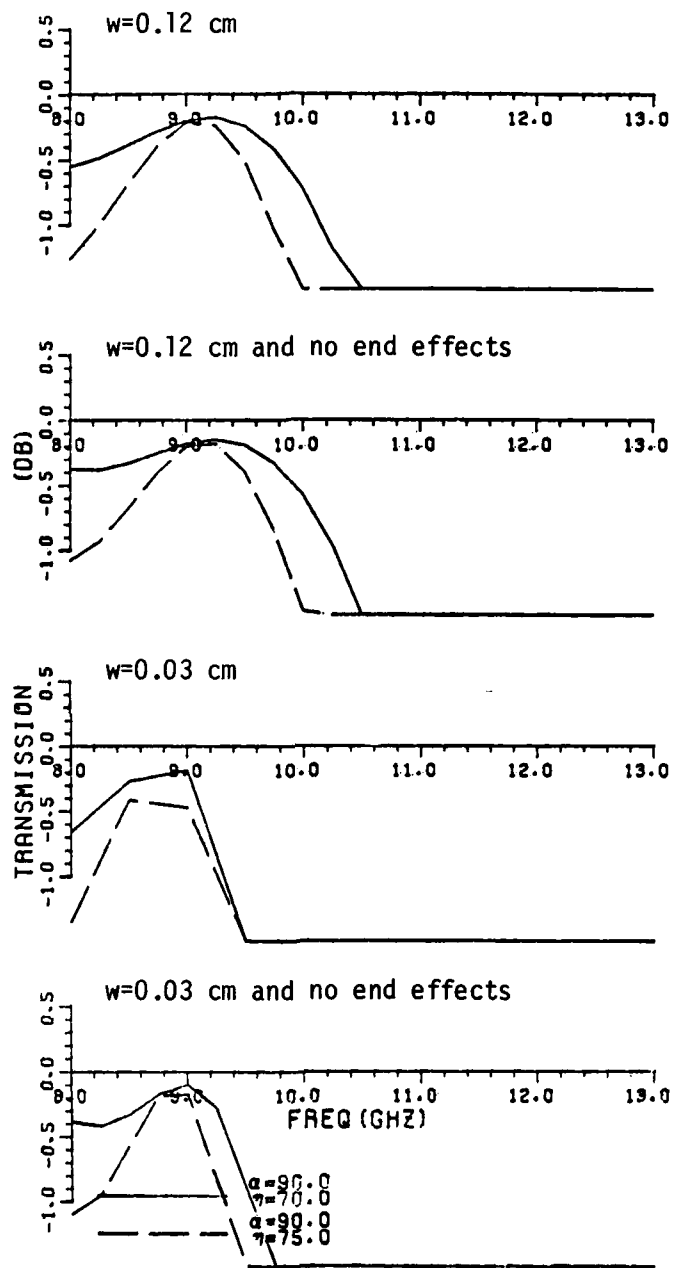


Figure 23. Transmission curves for parallel incident and parallel transmitted H-field for the various cases used in discussing the slight gain that occurs when using the voltage distributions of Equations (11) and (29). (Data set TS9A except where noted.)

evanescent waves begin to increase in strength and will destructively interfere with the principle wave at some frequency. This causes the mutual coupling between the straight slots to go to zero, hence zero transmission occurs. This is referred to as Luebbers anomaly [33].

In the $\alpha=90^\circ$ plane (θ -plane), the pattern factor limits the interference between the evanescent waves and the principle wave, consequently a null in the transmission curve corresponding to Luebbers anomaly is not observed for orthogonal polarization. Luebbers anomaly does exist in this plane for parallel polarization.

Since the starting data for the structure of this report came out of the above straight slot case, Luebbers anomaly was expected, but not observed for the computed transmission curves. However, an anomaly (i.e., a null in the transmission curves) does exist for parallel polarization in both the $\alpha=0^\circ$ and $\alpha=90^\circ$ planes. Investigation of this anomaly is done as before in the $\alpha=90^\circ$ plane (see p. 19). It will be recalled that for parallel polarization only the symmetric mode is excited. (Figure 7d). For a null in the transmission curve (Figures 15 and 17) the symmetric mutual coupling, y_{S1S2} or y_{S2S1} must go to zero for that point to be an anomaly. Examining results of the computer program shows this to be the case. In the $\alpha=0^\circ$ plane both the symmetric and asymmetric modes are excited but none of the modal admittances y_{S1S2} , y_{S2S1} , y_{A1A2} or y_{A2A1} goes to zero. However, the anomaly still exists. Hence the "effective mutual" coupling between the arrays must go to zero.

Luebbers anomaly and the newly attained anomaly are of different polarizations. Luebbers exists in the $\alpha=0^\circ$ plane for orthogonal polarization and in the $\alpha=90^\circ$ plane for parallel polarization, while the new anomaly exists in both the $\alpha=0^\circ$ and $\alpha=90^\circ$ planes for parallel polarizations.

Through the computer results, it was found that as a direct result of interlacing the slots, Luebbers anomaly changed to the new anomaly. The type of element did not affect the anomalies. Hence the new anomaly is referred to as the interlace anomaly.

This interlace anomaly limits the bandwidth at the upper frequency ends. As was previously stated, the interlace spacing and interelement spacings were reduced to raise the upper frequency end. This moved the anomaly up in frequency.

CHAPTER IV CONCLUSIONS

The transmission properties of a metallic radome configuration of two slot arrays consisting of three-legged elements imbedded in three dielectric layers has been investigated in order to design a bandpass filter with a large bandwidth. Only the symmetrical case consisting of two identical slot arrays with outer dielectric layers of the same material was considered.

A mathematical analysis was not attempted due to the complexity involved. A computer assisted design approach was used. The initial analysis used a sinusoidal voltage distribution. This was used in an iterative process to obtain as large a bandwidth as possible. Unfortunately, this was found, for a mono-planar configuration, to produce erroneous results at the upper portion of the frequency band. Thus, it became necessary to introduce a new cosinusoidal voltage distribution for unloaded three-legged slots in the non-transmitting (scattering) mode. This should improve the accuracy of the transmission curves above resonance. The transmission curves for the design were calculated. The bandwidth was then found to be somewhat smaller than the bandwidth calculated when using the sinusoidal voltage distribution. The bandwidth was also found to vary some with different angles of incidence and different polarization. For angles of incidence from normal (0°) to 60° the bandwidth has a range of 6.5 GHz to 10 GHz. Note that the iterations were not repeated when the cosinusoidal voltage mode was introduced. The data developed to that point was reused. It is, therefore, possible that slight improvements could be made to increase and stabilize the bandwidth. The final design still results in the largest and most constant bandwidth to date.

APPENDIX A
LIST OF ADMITTANCES FOR GIVEN STRUCTURE

In the main text, the admittances were defined and the general form was given. This appendix lists the admittances explicitly.

$$\begin{aligned}
 Y_{S1S1} &= -\frac{I_{S1S1}}{V_{ST}(0)} = \frac{\gamma_2}{2D_x D_z} \sum_{k=-\infty}^{\infty} \sum_{n=-\infty}^{\infty} \frac{e^{-j\beta_2 \frac{w}{4} r_{2y}}}{r_{2y}} \\
 &\quad [\downarrow P_2^{S1T} \downarrow P_2^{S1} \downarrow T_2(0, d_2) + \parallel P_2^{S1T} \parallel P_2^{S1} \parallel T_2(0, d_2)] \\
 &\quad + \frac{\gamma_3}{2D_x D_z} \sum_{k=-\infty}^{\infty} \sum_{n=-\infty}^{\infty} \frac{e^{-j\beta_3 \frac{w}{4} r_{3y}}}{r_{3y}} \\
 &\quad [\downarrow P_3^{S1T} \downarrow P_3^{S1} \downarrow T_3(0, d_3) + \parallel P_3^{S1T} \parallel P_3^{S1} \parallel T_3(0, d_3)] \tag{A1}
 \end{aligned}$$

$$\begin{aligned}
 Y_{S1A1} &= -\frac{I_{S1A1}}{V_{A1}(0)} = \frac{\gamma_2}{2D_x D_z} \sum_{k=-\infty}^{\infty} \sum_{n=-\infty}^{\infty} \frac{e^{-j\beta_2 \frac{w}{4} r_{2y}}}{r_{2y}} \\
 &\quad [\downarrow P_2^{S1T} \downarrow P_2^{A1} \downarrow T_2(0, d_2) + \parallel P_2^{S1T} \parallel P_2^{A1} \parallel T_2(0, d_2)] \\
 &\quad + \frac{\gamma_3}{2D_x D_z} \sum_{k=-\infty}^{\infty} \sum_{n=-\infty}^{\infty} \frac{e^{-j\beta_3 \frac{w}{4} r_{3y}}}{r_{3y}} \\
 &\quad [\downarrow P_3^{S1T} \downarrow P_3^{A1} \downarrow T_3(0, d_3) + \parallel P_3^{S1T} \parallel P_3^{A1} \parallel T_3(0, d_3)] \tag{A2}
 \end{aligned}$$

$$\gamma s1s2 = - \frac{I s1s2}{\gamma s2(0)} = \frac{\gamma_3}{2D_x D_z} \sum_{k=-\infty}^{\infty} \sum_{n=-\infty}^{\infty} \frac{e^{-j\beta_3 d_3 r_{3y}}}{r_{3y}}$$

$$\gamma^{s1a2} = -\frac{I^{s1a2}}{V^{a2}(0)} = \frac{\gamma_3}{2D_x D_z} \sum_{k=-\infty}^{\infty} \sum_{n=-\infty}^{\infty} \frac{e^{-j\beta_3 d_3 r_{3y}}}{r_{3y}} [P_3^{s1x} P_3^{a2} T_3(0,0) + " P_3^{s1x} " P_3^{a2} " T_3(0,0)] \quad (a4)$$

To define the remaining admittances,

superscript s superscript a
superscript a superscript s

which results in four more admittances.

Then

change from	to
superscript 1	superscript 2
superscript 2	superscript 1
subscript 2	subscript 4
$\left\{ \begin{array}{l} \uparrow \\ \downarrow \end{array} \right\} T_3(0, d_3)$	$\left\{ \begin{array}{l} 1 \\ u \end{array} \right\} T_3(d_3, 0)$

which again results in four more admittances.

The last four admittances are found by repeating the first set of changes. All admittances for the structure of Figure 1 are now specified.

APPENDIX B
T-FACTOR FOR THE STRUCTURE OF FIGURE 1

Note again that a slot can be considered as a magnetic element in front of an electrically perfectly-conducting ground plane. The reflection coefficient for the H -field from a ground plane is one. When calculating self admittances, the remaining arrays are short circuited causing them to become simply ground planes. Therefore, for either self or mutual admittance calculations the reflection coefficient at each slot array becomes one. For the structure of Figure 1, the reflection coefficients, $\{\frac{1}{n}\} \Gamma_{23}$, $\{\frac{1}{n}\} \Gamma_{32}$, $\{\frac{1}{n}\} \Gamma_{34}$, and $\{\frac{1}{n}\} \Gamma_{43}$ are equal to one.

For the self admittance calculations the reference point of the single test element is considered to be one quarter the slot width away from the reference point of the array by definition. However, the T-factor is calculated assuming the reference element and the array coincide. This discrepancy is negligible.

For mutual admittance calculations the reference element coincides with one of the arrays.

Using the above observations in the generalized non-normalized T-factor (Equation (17)) results in the following for the given structure for self admittance calculations;

$$\{\frac{1}{n}\} T_2(0, d_2) = 2.0 \quad \left(\frac{1 + \{\frac{1}{n}\} \Gamma_{2,1} e^{-j2\beta_2 d_2 r_{2y}}}{1 - \{\frac{1}{n}\} \Gamma_{2,1} e^{-j2\beta_2 d_2 r_{2y}}} \right) \quad (B1)$$

$$\{\frac{1}{n}\} T_3(0, d_3) = 2.0 \quad \left(\frac{1 + e^{-j2\beta_3 d_3 r_{3y}}}{1 - e^{-j2\beta_3 d_3 r_{3y}}} \right) \quad (B2)$$

$$\{\frac{1}{n}\} T_3(d_3, 0) = \{\frac{1}{n}\} T_3(0, d_3) \quad (B3)$$

$$\left\{ \frac{1}{n} \right\} T_4(0, d_4) = 2.0 \times \left(\frac{1 + \left\{ \frac{1}{n} \right\} \Gamma_{4,5} e^{-j2\beta_4 d_4 r_{4y}}}{1 - \left\{ \frac{1}{n} \right\} \Gamma_{4,5} e^{-j2\beta_4 d_4 r_{4y}}} \right) \quad (B4)$$

and for mutual admittance calculations

$$\left\{ \frac{1}{n} \right\} T_3(0,0) = 4 / \left(1 - e^{-j2\beta_3 d_3 r_{3y}} \right) \quad (B5)$$

This provides all necessary T-factors for admittance calculations.

The normalized T-factors needed for the structure of Figure 1 are:

$$\left\{ \frac{1}{n} \right\} T(0,0)_{2/1} = 2 \left(\frac{1 - \left\{ \frac{1}{n} \right\} \Gamma_{2,1}}{1 - \left\{ \frac{1}{n} \right\} \Gamma_{2,1} e^{-j2\beta_2 d_2 r_{2y}}} \right) \quad (B6)$$

and for transmitted H-field calculations

$$\left\{ \frac{1}{n} \right\} T(0,0)_{4/5} = 2 \left(\frac{1 - \left\{ \frac{1}{n} \right\} \Gamma_{4,5}}{1 - \left\{ \frac{1}{n} \right\} \Gamma_{4,5} e^{-j2\beta_4 d_4 r_{4y}}} \right) \quad (B7)$$

All T-factors have now been determined.

APPENDIX C
THE PLANE OF INCIDENCE AND THE PLANES OF SCATTERING

The following formulas were taken from Appendix B in [34] and are generalized and included here for completeness.

The plane of scattering is defined as the plane containing the vector normal to the dielectric interface, \hat{n}_0 , and the direction of propagation, \hat{r}_m , where m refers to the dielectric media.

For unit vectors, $\perp \hat{n}_m$, orthogonal to the plane of incidence

$$\perp \hat{n}_m = \frac{\hat{n}_0 \times \hat{r}_m}{|\hat{n}_0 \times \hat{r}_m|} = \frac{-\hat{x} r_{mz} + \hat{z} r_{mx}}{(r_{mx}^2 + r_{mz}^2)^{1/2}} \quad (C1)$$

For unit vectors parallel, $\parallel \hat{n}_m$, to the plane of scattering and orthogonal to the direction of propagation, \hat{r}_m .

$$\parallel \hat{n}_m = \perp \hat{n}_m \times \hat{r}_m = \frac{1}{(r_{mx}^2 + r_{mz}^2)^{1/2}} (-\hat{x} r_{mx} r_{my} + \hat{y} (r_{mx}^2 + r_{mz}^2) - \hat{z} r_{my} r_{mz}) \quad (C2)$$

The plane of incidence is defined as the plane containing the vector \hat{n}_0 normal to the dielectric interface and the direction of propagation \hat{s}_m ($=\hat{r}_m$ for $k=n=0$), cf. Figure D1.

APPENDIX D
REFLECTION COEFFICIENTS FOR THE H-FIELD

The following formulas are found in Appendix C in [35] and are listed here for completeness. The formulas correspond to the following generalized figure.

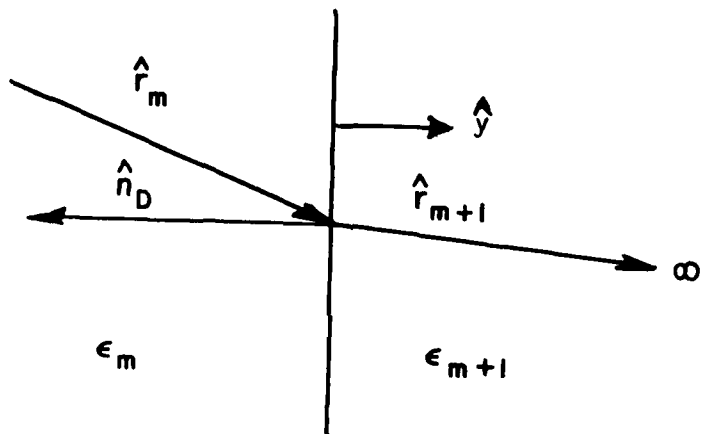


Figure D1. Incident wave on a dielectric boundary.

$$\downarrow \Gamma_{m,m+1} = \frac{\sqrt{\epsilon_{(m+1)}} r_{my} - \sqrt{\epsilon_m} r_{(m+1)y}}{\sqrt{\epsilon_{(m+1)}} r_{my} + \sqrt{\epsilon_m} r_{(m+1)y}} \quad (D1)$$

$$" \Gamma_{m,m+1} = \frac{\sqrt{\epsilon_{(m+1)}} r_{(m+1)y} - \sqrt{\epsilon_m} r_{my}}{\sqrt{\epsilon_{(m+1)}} r_{(m+1)y} + \sqrt{\epsilon_m} r_{my}} \quad (D2)$$

$$\frac{1 + \Gamma_{m,m+1}}{1 - \Gamma_{m,m+1}} = \frac{\sqrt{\epsilon_{(m+1)}} r_{my}}{\sqrt{\epsilon_m} r_{(m+1)y}} \quad (D3)$$

$$\frac{1 + \sqrt{\epsilon_{m,m+1}}}{1 - \sqrt{\epsilon_{m,m+1}}} = \frac{\sqrt{\epsilon_{(m+1)}} r_{(m+1)} y}{\sqrt{\epsilon_m} r_{(m+1)} y} \quad (D4)$$

$$\left\{ \frac{1}{n} \right\} F_{m,m+1} = - \left\{ \frac{1}{n} \right\} F_{m+1,m} \quad (D5)$$

APPENDIX E
MUTUAL ADMITTANCE (γ^{as} AND γ^{sa}) BETWEEN SYMMETRIC
AND ASYMMETRIC MODES

In this appendix we assume that the voltage distribution on the slots is of the same form for both the transmitting and non-transmitting modes, namely sinusoidal. The admittance relationship presented also holds for the cosinusoidal voltage distribution around resonance where the two voltage distributions are approximately equal. Any interlace spacing is allowed, i.e., the relationships hold for straight or interlaced array grids.

The relationships that follow are developed so that easy comparison of computer program results can be made between γ^{sa} and γ^{as} . Separating γ^{sa} into real and imaginary parts due to real and imaginary space* yields

$$\gamma^{sa} = \frac{(\text{Re}\gamma^{sa} + \text{Im}\gamma^{sa})_{\text{real}}}{\text{space}} + \frac{(\text{Re}\gamma^{sa} + \text{Im}\gamma^{sa})_{\text{imaginary}}}{\text{space}} . \quad (\text{E1})$$

Similarly

$$\gamma^{as} = \frac{(\text{Re}\gamma^{as} + \text{Im}\gamma^{as})_{\text{real}}}{\text{space}} + \frac{(\text{Re}\gamma^{as} + \text{Im}\gamma^{as})_{\text{imaginary}}}{\text{space}} . \quad (\text{E2})$$

Equating the components to each along with extensive use of Equations (B6), (B7) and (B8) in [36] it was found that

$$\frac{\text{Re}\gamma^{sa}_{\text{imaginary}}}{\text{space}} = - \frac{\text{Re}\gamma^{as}_{\text{imaginary}}}{\text{space}} \quad (\text{E3})$$

$$\frac{\text{Im}\gamma^{sa}_{\text{imaginary}}}{\text{space}} = + \frac{\text{Im}\gamma^{sa}_{\text{imaginary}}}{\text{space}} \quad (\text{E4})$$

*Real space pertains to propagating mode, i.e., $k=n=0$ for no grating lobes. Imaginary space pertains to evanescent modes, i.e., k and/or $n \neq 0$ for no grating lobes.

for a three-legged element, provided that the T-factor is real for imaginary space. This holds if the effective reflection coefficient is real, namely if

- 1) no grating lobes exist, anywhere, or
- 2) no dielectric exists (i.e., free space).

An additional case occurs if the reflection coefficient is complex but multiplied by a negligible number, effectively making the T-factor real. This is the case if

- 1) the electrical thickness $\beta_d r_m$, of the dielectric slabs is sufficient to insure that the exponentials in the T-factor be negligible.

Equations (E3) and (E4) correspond to Equation (B18) in [37].

For the three-legged elements

$$\hat{p}^{(1)} = \hat{z} \quad (E5)$$

$$\hat{p}^{(2)} = \hat{x} p_x^{(2)} + \hat{z} p_z^{(2)} \quad (E6)$$

$$\hat{p}^{(3)} = -\hat{x} p_x^{(2)} + \hat{z} p_z^{(2)} \quad (E7)$$

the relationship between γ_{sa} and γ_{as} in real space is

$$(\gamma_{sa})_{\substack{\text{real} \\ \text{space}}} = -(\gamma_{as})_{\substack{\text{real} \\ \text{space}}} * \quad (E8)$$

or

*Note Equation (E8) and Equation (B16) in [38] have differently defined quantities. Hence they do not contradict.

$$(ReY^{sa})_{\substack{\text{real} \\ \text{space}}} + (ImY^{sa})_{\substack{\text{real} \\ \text{space}}} = - (ReY^{as})_{\substack{\text{real} \\ \text{space}}} - (ImY^{as})_{\substack{\text{real} \\ \text{space}}}. \quad (E9)$$

For the above relationship to be true it was found that for the symmetric pattern factor, P^s , the \hat{x} and \hat{z} components had to be pure imaginary and pure real, respectively, and for the assymmetric pattern factor, P^a , the \hat{x} and \hat{z} components had to be pure imaginary and pure real respectively. This must also hold for the transmitting pattern factors. For the given three-legged elements this is indeed true only when the incident field is in the principle planes ($\alpha=0^\circ, 90^\circ$).

APPENDIX F
PATTERN FACTORS IN THE YZ-PLANE
FOR INTERLACE STRUCTURE

This appendix assumes that the voltage distribution on the slots is of the same form for both transmitting and non-transmitting modes. Certain properties of the composite pattern factors, $\{\frac{1}{n}\}^{pst}$, $\{\frac{1}{n}\}^{pat}$, $\{\frac{1}{n}\}^{ps}$ and $\{\frac{1}{n}\}^{pa}$, will be established for interlacing in the z direction only ($\Delta x=0$). The properties of the composite pattern factors for the non-interlace structure are a special case of those for the interlace structure treated here, (see Appendix D in [39]).

When the plane of incidence is the YZ-Plane, $s_{mx}=0$

$$\hat{r}_m = \hat{x} \left(k - \frac{n\Delta z}{D_z} \right) \frac{\lambda_m}{D_x} + \hat{y} r_{my} + \hat{z} \left(s_{mz} + \frac{n\lambda_m}{D_z} \right) \quad (F1)$$

where subscript m refers to the media.

Using a three-legged element that is symmetric with respect to the YZ-Plane, results in

$$\hat{p}^{(1)} = \hat{z} \quad (F2)$$

$$\hat{p}^{(2)} = \hat{x} p_x^{(2)} + \hat{z} p_z^{(2)} \quad (F3)$$

$$\hat{p}^{(3)} = -\hat{x} p_x^{(2)} + \hat{z} p_z^{(2)} \quad (F4)$$

Since the overall objective is to find certain properties between the composite patterns, certain properties between the patterns of each leg need be found.

To find those properties the following Equation (F5) is assumed since this relates the exponential factor of the patterns of each leg.

$$\hat{p}^{(2)} \cdot \hat{r}_m(k_2, n) = \hat{p}^{(3)} \cdot \hat{r}_m(k_3, n) \quad (F5)$$

where k_2 and k_3 refer to the summation indice k for leg 2 and 3, respectively.

Substituting Equation (F1) into Equation (F5) gives

$$\begin{aligned} p_x^{(2)} \left(k_2 - \frac{n\Delta z}{D_z} \right) \frac{\lambda_m}{D_x} + p_z^{(2)} \left(s_{mz} + \frac{n\lambda_m}{D_z} \right) \\ = - p_x^{(2)} \left(k_3 - \frac{n\Delta z}{D_z} \right) \frac{\lambda_m}{D_x} + p_z^{(2)} \left(s_{mz} + \frac{n\lambda_m}{D_z} \right) \end{aligned} \quad (F6)$$

so

$$k_2 - \frac{n\Delta z}{D_z} = \frac{n\Delta z}{D_z} - k_3 \quad (F7)$$

or

$$\frac{2n\Delta z}{D_z} - k_3 = k_2 \quad . \quad (F8)$$

The relationship between $r_{mx}(k_2, n)$ and $r_{mx}(k_3, n)$, where r_{mx} is the x component of \hat{r}_m , can now be found.

$$\begin{aligned} r_{mx}(k_2, n) &= \left(k_2 - \frac{n\Delta z}{D_z} \right) \frac{\lambda_m}{D_x} = \left(\left(\frac{2n\Delta z}{D_z} - k_3 \right) - \frac{n\Delta z}{D_z} \frac{\lambda_m}{D_x} \right) \\ &= \left(\frac{n\Delta z}{D_z} - k_3 \right) \frac{\lambda_m}{D_x} \end{aligned} \quad (F9)$$

or

$$r_{mx}(k_2, n) = - r_{mx}(k_3, n) \quad . \quad (F10)$$

Also by inspection $r_{mz}(k_2, n) = r_{mz}(k_3, n)$.

Substitution of Equations (F5) and (F8) into the equations for the pattern results in an equation of the form

$$p^v2 \left(\frac{2n\Delta z}{D_z} - k_3, n \right) = p^v3(k_3, n) \quad (F11)$$

$$p^v3 \left(\frac{2n\Delta z}{D_z} - k_3, n \right) = p^v2(k_3, n)$$

where p^v is the symmetric, asymmetric, non-transmitting (scattering) and transmitting patterns, p^s , p^a , p^{st} , p^{at} of each leg for scan in the YZ-Plane. v is a dummy variable.

Substituting Equation (F11) into (D10) in [40] with slight notational change yields

$$\begin{aligned} \downarrow p_m^s(k_2, n) &= \frac{1}{(r_{mx}^2(k_2, n) + r_{mz}^2(k_2, n))^{1/2}} \\ &[2r_{mx}(k_2, n)p^{s1}(k_2, n) + p_x r_{mz}(k_2, n)(p^{s2}(k_2, n) - p^{s3}(k_2, n) \\ &- p_z r_{mx}(k_2, n)(p^{s2}(k_2, n) + p^{s3}(k_2, n))] \\ &= \frac{1}{(r_{mx}^2(k_3, n) + r_{mz}^2(k_3, n))^{1/2}} \\ &\left[-2r_{mx}(k_3, n)p^{s1}(k_3, n) + p_x r_{mz}(k_3, n) \left(p^{s2}\left(\frac{2n\Delta z}{D_z} - k_3, n\right) - p^{s3}\left(\frac{2n\Delta z}{D_z} - k_3, n\right) \right) \right. \\ &\left. + p_z r_{mx}(k_3, n) \left(p^{s2}\left(\frac{2n\Delta z}{D_z} - k_3, n\right) + p^{s3}\left(\frac{2n\Delta z}{D_z} - k_3, n\right) \right) \right] \quad (F12) \\ &= \frac{1}{(r_{mx}^2(k_3, n) + r_{mz}^2(k_3, n))^{1/2}} \\ &[-2r_{mx}(k_3, n)p^{s1}(k_3, n) + p_x r_{mz}(k_3, n)(p^{s2}(k_3, n) + p^{s3}(k_3, n)) \\ &+ p_z r_{mx}(k_3, n)(p^{s2}(k_3, n) + p^{s3}(k_3, n))] \\ &= - \downarrow p_m^s(k_3, n) \end{aligned}$$

Substituting Equation (F7) into Equation (F12) yields

$$\perp P_m^S \left(\frac{2n\Delta z}{D_z} - k_3, n \right) = \perp P_m^S(k_3, n) \quad (F13)$$

Similar derivations using Equations (D11)-(D13) in [41] of non-transmitting modes for parallel and orthogonal components yields

$$|| P_m^S \left(\frac{2n\Delta z}{D_z} - k_3, n \right) = || P_m^S(k_3, n) \quad (F14)$$

$$\perp P_m^a \left(\frac{2n\Delta z}{D_z} - k_3, n \right) = \perp P_m^a(k_3, n) \quad (F15)$$

$$|| P_m^a \left(\frac{2n\Delta z}{D_z} - k_3, n \right) = - || P_m^a(k_3, n) \quad (F16)$$

The above four equations also hold for the transmitting case.

Note that for $k=n=0$.

$$\perp P_m^S(0,0) = || P_m^a(0,0) = 0$$

which is identical to Equation (D18) in [42]. This should be the case since at $k=n=0$ the principle propagating mode will be the same regardless of grid structure.

If $\Delta z=0$ (non-interlace structure) Equations (F13), (F14), (F15) and (F16) reduce to Equations (D14)-(D17) in [43] given for the non-interlace design.

Equations (D21) and (D22) in [44] only hold for the non-interlace structure.

APPENDIX G
 COMPUTER LISTING FOR BIPLANAR SLOT ARRAY
 OF THREE-LEGGED ELEMENTS IN A
 STRATIFIED DIELECTRIC MEDIUM

LIST OF IMPORTANT COMPUTER VARIABLES	EXPLANATION AT PROGRAM* LINE NUMBER
ABRS	91
ACPAT.	658
ALPHA.	17 DATA FILE
APATX.	641
APATZ.	642
BETA	85
BETAD.	891
BTD.	586
CA1.	1202
CS1.	1201
D.	11 DATA FILE
DELTZ.	26 DATA FILE
DX	24 DATA FILE
DZ	25 DATA FILE
EFFL	893
ELEMX.	894
ELEMZ.	894
ER	19 DATA FILE
ETA.	17 DATA FILE
EXPT	1127
EXPY.M.	1103
EXPYS.	1077
FINCRM	9 DATA FILE
FREQH.	8 DATA FILE
FREQL.	7 DATA FILE
IKK.	853
INN.	853
IOC.	52 PRINT
IVD.	888

* Except when noted otherwise. Explanation then exists at line number given in listed program.

LIST OF IMPORTANT
COMPUTER VARIABLES
(cont.)

EXPLANATION AT PROGRAM
LINE NUMBER
(cont.)

NADMT	587
NANGLS	15 DATA FILE
OHO.	1221
OHP.	1222
OPATC.	660
PATX	897
PATZ	897
PHO.	1223
PHP.	1224
PPATC.	661
RHO.	1042
RL	27 DATA FILE
RLA.	30 DATA FILE
RLAMDA	85
RLF.	585
RXKN	859
RYKN	859
RZKN	859
SCPAT.	624
SPATX.	637
SPATZ.	640
SX	105
SZ	105
TFACT.	997
THIK	29 DATA FILE
VA2.	1251
VS2.	1250
WIDTH.	28 DATA FILE
YADMT.	590
YADMTR.	591
YADMTR.	592

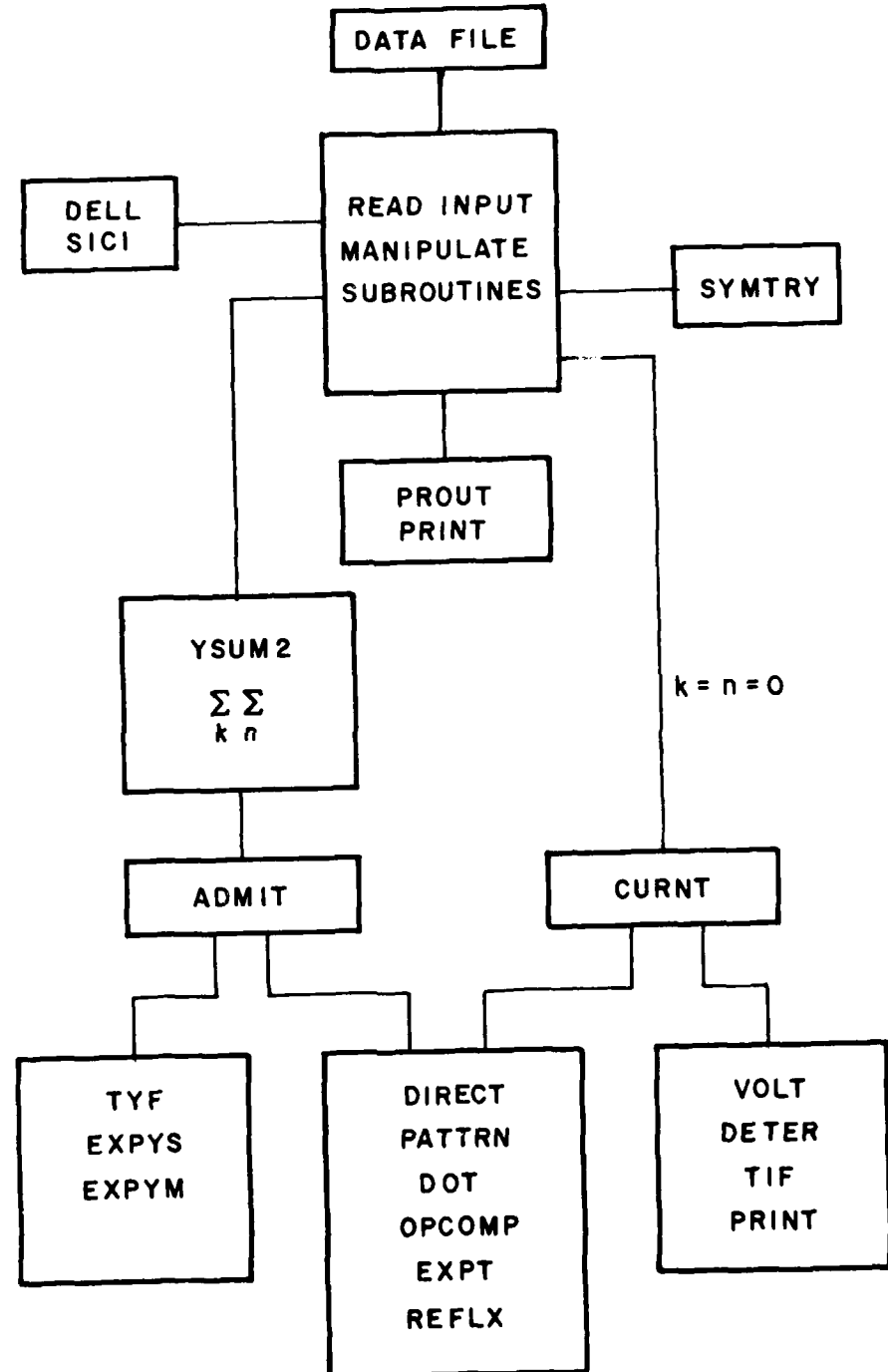


Figure G1. Program structure.

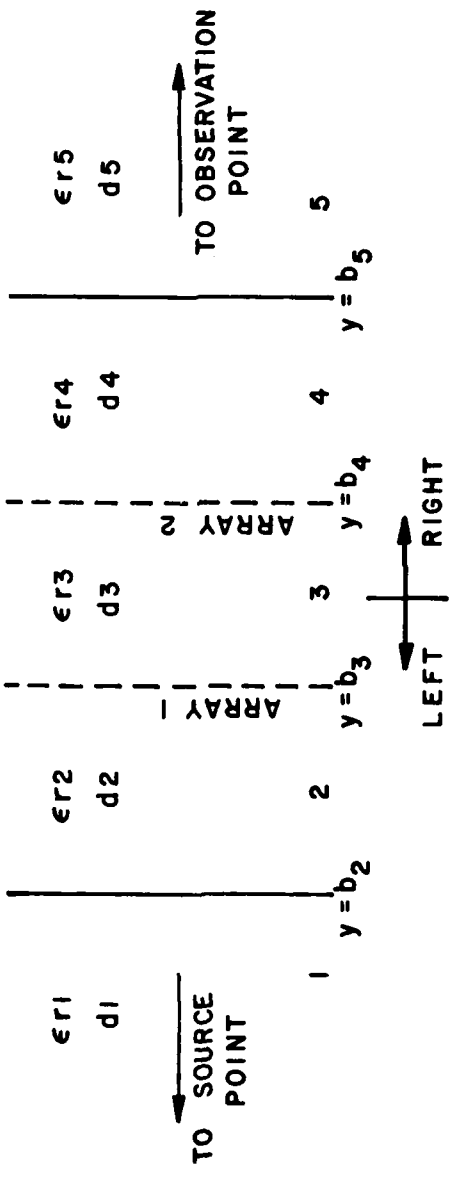


Figure G2. Defining the physical structure.

```

1 C
2 C      WRITTEN BY J.S.ERKST (UNLESS NOTED OTHERWISE)
3 C
4 C      THIS PROGRAM CALCULATES THE TRANSMITTED & FILED THRU STRUCTURE
5 C      OF FIGURE 1. THE SFLR AND SURFACE ADmittANCES ARE ALSO CALCULATED.
6 C
7 C      EXPLANATIONS OF VARIABLES ARE EXPLAINED THROUGHOUT THE PROGRAM
8 C
9 C      INCLUDE SYSTEM SOFTWARE FOR USE IN PRINT ROUTINES
10 C
11 C      INCLUDE FLTKS.H4;AUXLGP.H4;C
12 C      INCLUDE PACK.H;296.Y5
13 C      INCLUDE EISME;296.Y5
14 C      INCLUDE ETRLGR;296.Y5
15 C      INCLUDE EISNSD;296.Y5
16 C      INCLUDE PRIMTR;296.Y5
17 C      LOGICAL LOCAL
18 C      DIMENSION ELEM(2,5),ELEM(2,5),PLF(2),PTU(2),RLAMUA(5),
19 C      *SX(5),SC(5),ALPHA(10),FTA(10),ITMA1(5),ITMA2(3),ITMA3(3)
20 C      COMPLEX YAU1(15),YADM1(16),YADM1R(16)
21 C      COMMON /PR1NT/ IOC
22 C      COMMON /DISPLAY/ WIDTH
23 C      C---COMMON BLOCK
24 C      COMMON RXN,RXNRYKNN,RZKN,BETA,BETR
25 C      COMPLEX RYR(5),CJ,CZERO
26 C      DIMENSION RXR(5),RZRN(5),BETA(5),U(5),UR(5)
27 C      DATA CJ,ZERO/0.0,0.0/,(0.0,0.0)/
28 C      C---- DATA RYR,I/0.0174532925,0.14139265/
29 C      C*** COMPUTE' TIMING & FILE INITIALIZATION ***
30 C
31 C      GETTIME X IS USED TO GET THE TIME OF DAY & THE DATE
32 C      GETUP IS USED TO GET THE CURRENT CPU CLOCK IN 10'S OF SEC
33 C      CALL GETTIME(J1,W1)
34 C      CALL GETUP(J1,W1)
35 C      CALL GETTIME(J1,W1)
36 C      CALL GETUP(J1,W1)

```

```

11 *4=U
      CALL FGETL
36      SFT W, INITIALIZATION--SET DATA FILE
37      READ(5,5007)
38      READ(5,-)JV1
39      READ(5,5007)
40      READ(5,-)ISVY
41      READ(5,5007)
42      READ(5,-)JUC
43      READ(5,5007)
44      READ(5,-)JUC
45      READ(5,-)JUC
46      C     READ IN ELECTRIC PARAMETER AND ALL NO. ANTENNA
47      C     PARAMTERS--SFT DATA FILE
48      READ(5,5006)FPEL
49      READ(5,5006)FRESH
50      READ(5,5006)FINCHP
51      DU 10 I=1,5
52      READ(5,5006)L(I)
53      READ(5,5007)
54      READ(5,-)INANGS
55      READ(5,5007)
56      READ(5,-)ALPHAI(I)+TA(I),I=1,NANGS)
57      DU 15 I=1,5
58      READ(5,5006)TR(L)
59      READ(5,5006)DX
60      READ(5,5006)DZ
61      READ(5,5006)DT,L,IZ
62      READ(5,5006)WT,IP
63      READ(5,5006)WTRK
64      C     ASSUMPTIONS: LEG1 IS ON +Z AXIS, LEG2 AND LEG3 ARE IN
65      C     - Z DIRECTION -X+Y DIRECTION RESPECTIVELY
66      C
67      DU 20 LSLOT=1,2
68      READ(5,5007)
69      RTR(5,-)RLA
70      RLAK=RLA*RLB
71      ELEMX(( SLOT,1)=U,U

```

```

72      ELEM2((LSL01,1)=1.0
73      ELEMX((LSL01,2)=-SIN(RLR/2.0)
74      ELEM2((LSL01,2)=-(COS(RLR/2.0)
75      ELEMX((LSL01,3)=+SLIN((LSL01,2)
76 20    ELEM2((LSL01,3)=ELIN((LSL01,2)
77 5006   FORMAT(AX,F12.6)
78 5007   FORMAT(2X)
79       CALL GETCP(ITP2)
80 C      DETERMINE FREQ
81       NPNT=(FREQ*FREQ)/FINCH**1.2
82       DO 50 L=1,NPNT
83       FM=M-1
84       FREQ=FREQ+FM*FINCH
85 C      CALCULATE THE WAVELENGTH / NM PROPAGATION CONST
86 C      EACH ELECTRIC MEDIA
87       DO 25 I=1,5
88       RLAMDA(I)=30.0/(FREQ*SQRT(EK(I)))
89 25     ET(I)=2.*PI/RLAMDA(I)
90       CALCULATE THE EFFECTIVE LENGTH AND HTD FOR EACH ARRAY
91       APPSEOR((EP(2)+EP(5))/2.0)
92       RLAMDA(1)
93       CALL UFL((KL,WLTH,THK,PLAM,ABKS,UL))
94       RLF(1)=RL+UL
95       RIN(1)=ABKS*BFTA(1)/SIN(TLN(1))
96       ABRS=SINH((LN(3)+LN(4))/2.0)
97       CALL UFL(KL,WLTH,THK,PLAM,ABRS,UL)
98       RLF(2)=RL+UL
99       PTn(2)=ABKS*BFTA(1)/SIN(TLN(1))
100      DETERMINE THE SCATTER ANGLE
101      DO 45 I=1,NALCS
102      ALPHAH=RP*(ALPHAH+ALPHAH*LNX)
103      ETAR=RN*(ETAR*LNX)
104      DO 30 L=1,b
105      COMPONENTS OF INCIDENT PLANE WAVE SIGNIF.

```

```

105      SX(L)=SIN(TAF)*COS(ALPHAK)*COS(TER(J))/SIN(TER(J))
106      S/(L)=SIN(TAF)*SIN(ALPHAK)*SIN(TER(J))/SIN(TER(J))
107      DUMMY1=ALPHA(1)*DX
108      DUMMY2=ALPHA(2)*DX
109      CALL PRINT(FREQUENCIES(Y1+NUMY2))
110      SYMMETRY CONDITION USED
111      C
112      IXY=16
113      IF(IXY>Y*EG.1) IXY=6
114      DO 40 I=AUT+1,IXY
115      C      PERFORM THE PRODUCT SUMMATION TO CALCULATE PRELIMINARY
116      C      CALL Y(UM2*IVN*ELM*PLF*BTU*PLANAS)*SZ
117      C      *DX*DZ*DLT2*RL*ATM1*YADM1*YAMTL*YAPTR
118      C      YADM1(YADM1)=YADM1(YADM1)/(2.0*DZ*D7*576.82)
119      C      YAMTL(YAMTL)=YAMTL(YAMTL)/(2.0*DZ*D7*576.82)
120      C      YAPTR(YAPTR)=YAPTR(YAPTR)/(2.0*DZ*D7*576.82)
121      C      IF(IXY>Y*EG.1) CALL SYNT(YADM1,YAMTL,YAPTR,IY)
122      C      PRINT OUT ADMISSION RESULTS
123      C      CALL PCUT(YADM1,YAMTL,YAPTR,IY)
124      C      CONTINUE
125      C      CALCULATE THE TRANSMITTED FIELD
126      C      CALL CCRK(IVN*ELM*PLF*BTU*PLANAS)
127      A,SX,SZ,DZ,DLT2*RL*YADM1
128      ITM4=ITM4+1
129      40      CONTINUE
130      50      CONTINUE
131      C
132      C*** END OF SUB ***

133      C
134      C      CALL UTUP(ITM3)
135      C      CALL UTUP(ITM3)
136      C      ITM1=(ITM3-ITM1)/100
137      C      ITM4=((ITM3-ITM2)/ITM4)/100
138      C      CALL PRINT(ITM1,ITM2,ITM3,ITM4)
139      C      STOP
140      C      END

```

```

141 C ****
142 C ****
143 C ***SYMMTRY
144 C
145 C THIS SUBROUTINE USES SYMMETRY OF THE STRUCTURE TO REDUCE CALCULATION
146 C TIME. WITHIN SYMMETRIC ARRAY 1 IS THE SAME AS ARRAY 2 IN THE
147 C SAME PHYSICAL SURROUNDING. THE ADmittANCE'S CALCULATED FOR ARRAY 1
148 C ARE THE SAME AS THOSE OF ARRAY 2
149 C
150 C SUBROUTINE SYMMTRY(YADMT,YAUMT,YADMIL,YAUMTR)
151 COMPLEX YADMT(16),YAUMT(16),YADMIL,YAUMTR(16)
152 GOTO (1,1,1,2,2,2,2)*NAUT
153 1 YADMT(NAUT+12)=YAUMT(NAUT)
154 YAUMT(NAUT+12)=YAUMT(NAUT)
155 YAUMTR(NAUT+12)=YAUMTR(NAUT)
156 RETURN
157 2 YAUMT(NAUT+4)=YAUMT(NAUT)
158 RETURN
159 ENP
160 C ****
161 C
162 C ***PKOUT
163 C
164 C THIS SUBROUTINE JUSTS SETS UP THE LAPPING SYSTEM TO PRINT OUT
165 C DATA
166 C
167 C SUBROUTINE PKOUT(NAUT,YAUMT,YADMIL,YAUMTR)
168 COMPLEX YAUMT(16),YADMIL(16),YAUMTR(16)
169 DIMENSION LAB(2),LEFT(2),JKT(2)
170 DATA LB1,LB2,LBS,LBU,LYR,LYS,3H1A1,3H1S1/
171 DATA LH5,LH6,LH7,LRE,3H2A1,3H1A2,3H2S1,3H1S2/
172 DATA LH9,LE10,3H2A2,3H2S2/
173 DATA L11,L12,L13,L14,3HYL,3YRS,3HYLA,3HYRA/
174 C
175 C GOTO(1,2,3,4,5,6,7,8,9,10,11,12,13,14,15,16),NADMT

```

```

17b 1 LAR(1)=LB1
177 LAR(2)=LB4
17b LFT(1)=LB11
179 IKT(1)=LB14
180 IPNNT=*
181 GOTO 1/
LAR(1)=LB1
182 LAR(2)=LB3
183 LFT(1)=LB11
184 IRT(1)=LB12
185 IPNNT=*
186 GOTO 1/
LAR(1)=LB2
187 LAR(2)=LB4
188 LFT(1)=LB13
189 IKT(1)=LB14
190 IPNNT=*
191 GOTO 1/
LAR(1)=LB2
192 LAR(2)=LB3
193 LFT(1)=LB13
194 IKT(1)=LB14
195 IPNNT=*
196 GOTO 1/
LAR(1)=LB2
197 LAR(2)=LB3
198 LFT(1)=LB13
199 IKT(1)=LB14
200 IPNNT=*
201 GOTO 1/
LAR(1)=LB1
202 LAR(2)=LB6
203 LFT(1)=LB1
204 IRT(1)=LB6
205 IPNNT=*
206 GOTO 1/
LAR(1)=LB2
207 LAR(2)=LB6
208 IPNNT=*
209 GOTO 1/
LAR(1)=LB2
210 IPNNT=*

```

211 GOT0 15
212 E
213 LAB(1)=LB2
214 LAB(2)=LB6
IPRNT=6
215 GOT0 18
216 9
LAB(1)=LB1
LAB(2)=LB7
IPRNT=6
217
218
219 GOT0 18
220 10
LAB(1)=LB1
LAB(2)=LB5
IPRNT=6
221 GOT0 18
222
223
224 11
LAB(1)=LB2
LAB(2)=LB7
IPRNT=6
225 GOT0 18
226
227
228 12
LAB(1)=LB2
LAB(2)=LB5
IPRNT=6
229 GOT0 18
230
231
232 13
LAB(1)=LB1
LAB(2)=LB10
LFT(1)=LE11
IKT(1)=LB12
IPRNT=16
233 GOT0 17
234
235
236
237
238 14
LAB(1)=LB1
LAB(2)=LB9
LFT(1)=LE11
IKT(1)=LE12
IPRNT=15
239 GOT0 17
240
241
242
243
244 15
LAB(1)=LB2
LAB(2)=LB10

```

246      LFT(1)=LFT13
247      IRT(1)=L014
248      IPRINT=15
249      GOTO 17
250 16    LAP(1)=L02
251      LAP(2)=L03
252      LFT(1)=L013
253      IKT(1)=L014
254      IPRINT=16
255 17    LFT(2)=LAB(2)
256      IRT(2)=LAB(2)
257      CALL PRINCI(LFT,YADMT(NADM1)*52.0)
258      CALL PRINCI(IRT,YADMTR(NADM1)*52.0)
259      CALL PRINCI(LAR,YADM1(NADM1),IPRNT,n)
260      RETURN
261      END
262      ****
263      C
264      C***YSUM2
265      C
266      C WRITTEN BY C.J.LARSON--MULIFLU BY J.S.E.R.JST
267      C
268      C THIS SUBROUTINE PERFORMS THE DOUBLE SUMMATION IN THE POISSON
269      C SUM FORMULA AND CHECKS FOR CONVERGENCE
270      C
271      C THE VARIABLES ARE READ THRU AND REFINED IN GRAPH FARTS OF THE
272      C PROGRAM
273      C
274      C SUBROUTINE YSUM2(LV,ELEMX,ELEMZ,KLF,STN,RLANA,SX,SSZ
275      C
276      C DIMENSION ELEMX(12,3),ELEMZ(12,3),RLF(12,51),HT(12),RLANA(51)
277      C
278      COMPLEX YADM1(16),YADMTR(16),YADMTR(16)
279      COMPLEX Y,Y1,Y2,Y3,Y4,Y5,Y6,Y7,Y8,Y9
280      COMPLEX YLT,YLT1,YLT2,YLT3,YLT4,YLT5,YLT6,YLT7,YLT8,YLT9

```

```

281      Y1=Y1+YR2*YR3*YR4*YR5*YR6*YR7*YR8*YR9
282      INTEG1=TEST1*TEST2*TEST3*TEST4*TEST5*TEST6*TEST7.
283      TEST8*TEST9*TEST10*TEST11*TEST12
284      C---COMMON BLOCK
285      C
286      COMMON RXKN,KYKN,KZKN,HETA,RL,ER
287      COMPLEX KYKN(5)*CJ,CZERO
288      DIMENSION RXKN(5),KZKN(5),BFTA(5),U(5),FR(5)
289      DATA CJ,CZERO/(0.0,0.0),(0.0,0.0)/
290      C-----C
291      C
292      C
293      C CONVERGENCE NUMBER (COMPARE)
294      C
295      C
296      COMP=0.
297      DU 1 1=1,5
298      N=1-2
299      DO 1 M=1,3
300      K=M+2
301      CALL ALIMIT(IVD,ELEMX,ELEMZ,RLF,BTD,RLAMLA,SY,SZ
302      1*UX*DZ*DELTZ,RL,NADMT,K+N,YAMNT,YAMTR)
303      A=ABS(AIMAG(YADM1("AUMT")))
304      1      COMP=COMP+A
305      LCPA=COMP/1E+3
306      C
307      C      K=N=0. TERM
308      C
309      C
310      K=11
311      N=0
312      CALL ALIMIT(IVD,ELEMX,ELEMZ,RLF,BTD,PLAMDA,SY,SZ
313      1*UX*DZ*DELTZ,RL,NADMT,K+N,YAMNT,YAMTR)
314      Y1=YAMNT
315      YL1=YAMNT(NADMT)
316      YK1=YAMNT(MAT)
317

```

```

516 C SUM ALONG +K AXIS
517 C
518 C
519 C Y2=(0.0.0.)
520 C YL2=(0.0.0.)
521 C YR2=(0.0.0.)
522 C TEST1=1
523 C DO 2 1=1,200
524 K=1
525 KCONP=1
      CALL ADMIT(IVD,ELEMX,ELFMZ,RLF,BTL,PLAN,A,SX,SZ
526 1,UX,DZ,DEL,T2,RL,ADMT,K,N,YADM1,YADM2,YADM3)
527 Y2=Y2+YADM1
528 YL2=YL2+YADM1
529 YR2=YR2+YADM1
530 BB=AB(AIRAG(YADM1))
531 IF(PBS.LT.CMPA) GO TO 10
532 GO TO J1
533 J1
534 10 TEST1=TEST1+1
535 IF(TEST1.EQ.2) GO TO 12
536 GO TO J1
537 J1 TEST1=1
538 2 CONTINUE
539 C SUM ALONG -K AXIS
540 C
541 C
542 J2 Y3=(0.0.0.)
543 YL3=(0.0.0.)
544 YR3=(0.0.0.)
545 TEST2=1
546 DO 3 1=1,200
547 K=-1
548 KCONP=1
      CALL ADMIT(IVD,ELEMX,ELFMZ,RLF,BTL,PLAN,A,SX,SZ
549 1,UX,DZ,DEL,T2,RL,ADMT,K,N,YADM1,YADM2,YADM3)
550

```

```

351      Y3=Y3+YAUMT(NADM1)
352      YL3=YL3+YAUMTL(NADM1)
353      YR3=YR3+YAUMTR(NADM1)
354      C=ABS(YAMAG(YADM1(NADM1)))
355      IF(C.LT.COMPA)GO TO 20
356      GO TO 21
357 20   TEST2=TEST2+1
358      IF(TEST2.EQ.3)GO TO 22
359      GO TO 3
360 21   TEST2=0
361 3    CONTINUE
362 C
363 C    SUM ALONG +N AXIS
364 C
365 22   K=0
366      YL4=(0.0.0.)
367      YR4=(0.0.0.)
368      Y4=(0.0.0.)
369      TEST3=U
370      DO 4 I=1,200
371      N=I
372      NCNP=I
373      CALL AUMIT(LV,DZ,DELTZ,KL,NADM1,KM,YAMMT,YADM1,MTR)
374      Y4=Y4+YAUMT(NADM1)
375      YL4=YL4+YAUMTL(NADM1)
376      YR4=YR4+YAUMTR(NADM1)
377      DAB=ABS(YAMAS(YAUMT(NADM1)))
378      IF(DAB.LT.CMPA)GO TO 30
379      GO TO 31
380 30   TEST3=TEST3+1
381 31   IF(TEST3.EQ.3)GO TO 32
382      GO TO 4
383 32   TEST3=1
384 31   CONTINUE
385 4

```

```

386 C SUM ALONG -R AXIS
387 C
388 C
389 32 Y5=(0.0 0.0)
390 YL5=(0.0 0.0)
391 YR5=(0.0 0.0)
392 TEST4=1
393 DO 5 I=1,200
394 N=-1
395 NCNAME=''
396 CALL ALIMIT(LVDO,ELTMAX,ELTMIN,ELTMIN,ELTMAX,ELTMAX,ELTMIN,ELTMIN)
397 100 DZ=DTLTZ,PL=PLATLT,PA=PAALT,YA=YAALT,YAU=YAULT
398 Y5=Y5+YALT(NANLT)
399 YL5=YLB+YAPLT(NALPLT)
400 YR5=YRB+YAPLT(NALPLT)
401 E=ABS(STAIR5(YAPLT(NALPLT)))
402 IF (IE.LT.COMMA) GO TO 40
403 GO TU 41
404 40 TEST4=TEST4+1
405 IF (TEST4.EC.3) GO TO 42
406 GO TO 5
407 41 TEST4=0
408 5 CONTINUE
409 C
410 C SUM IN FIRST GRID K(+) N(+)
411 C
412 42 Y6=(0.0 0.0)
413 YL6=(0.0 0.0)
414 YR6=(0.0 0.0)
415 TEST5=1
416 TEST6=1
417 DU 6 I=1,200
418 K=1
419 CALL ALIMIT(LVDO,ELTMAX,ELTMIN,ELTMIN,ELTMAX,ELTMAX,ELTMIN,ELTMIN)
420

```

```

421      L0X•U2•DE•L2•RL•SACMT•K•N•YDNT•YAUMTL•YAUMTR)
422      Y0=Y6+YALW•T(NADM1)
423      YLF=YL2+YALW•T(NPWT)
424      YRK=YR6+YALW•TR(NADM1)
425      F=ABS(SA1MAG(YADM1)(VALWT)))
426      IF(I•LT•COMPAG)GO TO 50
427      GO TO 31
428      TEST5=TEST5+1
429      IF( TEST5•E•3 )GO TO 55
430      GO TO 32
431      TEST5=1
432      TEST6=0
433      DO 7 M=2•200
434      K=M
435      CALL AIMIT(LIVP•ELIMZ•RLF•BTU•PLAMRA•SX•SZ
436      •DX•NZ•NEL1•Y•RL•NAUMT•K•N•YADM1•YAUMTL•YAUMTR)
437      Y6=Y6+YADM1
438      YL6=YL6+YADM1
439      YR6=YR6+YADM1
440      G=ABS(SA1MAG(YADM1)(NAUMT)))
441      IF(I•GLT•COMPAG)GO TO 53
442      GO TO 54
443      TEST6=TEST6+1
444      IF( TEST6•E•6 )GO TO 60 6
445      GO TO 7
446      TEST6=
447      CONTINUE
448      CONTINUE
449      C
450      C      SUM IN SEC(6.0 QURE( K(-) E(+))
451      C      Y7=(0•0•0•)
452      C      YL7=(0•0•0•)
453      C      YR7=(0•0•0•)
454      C      TEST7=1

```

```

16 TEST
  L0 6 I=1•200
  K=-1
  N=1
  CALL ALMMIT(LV),ELM,X•ELM,Z•KIF•BTDF•FLMDA•SX•SZ
  1•UX•DZ•DLT2•PL•ALMT•K•YAMT•YAMTL•YAMTR
  Y7=Y7+YAMT(GAMMT)
  YL7=YL7+YAMT(GAMMT)
  YR7=YR7+YAMT(GAMMT)
  H=ABS(YAMT(YAMT(GAMMT)))
  IF(H.LI•COMPAG) GO TO 60
  GOTO 61
  TEST7=TEST7+1
  IF(IES7•3) GO TO 65
  60 TO 62
  TEST7=0
  61
  TEST6=0
  62
  60 9 M=2•200
  K=-M
  CALL ALMMIT(LV),ELM,X•ELM,Z•KIF•BTDF•FLMDA•SX•SZ
  1•UX•DZ•DLT2•PL•ALMT•K•YAMT•YAMTL•YAMTR
  Y7=Y7+YAMT(GAMMT)
  YL7=YL7+YAMT(GAMMT)
  YR7=YR7+YAMT(GAMMT)
  O=ABS(YAMT(YAMT(GAMMT)))
  IF(O.LT•COMPAG) GO TO 55
  60 TO 54
  TEST8=TEST8+1
  IF(IES8•3) GO TO 68
  60 TO 67
  TEST8=0
  64
  CONTINUE
  CONTINUE

```

```

489 C
490 C SUM IN THIRD QUADRANT F(-) F(-)
491 C
492 F5 YB=(0.0.0.)
493 YLB=(0.0.0.)
494 YRB=(0.0.0.)
495 TEST9=0
496 TEST10=0
497 DO 13 I=1,260
498 K=-1
499 N=-I
500 CALL ADUMIT1V0,EL,EX,ELEM2,PLF,BTC,PLA,SA,SZ
501 1,UX,DZ,DLTZ,RL,NAUMT,K,N,YADM1,YADMTR,
502 YB=YB+YADM1(NADM1)
503 YLB=YL3+YADM1(NADM1)
504 YRB=YR6+YADM1(NADM1)
505 P=ABS(CAIMAG(YADM1(NADM1)))
506 IF(P.LT.COMPA)GO 1C 70
507 GO TO 71
508 TEST9=TEST9+1
509 IF(TEST9.EQ.3)GO 10 75
510 GO TO 72
511 71 TEST9=0
512 72 TEST10=0
513 DO 14 I=2,200
514 K=N
515 CALL ADUMIT1V0,EL,EX,ELEM2,PLF,BTC,PLA,SA,SZ
516 1,UX,DZ,DLTZ,RL,NAUMT,K,N,YADM1,YADMTR,
517 YB=YB+YADM1(NADM1)
518 YLB=YLB+YADM1(NADM1)
519 YRB=YR6+YADM1(NADM1)
520 P=ABS(CAIMAG(YADM1(NADM1)))
521 IF(P.LT.COMPA)GO 10 75
522 GO TO 74
523 73 TEST10=TEST10+1

```

```

524 IF (TEST12U.EQ.3) GO TO 13
525 GO TO 4
526 74 TEST16=0
527 14 CONTINUE
528 15 CONTINUE
529 C SUM IN FUNKTION QUAD K(+) K(-)
530 C
531 C
532 75 Y9=(0.,0.)
533 YL9=(0.,0.)
534 YR9=(0.,0.)
535 TEST11=0
536 TEST12=0
537 DO 15 I=1,200
538 K=1
539 N=-1
540 CALL ALUMIT(IVD,ELEM2,ELM2,RIF,ETU,RLA,MRA,SX,SZ
541 1,UX,UZ,DLL,T2,ELNAMT,K,N,YAMT,YAUMT,YALMT,YALMTR)
542 Y9=Y9+YAUMT(INADM1)
543 YL9=YL9+YAUMT(INAUT)
544 YR9=YR9+YALMTR(INAUT)
545 R=ABS(CAIMAG(YAMT(INADM1)))
546 IF(R.LT.COMPA)GO TO 80
547 GO TO 31
548 P0 TEST11=TEST11+1
549 IF (TEST11.EQ.3) GO TO 85
550 GO TO 82
551 61 TEST11=0
552 62 TEST12=0
553 DO 16 M=2,200
554 K=M
555 CALL ALUMIT(IVD,ELEM2,ELM2,FRTD,PLA,MRA,SX,SZ
556 1,UX,UZ,OEL,T2,RL,NADM1,K,N,YAMT,YAUMT,YALMT,YALMTR)
557 Y9=Y9+YAUMT(INADM1)
558 YL9=YL9+YAUMT(INAUT)

```

```

559      YK9=YK8+YAL+T(RINPUT)
560      S=ABS(YAL)*AG(YADM1*(NAUMLY)) )
561      IF (S.LT.0.0001) GO TO 83
562      GO TO 34
563  P5      TEST12=TEST12+1
564      IF (TEST12.EQ.3) GO TO 15
565      GO TO 16
566  F4      TEST12=0
567  I6      CONTINUE
568  I5      CONTINUE
569  C
570  R5      Y=Y1+Y2+Y3+Y4+Y5+Y6+Y7+Y8+Y9
571      YLT=YL1+YL2+YL3+YL4+YL5+YL6+YL7+YL8+YL9
572      YKT=YK1+YK2+YK3+YK4+YK5+YK6+YK7+YK8+YK9
573      YADM1*(NAUMLY)=YL1
574      YADM2*(NAUMLY)=YR1
575      YADM3*(NAUMLY)=YR2
576      RETURN
577      END
578  C *****
579  C *****
580  C ***NAUMLY
581  C THIS SUBROUTINE CALCULATES THE SELF AND MUTUAL ADMITTANCES
582  C
583  C INPUT VARIABLES
584  C RIF(A)=EFFECTIVE LENGTH OF EACH ARRAY
585  C ETG(A)=EFFECTIVE PROPAGATION CONSTANT OF EACH ARRAY A
586  C NAUMLY=OLCIUES WHICH ADMITTANCE IS BEING CALCULATED, THE NUMBER
587  C FOLLOWING THE COMMENTS ON THE ADMITTANCES BELOW IS NAUMLY
588  C OUTPUT VARIABLES
589  C YADM1=TOTAL ADMITTANCE FOR EACH INK. INT
590  C YADM2=ADMITTANCE LOOKING LEFT
591  C YADM3=ADMITTANCE LOOKING RIGHT
592  C
593  C

```

```

594 C THE REAL-TIME VARIABLES ARE EXPLAINING IN THE INDIVIDUAL SUBROUTINES
595 C
596 SUBROUTINE SPLIT(UN,ELMAX,ELFMZ,HLF,ELFMZ,HLMA)
597 1. SY*SZ*DX*(Z*DFLIZ*KL*NAME1*TKA1K1*YAU1)
598 2. YACM1*YAU1*TR
599 COMPLEX FATX(3)*PAT2(3)*SPATX(2,2)*SPATZ(2,2)
600 3. ATAX(2,2)*PAT(2,2)*XFAT*PAT*SCP1(2,2,2)
601 2*ACPA1(2,5,2)*FACT(2,5)*YACM1(16)*DFATC*DPATC*EXPYS*EXPYI
602 COMPLEX YAU1TL(16)*YAU1TR(16)
603 DIMENSION ELMAX(12,3),ELFMZ(2,3),HLAMA(5),SX(5),SZ(5)
604 1.HTU(2)*HLF(2)
605 C---COMMON BLOCK
606 C
607 COMMON RAKR,RYKN,RZKN,PETA,D,EK
608 COMPLEX HYKA(5)*CJ,CZERO
609 DIMENSION RXKN(5)*PZKN(5)*BFTA(5)*U(5)*FR(5)
610 DATA CJ*CZERO/(U,U,1.0)/(0.0,0.0)/
611 C-----
612 CALL DIRECT(IKK1NN*KLAMA*SY*SZ*DZ*(TELZ)
613 C SHIFT UP MEDIA NUMBERS AND SLN1 NUMBERS ACCURNING TO NADM1
614 GOTO (20,26,20,20,25,25,25,25,25,25,31,30,30,30),NAUMT
615 20 MZDL=2
616 MDR=5
617 LS1=1
618 LS2=1
619 GOTO J1,
620 25 MFL=3
621 MDR=3
622 LS1=1
623 LS2=2
624 GOTO J2,
625 30 MFL=3
626 MDR=4
627 LS1=2
628 LS2=2

```

```

629      GOTO 35
630      35      DO 40 LSLOT=LS1+LS2
631      DO 40 ATNS=1,2
632      RETAD=HTU(LSLOT)
633      EFLF=RLF(LSLOT)
634      CALL PATTR(IVN,NTNS,RETAL,PL,EFF,ELEx,ELFz,LSLOT
1•PATX,PATZ)
635
636      C
637      C SPATX(A,B)=X COMPONENT OF SYMMETRIC PATTERN
638      C WHERE A=A(MKAY NUMBER
639      C B=1(TRANSMITTING),2(NON-TRANSMITTING)
640      C SPATZ(A,B)=Z COMPONENT
641      C APATX(A,B)=X COMPONENT OF ASYMMETRIC PATTERN
642      C ADATZ(A,B)=Z COMPONENT
643
644      SPATX(LSLOT,NTNS)=2.0*PATX(1)-PATX(2)
1•PATX(2)
645      SPATZ(LSLOT,NTNS)=2.0*PATZ(1)-PATZ(2)
1-PATZ(2)
646      SPATX(LSLOT,NTNS)=PATX(2)-PATX(3)
647      SPATZ(LSLOT,NTNS)=PATZ(2)-PATZ(3)
648      CONTINUE
649
650      40
651      C
652      C DEFINING VARIABLES FOR THE REST OF THE SUBROUTINE
653
654      C SRPAT(A,B,C)=SYMMETRIC COMPOSITE PATTERN FACTOR
655      C WHERE A=1(UORTHOGONAL),2(PARALLEL)
656      C B=MEDIA NUMBER
657      C C=1(TRANSMITTING),2(NON-TRANSMITTING)
658      C ARPAT(A,B,C)=ASYMMETRIC COMPOSITE PATTERN FACTOR
659      C WHERE A,B,C ARE DEFINED ABOVE
660      C OPATC=ORTHOGONAL PATTERN COMPONENT
661      C PPATC=PARALLEL PATTERN COMPONENT
662
663      C GOTO (1,2,3,4,5,6,7,8,9,10,11,12,1,2,3,4),NNT

```

```

664 C Y(S1,S1) #1 OF Y(S2,S2) #1
665 C
666 C DU 16 EUDIA=MEDL+MEDI
667 I DU 16 TNS=1,2
668 XPATE=SPATX(LS1,NTRIS)
669 ZPATE=SPATZ(LS1,NTRIS)
670 CALL UPCOMP(MEDIA,2)=PATC,PPATC
671 SCPAT(1,MEDIA,NTRIS)=UPATC
672 SUPAT(2,MEDIA,NTRIS)=PPATC
673 16 CALL TYF(NADM1,FACT1)
674
675 C YADM1(NADM1)=EXPYS(MEDL)*(SCPAT(1,MEDL)*SCPAT(1,MEDL))
676 1*FACT1*(MEDL)+SCPAT(2,MEDL)*SCPAT(2,MEDL,2)*FACT2(FEUL)
677 YADM1(NADM1)=
678 EXPYS(MEDL)*(SCPAT(1,ENR,2)*SCPAT(1,ENR,2)*TFAC1(1,FEUR)
679 +SCPAT(2,MEDL)*SCPAT(2,ENR,2)*FACT2(FEUR))
680 YADM1(NADM1)=YADM1(NADM1)+YADM1(NADM1)
681 RETURN
682
683 C Y(S1,A1) #2 OF Y(S2,A2) #1
684 C
685 C DU 22 EUDIA=MEDL+MEDIA
686 2 XPATE=SPATX(LS1,1)
687 ZPATE=SPATZ(LS1,1)
688 CALL UPCOMP(MEDIA,XPAT,ZPAT,UPATC,PPATC)
689 SCPAT(1,MEDIA,1)=UPATC
690 SCPAT(2,MEDIA,1)=PPATC
691 XPATE=SPATX(LS1,2)
692 ZPATE=SPATZ(LS1,2)
693 CALL UPCOMP(MEDIA,XPAT,ZPAT,UPATC,PPATC)
694 ACPAT(1,MEDIA,2)=UPATC
695 ACPAT(2,MEDIA,2)=PPATC
696 ?2 CALL TYF(NADM1,FACT1)
697 YADM1(NADM1)=EXPYS(MEDL)*(SCPAT(1,MEDL)*SCPAT(1,MEDL,2))
698

```

```

699 1*TFACT(1*MFL)+SCPAT(2*MFUL,1)*ACPAT(2*FDL,2)*TFACT(2*MELL)
700 YADMTR(NADM)=
701 < EXPYS(MEDR)*(SCPAT(1*MENK,1)*ACPAT(1*MEDR,2)*TFACT(1*MEDR)
702 >+SCPAT(2*MEDR,1)*ACPAT(2*MEDR,2)*TFACT(2*MELR)
703 YADMTR(YADM)=YADMTR(NADM)+YADMTR(NADM)
704 RETURN
705 C
706 C Y(A1,S1) #5 UK Y(A2,S2) #15
707 C
708 3 DO 32 MFUL=MFL,MEDR
709 XPAT=APATX(LS1,1)
710 ZPAT=AFATZ(LS1,1)
711 CALL OPCUMP(MFDIA*XPAT,ZPAT,PPATC,PPATC)
712 ACPAT(1*MELA,1)=GPATC
713 ACPAT(2*MELA,1)=PPATC
714 XPAT=SPATX(LS1,2)
715 ZPAT=SPATZ(LS1,2)
716 CALL OPCUMP(MMEDIA*XPAT,ZPAT,PPATC,PPATC)
717 SCPAT(1*MEDIA,2)=PPATC
718 32 SCPAT(2*MEDIA,2)=PPATC
719 CALL TYP(NADM),IFAC1)
720 YADMTR(NADM)=FPYS(MFL)*(ARPAT(1*MFUL,1)*SCPAT(1*MEDL,2))
721 *TFACT(1*MFL)+ACPAT(2*MFDL,1)*TFACT(1*MEDL,2)
722 YADMTR(NADM)=
723 < EXPYS(MEDR)*(ACPAT(1*MENK,1)*SCPAT(1*MEDR,2)*TFACT(1*MEDR)
724 >+ACPAT(2*MEDR,1)*SCPAT(2*MEDR,2)*TFACT(1*MELR)
725 YADMTR(YADM)=YADMTR(NADM)+YADMTR(NADM),
726 RETURN
727 C
728 C Y(A1,A2) #4 CP Y(A2,A2) #16
729 C
730 4 DO 42 MFUL=MFL,MEDR
731 42 JTRN=1,2
732 XPAT=APATX(LS1,NIKAS)
733 ZPAT=APATZ(LS1,NIKAS)

```

```

734      CALL UPCUMP(MEDIA,XPAT,ZPAT,OPATC,PPATC)
    ACPAT(1,MEDIA,NFACT)=OPATC
    ACPAT(2,MEDIA,NFACT)=PPATC
    CALL TYP(FAC1,T,FAC1)
    YAMML(YAUMT)=EXP(Y(S1)*MPL)*(ACPAT(1,MELL,1)*ACPAT(1,MELL,2)
    *IFACT(1,MELL)+ACPAT(2,MELL,1)*ACPAT(2,MELL,2))*IFACT(2,MELL))
    YAMMT(YAUMT)=
    < EXP(Y(S1)*ACPAT(1,MENK,1)*ACPAT(1,MENK,2)*TFACT(1,1,MENK)
    *ACPAT(2,MENK,1)*ACPAT(2,MENK,2)*TFACT(2,MENK))
    YAMMT(YAUMT)=YAMML(YAUMT)+YAMTF(YAUMT)
    RETURN

745      C   Y(S1,S2) #5 UK Y(S2,S1) #9
746      C   XPAT=S'AIX(LS1,1)
747      C   ZPAT=S'ATZ(LS1,1)
748      C   CALL UPCUMP(3,XPAT,ZPAT,OPATC,PPATC)
749      C   SCFAT(1,3,1)=OPATC
750      C   SCFAT(1,3,1)=PPATC
751      C   SCPAT(2,2,1)=OPATC
752      C   XPAT=S'ATX(LS2,2)
753      C   ZPAT=S'ATZ(LS2,2)
754      C   CALL UPCUMP(3,XPAT,ZPAT,OPATC,PPATC)
755      C   SCPAT(1,5,2)=OPATC
756      C   SCPAT(2,5,2)=PPATC
757      C   CALL TYP(FAC1,T,FAC1)
758      C   YAMML(YAUMT)=EXP(Y(S1)*(SCPAT(1,3,1)*SCPAT(1,3,2)
759      C   *IFACT(1,3)+SCPAT(2,3,1)*SCPAT(2,3,2)*IFACT(2,3))
760      C   YAMML(YAUMT)=(U,U,U,U)
761      C   YAMMT(YAUMT)=(U,U,U,U)
762      C   RETURN

763      C   Y(S1,A2) #6 UK Y(S2,A1) #1n
764      C   XPAT=S'AIX(LS1,1)
765      C   ZPAT=S'ATZ(LS1,1)

```

```

769    CALL OPCUMP(3,XPAT).ZPAT.CPATC.PPATC)
770    SCPAT(1,3,1)=(CPATC
771    SCPAT(2,3,1)=PPATC
772    XPAT=APATX(LS2,2)
773    ZPAT=APATZ(LS2,2)
774    CALL OPCUMP(3,XPAT.ZPAT.OPATC.PPATC)
775    ACPAT(1,3,2)=OPATC
776    ACPAT(2,3,2)=PPATC
777    CALL TYF(NAUMT.FAC1)
778    YAMMT(NAUMT)=FXPYM(3)*(SCPAT(1,3,1)*ACPAT(1,3,2)
779    1*FACT(1,3)+SCPAT(2,3,1)*ACPAT(2,3,2)*FACT(2,3))
780    YAMTL(NADMT)=(U,U,U,U)
781    YAMTR(NAUT)=(U,U,U,U)
782    RETURN
783 C
784 C   Y(A1,S2) #7 CR Y(A2,S1) #11
785 C
786    XPAT=PAIX(LS1,1)
787    ZPAT=APATZ(LS1,1)
788    CALL OPCUMP(3,XPAT.ZPAT.OPATC.PPATC)
789    ACPAT(1,3,1)=OPATC
790    ACPAT(2,3,1)=PPATC
791    XPAT=SPATX(LS2,2)
792    ZPAT=SPATZ(LS2,2)
793    CALL OPCUMP(3,XPAT.ZPAT.CPATC.PPATC)
794    SCPAT(1,3,2)=OPATC
795    SCPAT(2,3,2)=PPATC
796    CALL TYF(NAUMT.FAC1)
797    YAMMT(NAUMT)=FXPYM(3)*(ACPAT(1,3,1)*SCP, F(1,3,2)
798    1*FACT(1,3)+ACPAT(2,3,1)*SCPAT(2,3,2)*FACT(2,3))
799    YAMTL(NADMT)=(U,U,U,U)
800    YAMTR(NAUT)=(U,U,U,U)
801    RETURN
802 C   Y(A1,A2) #5 OR Y(A2,A1) #12
803 C

```

```

804 C
805 S      XPAT=A, A1)(LS1,1)
806      ZPAT=APAT2(LS1,1)
     CALL OPROMP(3,XPAT,ZPAT,OPATC)
807      ACAT(1,3,1)=OPATC
808      ACAT(2,3,1)=OPATC
809      ACAT(3,3,1)=OPATC
     XPAT=APATX(LS2,2)
810      ZPAT=APAT2(LS2,2)
     CALL OPCUMP(3,XPAT,ZPAT,OPATC)
811      ACAT(j,j,e)=CPATE
812
813      ACAT(2,3,2)=PPATC
     CALL TTF(NAUMT,IFAC1)
814      YAMT(NAUMT)=EXP((5)*(ACPAT(1,3,1)*ACPAT(1,3,2)
815      *IFACT(1,3)+ACPAT(2,3,1)*ACPAT(2,3,2)*IFACT(3,3)))
816      YAMTL(NAUMT)=U,U,U,U
817      YAMTR(NAUMT)=U,U,U,U
818
819
820      RETURN
821      Y(S2,S1) #9
822 C
823 C
824 9      LS1=2
825      LS2=1
826      GOT0 5
827 C      Y(S2,A1) #10
828 C
829 C
830 10      LS1=2
831      LS2=1
832      GOT0 6
833 C      Y(A2,S1) #11
834 C
835 C
836 11      LS1=2
837      LS2=1
838      GOT0 7

```

```

839 C
840 C      Y(AZ,AJ) =12
841 C
842 J2      LS1=2
843      LS2=1
844      GOTO 0
845      E1Y
846 C ****
847 C
848 C ***DIRECT
849 C
850 C THIS SUBROUTINE CALCULATES THE DIRECTIONS THE WAVE IS PROPAGATING
851 C
852 C INPUT VARIABLES
853 C IKK,I,IE,SURFACE INDICES
854 C RCLAMUA=WAVELENGTH IN FACH DIELECTRIC
855 C SX,SZ=X,Z COMPONENTS OF INCIDENT WAVE VECTOR
856 C UX,UZ=X,Z INTERELEMENT SPACING
857 C UFL,TZ=ELMPLACET SPACING IN Z DIRECTION
858 C OUTPUT VARIABLES
859 C RAKK,RKMN,RZN=X,Y,Z COMPONENTS OF PROPAGATING WAVE
860 C
861 C SURROUNING SURFACE (IKK,I,NN,RCLAMUA,SX,SZ,UX,DZ,DELTAZ)
862 C DIMENSION RAKK(5),SX(5),SZ(5)
863 C---COMMON BLOCK
864 C
865 C COMMON RAKK,NYKN,RZKN,BETA,D,ER
866 C COMPLEX RYKN(5)*(JCZLPO
867 C DIMENSION RAKK(5),RZKN(5),BETA(5),U(F),U(L),U(0,0,0,0)/
868 C
869 C-----L=1,L=1.5
870 C
871 RXXN(L)=SY(L)+IKK*RCLAMUA(L)/NX-INN*RI AMIN(L)*NFLTZ/(DX*UZ)
872 FZ(L)=SZ(L)+INN*RCLAMUA(L)/NZ
873 YK=1.0-RXK(L)*RXK(L)-RZK(L)*RZK(L)

```

```

874      IF(YR .LT. 0.0) RYR(L)=COMPLX(0.0,-SQR(-YR))
875      IF(YR .GT. 0.0) RYR(L)=COMPLX(SQR(YR),0.0)
876 1      CONTINUE
877      RETURN
878      END
879      ****
880      ****PATTERN
881      ****
882      THIS SUBROUTINE CALCULATES THE PATTERN FUNCTION ASSUMING
883      EITHER A SINEUSOIDAL OR COSINEUSOIDAL VOLTAGE DISTRIBUTION
884      FOR TRANSMITTING AND RECEIVING TRANSMITTING NODES (SET IVN)
885      ****
886      INPUT VARIABLES
887      IVN=1(SINEUSOIDAL V OSTR IS USED FOR I AND NT MODES)
888      =2(COSINEUSOIDAL V OSTR IS USED FOR I MODE AND COSINEUSOIDAL
889      IS USED FOR NT MODE)
890      BETAD=RELATIVE PROPAGATION CONSTANT
891      RLEG=LEGTH OF EACH LEG
892      EFFLE=EFFCTIVE LENGTH OF EACH LEG
893      ELEMX=ELEM<=X,Z COMPONENTS OF LEG DIRECTIONS
894      LSL01=1(ONE ARRAY),=2(THE OTHER ARRAY)
895      OUTPUT VARIABLS
896      PATX,YIZE,X,Z COMPONENTS OF THE TOTAL PATTERN OF EACH LEG
897      ****
898      ****
899      SUBROUTINE PATTN(IVN,NTNS,BETAL,RLEG,LSELMX
900      LLEMZ,LSLU1,PATX,PATZ)
901      COMPLEX PATX(3),PATZ(3),PAT,CLEMX,CLEMZ,DF
902      1,CPLYK,N,CZKN,DF
903      2,CXP1,CXP2,CXP3,CXF4
904      DIMENSION ELEMX(2,3),ELEMZ(2,3)
905      C=-CUNMND DLCK
906      COMMON KAR,KRYKN,KZKN,META,D,ER
907      COMPLEX KYNL(5),CL,CZEN

```

```

909      DATA CJ,CZ/R0/(0.0,1.0),U(0.0,0.0)/
910      C=--=-
911      CKXKN=CMLPLX(RXKN(1),0.0)
912      CRZKN=CMLPLX(RZKN(1),0.0)
913      IF(CVU,EW,1) GOTO 1
914      GOTO 1,3,MTRN
915
916      C ASSUMES SINUSOIDAL VOLTAGE DISTRIBUTION
917      ELECR=TAUE*EFFL
918      DE NOM=2.0*SIN(REAL)
919      BTME=REAL(1)
920      IF(MTRN<=E&E>BTME)
921      DO 2 L=1,5
922      CELFM=X=CMLPLX(FLEM*(LSLOT*LEG)+0.0)
923      CELFMZ=CMLPLX(FLEMZ*(LSLOT*LEG)+0.0)
924      DP=DOT(CELFM*X,CZK0*CELEMZ,CXKN(1)*CRZKN)
925      PAT=(CXP((J*RL)*(REL-E*TAD-BTME*UP*PL))-
926      1-CXP((J*RL)/(E*TAD-BTME*NP))+
927      2+(CEXP((-CJ*(BELE-BETAD*RL-BTME*UP*RL))-
928      3-CEXP((-CJ*BEELF)/(E*TAD+BTME*UP))-
929      PAT(X(LEG)=CELEMZ*(LSLOT*LEG)*PAT/LFNM
930      PAT(Z(LEG)=CELEMZ*(LSLOT*LEG)*PAI/DENOM
931      RETURN
932      C ASSUMES COSINUSOIDAL VOLTAGE DISTRIBUTION
933      X
934
935      CXP2=CXP((J*BETAD*RL)
936      CXP3=CXP(-CJ*BETAD*RL)
937      RELEC=CON(BETAN*FL)
938      DE NOM=2.0*(1.0-BEFLC)
939      DO 4 L=1,5
940      CELFM=X=CMLPLX(FLEM*(LSLOT*LEG)+0.0)
941      CELFMZ=CMLPLX(FLEMZ*(LSLOT*LEG)+0.0)
942      DP=DOT(CELFM*X,CZK0*CELEMZ,CXKN(1)*CRZKN)
943      CXP1=CXP((CJ*RETA(1)*RL*DP)
944      CXP4=CXP((CJ*MF,0.0) CXP4=(1.0-CXP1)/(BTM(1)*RP)

```

AD-A084 663

OHIO STATE UNIV COLUMBUS ELECTROSCIENCE LAB
BROADBAND METALLIC RADOME. (U)

F/6 9/5

SEP 79 J S ERNST
ESL-784346-11

F33615-76-C-1024

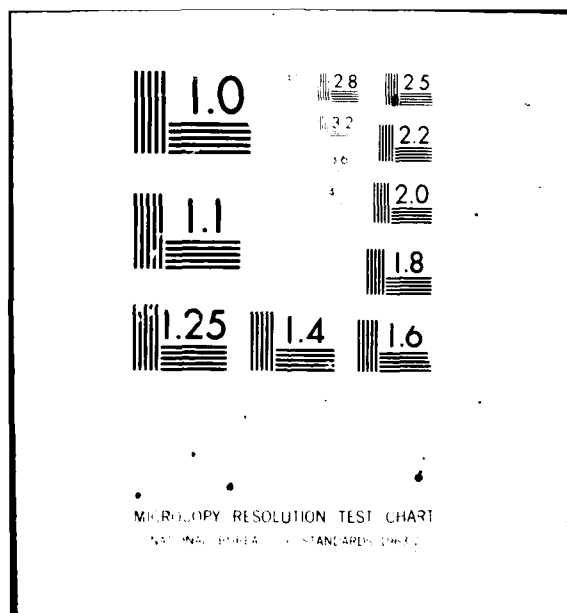
NL

UNCLASSIFIED

AFAL-TR-79-1142

2 OF 2
40
4084963

END
DATE FILMED
6-80
DTIC



```

944      PAT=(1.0-CXP2*CXP1)/(PF.TAU+RFTA(1)*NFI)
945      1+(CXP3+CXP1-1.0)/(RFTA(1)-RFTA(1)*NFI)
946      C   2=2.0*B1*Lc*(CXP4
947      C   COMPONENTS OF THE PATTERN DUE TO EACH LEG
948      C   PATX(LLG)=ELF*Y(LLSLG)*FA1*CJ/UFUN
949      C   PATZ(LLG)=ELF*Z(LLSLG)*PA1*CJ/UFUN
950      RRETURN
951      ENN
952      C
953      C***OPCOMP
954      C
955      C THIS SUBROUTINE CALCULATES THE ORTHOGONAL AND PARALLEL
956      C COMPONENTS OF THE COMPOSITE PATTERN FACTORS
957      C
958      C INPUT VARIABLES
959      C MEDIA=MEDIA IN WHICH PROPAGATION VECTOR IS CALCULATED
960      C CXCOMP,CYCOMP,CZCOMP=VECTOR COMPONENTS OF WHICH ORTHOGONAL
961      C OR PARALLEL COMPONENTS TO PLANE OF INCIDENCE IS DESIRED
962      C OUTPUT VARIABLES
963      C OTOT=ORTHOGONAL RESULT
964      C PTOT=PARALLEL RESULT
965      C
966      C SURROUNING UPCM(MEDIA,CXCMP,CZCUMP,OTOT,PTOT)
967      C COMPLEX CXCOMP,CZCOMP,OTOT,PTOT,CRXKN,CRZKN,OTOT
968      C---COMMON BLOCK
969      C
970      COMMON RXKN,RYKN,RZKN,BETA,D,ER
971      COMPLEX KYKN(5),CJ,CZERO
972      DIMENSION RXKN(5),PZKN(5),EETA(5),U(5),ER(5)
973      DATA CJ,CZERO/(0.0,1.0),(0.0,0.0)/
974      C-----+
975      CRXKN=IMPLX(RXKN(MEDIA),0.0)
976      CRZKN=IMPLX(RZKN(MEDIA),0.0)
977      RXZ=SURT(RXKN(MEDIA)*RYKN(MEDIA)+RZKN(MEDIA))*PTKN(MEDIA))
978      C   CALCULATE THE ORTHOGONAL PATTERN FACTOR

```



```

1014      CALL RFLX(LORTH0,1,RHO)
1015      TFACT((LORTH0,2)=2.0*(1.0+RHO*(2.0))
1016      *EXP2)/(1.0-RHO*(2.0)*EXP2)
1017      TFACT((LORTH0,3)=2.0*(1.0+EXP3)/(1.0-RHO*(3.0))
1018      RETURN
1019      EX1=SET(PI(3.0,2.0))
1020      DO 5 LORTH0=1.2
1021      TFACT((LORTH0,3)=4.0/(1.0+EXP3))
1022      RETURN
1023      EXP4=EXP1(4.0,2.0)
1024      EXP5=EXP1(5.0,2.0)
1025      DO 6 LORTH0=1.2
1026      CALL RFLX(LORTH0,4)
1027      TFACT((LORTH0,4)=2.0*(1.0+RHO*(4.0,
1028      *EXP4)/(1.0-RHO*(4.0)*EXP4)
1029      TFACT((LORTH0,3)=2.0*(1.0+EXP3)/(1.0-RHO*(3.0))
1030      RETURN
1031      END
1032      C***RFLX
1033      C***RFLX
1034      C THIS SUBROUTINE CALCULATES THE REFLECTION COEFFICIENTS FOR
1035      C H-FIELD AT DIELECTRIC INTERFACES
1036      C
1037      C INPUT VARIABLES
1038      C LORTH0=(ORTHOGONAL),2(PARALLEL) RHO IS CALCULATED
1039      C LEMEDIA NUMBER OR ONE OF THE DIELECTRICS RHO IS NEEDED
1040      C
1041      C OUTPUT VARIABLES
1042      C RHO=REFLECTION COEFFICIENT
1043      C
1044      C SUBROUTINE RFLX(LORTH0,1,RHO)
1045      C COMPLEX RHO(15,3)
1046      C ---COMMON BLOCK
1047      C
1048      COMMON RHO1,RHO2,RHO3,RHO4,RHO5,RHO6,RHO7
1049      COMMON RHO8,RHO9,RHO10,RHO11,RHO12,RHO13,RHO14
1050      COMMON RHO15,RHO16,RHO17,RHO18,RHO19,RHO20,RHO21

```

```

1050      DIMENSION RYKN(5),RZKN(5),BFTA(5),U(5),RK(5)
1051      DATA CJ,CZEKO/(0.0,1.0),(0.0,0.0)/
1052      C----- S1=SURT(L-1)
1053      S2=SURT(L)
1054      GTO (1,2),LORTHU
1055      C      ORTHOGONAL H
1056      C      RHO(L-1,L)=(SQ2*RYKN(L-1)-SC1*
1057      1*RYKN(L))/(SQ2*RYKN(L-1)+SC1*RYKN(L))
1058      RHO(L,L-1)=RHO(L-1,L)
1059      RETURN
1060
1061      C      PARALLEL H
1062      2      RHO(L-1,L)=(SQ2*RYKN(L)-SC1*
1063      1*RYKN(L-1))/(SQ2*RYKN(L)+SC1*RYKN(L-1))
1064      RHO(L,L-1)=RHO(L-1,L)
1065      RETURN
1066      END
1067      ****
1068      C***FXPY
1069      C***FXPY
1070      C
1071      C      THIS FUNCTION SUBROUTINE CALCULATES THE NEEDED EXPONENTIAL
1072      C      FOR SELF ADMITTANCE CALCULATIONS
1073      C
1074      C      INPUT VARIABLES
1075      C      MEDIA=DETERMINES IN WHICH DIELECTRIC CALCULATIONS ARE MADE
1076      C      OUTPUT VARIABLES
1077      C      EXPY=COMPLEX EXPONENTIAL ADMITTANCE SELF
1078      C
1079      C      COMPLEX FUNCTION EXPY(MFUN),
1080      C      COMPLEX ARGUM.PHASE
1081      C      COMMON/EXPY/WITH
1082      C      ---COMMON BLOCK
1083      C
1084      C

```

```

1085      COMMON PXYK,RYK,NHZN,HTA,D,ER
1086      COMPLEX RYK(5),D,CZT(5)
1087      DIMENSION PXYK(5),HZN(5),HTA(5),U(5),V(5)
1088      DATA C,CZT/0.0,1.0,0.0,0.0,1/
1089      -----
1090      ARGUM=REAL(MEDIA)*IMAG(ARGM)/C*RYK(NMEN)
1091      C   THE FOLLOWING TWO STATEMENTS TERMINATE ANY ERROR MESSAGES
1092      C   WHEN :XFONENTIALS EXCEED CERTAIN LIMITS--INC ACTUAL ERROR
1093      IF (AIMAG(ARGM).LT.-50.0) PHASE=CMLX(0.0,0.0)
1094      IF (AIMAG(ARGM).GT.-50.0) PHASE=CMLX(0.0,0.0)
1095      IF (REAL(RYK(NMEN)).NE.0.0) PHASE=CMPLX(1.0,0.0)
1096      RAPYS=SQRT(ER(MEDIA))*PHASE*CMPLX(1.0,0.0)
1097      RETURN
1098      END
1099      ****
1100      C ***EXPM
1101      C
1102      C THIS FUNCTION SUBROUTINE CALCULATES THE NEEDED EXPONENTIAL
1103      C FOR MUTUAL ADMITTANCE CALCULATIONS
1104      C
1105      C INPUT VARIABLES
1106      C   MFIDIA=DETERMINES IN WHICH DIELECTRIC CALCULATIONS ARE MADE
1107      C
1108      C OUTPUT VARIABLES
1109      C   FXPY=COMPLEX EXPONENTIAL ADMITTANCE MATRICES
1110      C
1111      C COMPLEX FUNCTION EXPYM(MEN)
1112      C   COMPLEX EXPY
1113      C---COMPLEX BLOCK
1114      C
1115      COMMON RXK,RYK,NHZN,HTA,D,ER
1116      COMPLEX RYK(5),D,CZT(5)
1117      DIMENSION PXYK(5),HZN(5),HTA(5),U(5),V(5)
1118      DATA C,CZT/0.0,1.0,0.0,0.0,1/
1119      -----

```

```

1120      EXPMGNT(ER(MEDIA))*EXP((MFDA,1.0)/RYKN(MFDA))
1121      RETURN
1122      END
1123      ****
1124      ****
1125      ****FAPT
1126      ****
1127      THIS FUNCTION SUBROUTINE CALCULATES A FREQUENTLY USED
1128      COMPLEX EXPONENTIAL
1129      C
1130      INPUT VARIABLES
1131      R'VUL'ERAL MULTIPLIER VALUE DEPENDS ON PHYSICAL SITUATION
1132      MEDIA=TERM'S IN WHICH ELECTRIC CALCULATIONS ARE MADE
1133      OUTPUT VARIABLES
1134      EXPTE ORPLEX EXPONENTIAL
1135      COMPLEX FUNCTION EXP((MEDIA*RMULT)
1136      COMPLEX ARGUM
1137      COMPLEX ARGUM
1138      C--COMMON BLOCK
1139      C--COMMON: BLOCK
1140      COMMON RXKN,RYKN,RZKN,BETA,D,ER
1141      COMPLEX RYKN(5),CJ,CZERO
1142      DIMENSION RXKN(5),RZKN(5),BETA(5),D(5),FR(5)
1143      DATA CJ,CZERO/(0.0,1.0),(0.0,0.0)/
1144      C----*
1145      ARGUM=RMULT*BETA(MEDIA)*D(MEDIA)*RYKN(MFDA)
1146      SEE COMMENT IN PREVIOUS SUBROUTINE EXPYS
1147      IF(CAIMAG(ARGUM)<1.0-50.0)EXPTE=CEXP(-CJ*PRGUN)
1148      IF(CAIMAG(ARGUM)>LE-50.0)EXPTE=CMPLX(0.0,0.0)
1149      RETURN
1150
1151      END
1152      ****
1153      C
1154      C**CURRENT
1155      C

```

```

1156 C THIS SUBROUTINE CALCULATES THE INCIDENT AND TRANSMITTED H FIELD
1157 C
1158 C
1159 C
1160 C
1161 C* SY*SZ*PX*LZ*PFL*1*KL*YAMDA
1162 C* PFL,L,PATX(3),PATY(3),PATZ(3),SPATX(2),SPATY(2),SPATZ(2)
1163 C* APATX(2,2),APATY(2,2),APATZ(2,2),SPATX(2,5,2)
1164 C* ACATX(2,5,2),TFACT(2,5),YAM(16),OPATC,OPATC,EXPF
1165 C* FACTUR,CSJ(2),CA1(2),VS2(2),VA2(2),(CH,CHP,PHO,PHP
1166 C* DIFENS(1,1),MX(2,3),ELEM(2,3),PLAM(5),SY(5),SZ(5)
1167 C* BT(2),BLF(2)
1168 C---COMMON BLOCK
1169 C
1170 COMMON RXN,RKRN,RZRN,PETA,E,ER
1171 COMPLEX RYR,(5),CJ,CZRC
1172 DIMENSION RXN(5),RZRN(5),BETA(5),U(5),ER(5)
1173 DATA CJ,CZRC/(0.0,1.0)/(0.0,0.0)/
1174 C---- CALL DIRECT(C,0,0,0,PLAMA,SY,S7,DX,DZ,ELTZ)
1175 DO 1 LSLOT=1,2
1176 1 THE FOLLOWING STATEMENT JUST WORKS, NO PHYSICAL MEANING
1177 C
1178 NTRNSLSELCT
1179 RETADENT(LSLOT)
1180 EFLRFL(LSLOT)
1181 CALL PATRK(JVD,NTRNS,SHETA),RLEFFL,ELEN,X,ELFMZ,LSLOT
1182 1-PATX,PATZ)
1183 SPATX(LSLOT,NTRNS)=2.0*PATX(1)-PATX(2)
1184 1-PATX(3)
1185 SPATZ(LSLOT,NTRNS)=2.0*PATZ(1)-PATZ(2)
1186 1-PATZ(3)
1187 APATX(LSLOT,NTRNS)=PATX(2)-PATX(3)
1188 1 APATZ(LSLOT,NTRNS)=PATZ(2)-PATZ(3)
1189 XRATE=SPATX(1,1)
1190 ZRATE=SPATZ(1,1)

```

```

1191 CALL UPCURIP(1,XPAT,ZPAT,OPATC,PPATC)
1192 SCPAT(1,1,1)=CPATC
1193 SCPAT(2,1,1)=PPATC
1194 XPAT=APAT(1,1)
1195 ZPAT=APATZ(1,1)
1196 CALL OPCUMP(1,XPAT,ZPAT,OPATC,PPATC)
1197 ACPAT(1,1,1)=OPATC
1198 ACPAT(2,1,1)=PPATC
1199 DO 2 LURTHO=1,2
1200 CALL TIF(LURTHO,IFACT)
1201 C CS1(A)=SYMMETRIC CURRENT OF ARRAY 1
1202 C CA1(A)=ASYMMETRIC CURRENT OF ARRAY 2
1203 C WHERE A=1(ORTHOGENAL)*2(PARALLEL)
1204 CS1(LOPTHU)=SCPAT(LURTHO,1,1)*IFACT(LURTHU,2)*FXFT(2,1,0)
1205 1*EXPT(1,1,0)
1206 2 CA1(LOPTHU)=ACPAT(LURTHO,1,1)*IFACT(LURTHU,2)*FXPT(2,1,0)
1207 1*EXPT(1,1,0)
1208 CALL VOLT(YAUMT,US1,CA1,V$2,VAC)
1209 XPAT=APAT(2,2)
1210 ZPAT=SPAT(2,2)
1211 CALL OPCUMP(5,XPAT,ZPAT,OPATC,PPATC)
1212 SCPAT(1,5,2)=OPATC
1213 SCPAT(2,5,2)=PPATC
1214 XPATEPAT(2,2)
1215 ZPAT=APATZ(2,2)
1216 CALL OPCUMP(5,XPAT,ZPAT,OPATC,PPATC)
1217 ACPAT(1,5,2)=OPATC
1218 ACPAT(2,5,2)=PPATC
1219 FACTOR=EXPT(4,1,0)*EXPT(5,1,0)*SQRT(EN(1))/1(RYKN(5)*2.0*DX*UX*576.82)
1220 OH0=ORTHOGENAL INCIDENT H FIELD ORTHOGONAL TRANSMITTED
1221 OH0=" " " PARALLEL "
1222 OH0=" " " ORTHOGONAL "
1223 OH0= PARALLEL " " " PARALLEL "
1224 OH0=" " " " PARALLEL "
1225 OH0=(V$2(1)*SCPA1(1,5,2)+VA2(1)*ACPAT(1,5,2))
1226 1*TFACT(1,4)*FACTOH

```

```

1227      CHP=(V<2*(1)*SCPAT(2,3,2)+VA2(1)*ALPHAT(2,3,2))
1228      1*TFACT(2,4)*FACTOR
1229      PH0=(V<2*(2)*SCPAT(1,3,2)+VK2(2)*ACPAT(1,5,2))
1230      1*TFACT(1,4)*FACTOR
1231      PHF=(V<2*(2)*SCPAT(2,3,2)+VK2(2)*ACPAT(2,5,2))
1232      1*TFACT(2,4)*FACTOR
1233      CALL PINTC(6HCHU.....0H0.1*1)
1234      CALL PINTC(6H0H0.....0HP.1*1)
1235      CALL PINTC(6HPH0.....PH0.1*1)
1236      CALL PINTC(6HPHF.....PHP.1*1)
1237      RETURN
1238      END
1239      ****
1240      C
1241      C***VULT
1242      C
1243      C THIS SUBROUTINE SETS UP THE MATRICES FOR CALCULATING THE
1244      C VOLTAGES ON SLOT ARRAY NUMBER 2
1245      C
1246      C INPUT VARIABLES
1247      C YADMT=THE ADMITTANCES
1248      C CS1=SEE SUBROUTINE CURNT
1249      C OUTPUT VARIABLES
1250      C VS2(A)=SYMMETRIC VOLTAGE OF ARRAY 2
1251      C VA2(A)=ASYMMETRIC VOLTAGE OF ARRAY 2
1252      C WHERE A=1(ORTHOGONAL),2(PARALLEL)
1253      C
1254      C SUBROUTINE VULT(YADM1,CS1,CA1,VS2,VA2)
1255      C COMPLEX YADM(16),CS1(2),CA1(2),VS2(2),VA2(2),7(4,4)
1256      C DET,UTL
1257      DO 1 I=1,5
1258      Z(1,1)=YADM(1)
1259      Z(1,2)=YADM(2)
1260      Z(2,1)=YADM(3)
1261      Z(2,2)=YADM(4)

```

```

1262      Z(3,1)=YAUMT(9)
1263      Z(3,2)=YACFT(10)
1264      Z(4,1)=YAUMT(11)
1265      Z(4,2)=YAUMT(12)
1266      GOTO (2*3*4,4)*1
1267      2
1268      Z(1,3)=YAUMT(5)
1269      Z(1,4)=YADMT(6)
1270      Z(2,5)=YADMT(7)
1271      Z(2,4)=YALMT(6)
1272      Z(3,5)=YAUMT(13)
1273      Z(3,4)=YAUMT(14)
1274      Z(4,3)=YAUMT(15)
1275      Z(4,4)=YAUMT(16)
1276      CALL UETR(2,DET)
1277      DET=DET
1278      GOTO 1
1279      LORTHU=I-1
1280      Z(1,3)=CS1(LORTHU)
1281      Z(1,4)=YAUMT(6)
1282      Z(2,3)=CA1(LORTHU)
1283      Z(2,4)=YAUMT(8)
1284      Z(3,5)=CMFLX(0,0,0,0)
1285      Z(3,4)=YADMT(14)
1286      Z(4,3)=CMPLX(0,0,0,0)
1287      Z(4,4)=YAUMT(16)
1288      CALL UETR(2,DET)
1289      VS2(LORTHU)=DET/DET
1290      GOTO 1
1291      LORTHU=I-3
1292      Z(1,3)=YAUMT(5)
1293      Z(1,4)=CS1(LORTHU)
1294      Z(2,5)=YAUMT(7)
1295      Z(2,4)=CA1(LORTHU)
1296      Z(5,3)=YADMT(13)
1297      Z(3,4)=CMFLX(0,0,0,0)
1298      Z(4,5)=YAUMT(15)

```

```

1298      Z(4,4)=C*PL*(0.0,U,U,U)
1299      CALL D*TRN(2,RT)
1300      VA2(ILUTHO)=LT/UL19
1301      CURTINP
1302      RETURN
1303      END
1304      ****
1305
1306      ****TIF
1307
1308      THIS SUBROUTINE CALCULATES THE NORMALIZED TRANSFORMATION FUNCTION
1309      NEEDED IN CALCULATING THE INCIDENT FIELD AND TRANSMITTED FIELD
1310
1311      SELF SUBROUTINE TIF FOR VARIABLE LISTING
1312
1313      SUBROUTINE TIF(LURTHO,TFACT)
1314      COMPLEX TFACT(2,5),RHO(5,5),EXPT
1315      C--COMMON BLOCK
1316
1317      COMMON RXKN,RYKN,RZKN,RETA,D,ER
1318      COMPLEX KYKN(5),(J,CGERO
1319      DIMENSION RXKN(5),RZKN(5),RETA(5),U(5),FR(5)
1320      DATA CJ,CGERO/(0.0,1.0),(0.0,0.0)/
1321      C----- CALL KFLX(LURTHO,2)
1322      TFACT(LURTHO,2)=2.0*(1.0-KH0(2,1))
1323      1/(1.0-KH0(2,1))*EXPT(2,2,0)
1324      CALL KFLX(LURTHO,5,KH0)
1325      TFACT(LURTHO,4)=2.0*(1.0-KH0(4,5))
1326      1/(1.0-KH0(4,5))*EXPT(4,2,0)
1327      RETURN
1328
1329
1330      ****
1331
1332      C**DETER
1333

```

```

1334 C WRITTEN JACK RICHMOND--MODIFIED BY JOSEPH RNST
1335 C
1336 C THIS SUBROUTINE CALCULATES THE DETERMINATE OF THE ADMITTANCE
1337 C MATRIX
1338 C
1339 C INPUT VARIABLE
1340 C Z=YADT=SELF AND MUTUAL ADMITTANCES
1341 C OUTPUT VARIABLE
1342 C DET=DETERMIMATE
1343 C
1344 C SUBROUTINE DETERM(Z,DET)
1345 COMPLEX Z(4,4)*B16Z*MOLD.LET
1346 DIMENSION L(4),M(4)
1347 N=4
1348 DET=(1.0,0.0)
1349 DO 60 K=1,N
1350 L(K)=K
1351 M(K)=K
1352 BIGZ=Z(K,K)
1353 DO 20 J=K,N
1354 CO 20 I=K,N
1355 10 IF(CABS(BIGZ)-CABS(Z(I,J)))15,19,19
1356 15 BIGZ=Z(I,J)
1357 L(K)=I
1358 M(K)=J
1359 19 CONTINUE
1360 20 CONTINUE
1361 J=L(K)
1362 1F 1=J-K)35,45,25
1363 25 CONTINUE
1364 26 CONTINUE
1365 27 CONTINUE
1366 28 CONTINUE
1367 30 Z(J,I)=HOLD
1368 35 I=M(K)

```

```

1369      IF(I=K) 45,45,36
1370      CONTINUE
1371      DO 40 J=1,N
1372      H(U)=Z(J,K)
1373      Z(J,K)=Z(J,I)
1374      40   Z(J,I)=H(U)
1375      CONTINUE
1376      DO 55 I=1,N
1377      IF(I-K)50,50,50
1378      50   Z((I,K)=Z((I,J)/(I-P1(Z))
1379      CONTINUE
1380      DO 65 I=1,N
1381      DO 65 J=1,N
1382      IF(I-K)60,64,60
1383      IF(J-K)62,64,62
1384      62   Z(I,J)=Z(I,K)*Z(K,J)+Z(I,J)
1385      CONTINUE
1386      65   CONTINUE
1387      DO 75 J=1,N
1388      IF(J-K)70,75,70
1389      70   Z(K,J)=Z(K,J)/RIGZ
1390      75   CONTINUE
1391      DET=DET*B16Z
1392      Z(K,K)=1./B16Z
1393      P0   CONTINUE
1394      RETURN
1395      END
1396      ****

```

```

1 C PRINT SUBROUTINES FOR 2909M V:04
2 C J.F.SYNTHIC NOV.6.78
4 C
5 C*****S
6 C
7 C SURROUNTING PRINTK(LAB,X,IVAR,IUB)
8 C PRINT REAL X; VALUE,(OPTION,OB)
9 C
10 C IN LAB :A 6 CHARACTER HOLLOW IDENTIFIER
11 C IN X :THE VARIABLE TO BE PRINTED
12 C IN IVAR :THE BINARY CODE OF THIS VARIABLE
13 C IN IUB :IF IVAR < 0, A BLANK LINE IS PRINTED FIRST
14 C   :IF IVAR > 0, NO BLANK LINE IS PRINTED
15 C   :IF IVAR = 0, MAGNITUDE IS ALSO PRINTED IN OB
16 C IN IUB :IS THE I/U CODE, BINARY SUM OF DESIRED OUTPUTS
17 C COM IUC
18 C
19 DIMENSION LAB(2),
20 COMMON /PRINT/, IUC
21 C
22 IF((IAHS(IVAR).AND.100).EQ.0) RETURN
23 IF(IVAH.LT.0) WRITE(6,10)
24 10 FORMAT(*,*)
25 IF((I0B+NL+1) GTR 120
26 B=-100.0D
27 IF(X.GT.0.0) B=20.0* ALOG10(X)
28 WRITE(6,40) LAB,X,B
29 40 FORMAT(1X,A3,=(1X,1F6.3,4),2X,0PF0.4)
30 RETURN
31 120 WRITE(*,40) LAB,X
32 RETURN
33 END
34 C*****S
35 C*****S

```

```

36 C
37 C SUBROUTINE PRINTC(LAB,X,IVAR,IUR)
38 C
39 C PRINT COMPLEX X; REAL, IMAGINARY, MAGNITUDE, PHASE(NEG), MAG, DBJ
40 C
41 C
42 C COMPLEX X
43 C DIMENSION LNH(2)
44 C COMMON /PRINT/ IUC
45 C
46 C IN LAP :A 6 CHARACTER HOLLERITH IDENTIFIER
47 C IN X :THE VARIABLE TO BE PRINTED
48 C IN IVAR :THE BINARY CODE OF THIS VARIABLE
49 C          :IF IVAR < 0, A BLANK LINE IS PRINTED FIRST
50 C          :IF IVAR > 0, NO BLANK LINE IS PRINTED
51 C IN IUR :IF IUR=1, MAGNITUDE IS ALSO PRINTED IN DB
52 C COM IOC :IS THE I/O CODE. A IRARY SUM OF DESIRED OUTPUTS
53 C
54 IF((IVAR).NE.0) RETURN
55 IF(IVAR.LT.0) WRITE(6,10)
56 10 FORMAT(1*0)
57 A$CABS(X)
58 P=57.295779*ATAN2(AIMAG(X),RREAL(X))
59 IF(10b.NE.1) GOTO 120
60 B=-100.0U
61 IF(A.GT.0.0) R=20.0*A LOG10(A)
62 WRITE(b,30) LAB,X,A,P
63 30 FORMAT(2A3=3(ix,1P6.4),1Y,0PF7.2,1X,0PF8.0)
64 RETURN
65 120 WRITE(6,30) LAB,X,A,P
66 RETURN
67 END
68 C
69 C
70 C

```

```

71      SUBROUTINE PRINT(LAB,II,X,IVAR,IDE)
72      C PRINT COMPLEX *X* WITH SINGLE INDEX (SEE 'PRINTC')
73      C
74      C IN LAB : A 6 CHARACTER HOLLERTH IDENTIFIER
75      C          : THE LAST TWO CHARACTERS ARE REPLACED
76      C IN II : INDEX OF VARIABLE NAME
77      C
78      C
79      COMPLEX X
80      DIMENSION LAB(2)
81      C
82      LAB(2)=LAB(2)*AND(.77600000
83      LAB(2)=LAB(2)+(.54)*256+(.60+II)
84      CALL PRINTC(LAB,X,IVAR,IDE)
85      RETURN
86      END
87      C
88      C
89      C
90      C
91      C
92      C PRINT COMPLEX *X* WITH DOUBLE INDICES (SEE 'PRINTC')
93      C
94      C IN LAB3 : A 3 CHAPACIER HOLLERTH IDENTIFIER
95      C IN II,II2 : ARE THE INDICES OF THE VARIABLE
96      C
97      COMPLEX X
98      DIMENSION LAB(2)
99      C
100     LAB(1)=LAB3
101     LAB(2)=(.60+II)*65536+(.54)*256+(.60+II2)
102     CALL PRINTC(LAB,X,IVAR,IDE)
103     RETURN
104     END

```

```

105 C
106 C*****  

107 C
108 C      SUBROUTINE PRINTL  

109 C
110 C      INITIALIZATION  

111 C
112 C      DIMENSION IRUF(24),IFILE(2),IUSER(2)
113 C      LOGICAL LOGIC
114 C      DATA IENU/3H EN/
115 C*** ASSIGN NAMES TO INPUT(5) & OUTPUT(6) FILES ***
116 C
117 C
118 100  WRITE(6,10)
119 10  FORMAT('INPUT')
120  CALL RUFLN(IFILE,IUSER)
121  CALL ASSIGN(IFILE,IUSER,5,$100)
122 110  WRITE(6,11)
123 11  FORMAT('OUTPUT')
124  CALL RUFLN(IFILE,IUSER)
125  CALL AONWOL(IFILE,IUSER,6,$110)
126 C
127 C*** DECISION ON BACKGROUND PROCESSING. PROGRESS(4) FILE ***
128 C
129 12  WRITE(6,12)
130 12  FORMAT('BACKGROUND (T OR F) ?')
131  READ(6,--) LOGIC
132  IF(.NOT.LOGIC) GOTO 140
133 120  WRITE(6,13)
134 13  FORMAT('PROGRESS?')
135  CALL RUFLN(IFILE,IUSER)
136  CALL ASSIGN(IFILE,IUSER,4,$130)
137  CLOSE 4
138  CALL DEASSN
139 140  CONTINUE

```

```

140 C*** UELFTE THE TEMPORARY FILE CREATED BY THE COMPUTER ***
141 C
142 C
143 C CALL LLDELL(3)
144 C
145 C*** TRANSFER THE INPUT FILE TO THE OUTPUT FILE ***
146 C
147 150 READ(5,30) (IBUF(I),I=1,24)
148 30  FORMAT(24A3)
149      WRITE(6,40) (IBUF(I),I=1,24)
150 40  FORMAT(1H *24A3)
151      IF (IBUF(2).NE.TEND) GOTO 150
152 C
153 C*** PRINT THE OUTPUT HEADER ***
154 C
155 C CALL PRINTH
156 C
157 C CLOSE 5
158      RETURN
159      END
160 C
161 C*****S
162 C SURROUNING PRINTH
163
164 C
165 C PRINT AN OUTPUT HEADER
166 C
167 WRITE(6,30)
168 90  FORMAT('COMPLEX VALUES: REAL, IMAGINARY, MAGNITUDE, '
169      & 'PHASE (DEG), [MAG*(1H)]'
170      & '/ FREQUENCY, ALPHAEITA(neg), AMITTANCE(MHOS)')
171      RETURN
172      END
173 C*****S
174 C*****S
175 C

```



```

1 C WRITTEN BY C.J.LARSON--MODIFIED BY J.F.SLOSSIC
2 C GENERAL SUBROUTINES NEEDED FOR PROGRAM
3 C
4 C*****S
5 C
6 C FUNCTION DOT(AX,AY,AZ,RX,EY,PZ)
7 C COMPUTE THE DOT PRODUCT OF TWO COMPLEX VECTORS
8 C IN AX,AY,AZ : X,Y,Z COMPONENTS OF THE A VECTOR
9 C IN RX,EY,EZ : X,Y,Z COMPONENTS OF THE P VECTOR
10 C
11 C
12 COMPLEX AX,AY,AC,BY,BZ,BZ,DOT
13 DOT=AX*BX+AY*BY+AZ*BZ
14
15 RETURN
16 C
17 C*****S
18 C
19 C SUBROUTINE DELLHL(W,T,RLAMDA,SRER,DL)
20 C
21 C CALCULATION OF AN INCREMENTAL LENGTH TO BE ADDED TO
22 C A SLOP OR FLAT WIREF DIPOLE DUE TO END EFFECTS.
23 C SEE DISSERTATION BY R. MUNK, APPENDIX A
24 C WHAT: FQ(A-19), XHAT: E,(A-33), RL: EG(A-23) & E,(A-30)
25 C
26 C ALL OF THE DIMENSIONS HAVE THE SAME UNITS. EG. CM
27 C IN HL : HALF-LENGTH
28 C IN W,T : WIDTH & THICKNESS OF SLOT OR LIPSE
29 C IN RLAMDA : FREE SPACE WAVELENGTH
30 C IN SRER : SQUARE ROOT OF EFFECTIVE DIELECTRIC CONSTANT
31 C OUT DL : DELTA L2 TO BE ADDED TO HALF-LENGTH
32 C
33 DATA PI,R12 /3.14159265, 1.57079635/
34 B=2.0*PI/RLAMDA
35 C

```

```

56 C*** CALCULATE ELECTRICAL LENGTHS ***
57 C
58 EL=ABS(HL)*SREF
59 E=w*SREF
60 ET=T*SREF
61 RL=H*EL
62 PL2=2.0*BL
63 PL4=4.0*BL
64 C
65 CALL SICI(SHL,CIHL,HL)
66 SIPL=SI2BL+PI2
67 CALL SICI(SI2BL,CI2BL,PL2)
68 SI2BL=SI2BL+PI2
69 CALL SICI(SI4BL,CI4BL,PL4)
70 SI4BL=SI4BL+PI2
71 C
72 KHAT=120.0*(ALOG(HLAMDA/(PL*FW))+CIPL+0.769357926)
73 IF(2.0+EL/EW.LT.10.0)KHAT=KHAT-41.588888888888888
74 C
75 XHAT=60.0*SI2BL+30.0*(2.0*SI2BL-SI4BL)*COS(PI2)+30.0*(CIPL-
76 # +2.0*CIPL-2.0*CI2BL-ALOG(HL4))+2.19537305)*SIIN(BL2)
77 C
78 EUL=XHAT/(B*KHAT)+1.8E-3*EL*KHAT/ALOC(1.5*EV/ET)
79 C
80 OL=EDL/SREF
81 C
82 RETURN
83 END
84 C
85 C*****S
86 C
87 SUBROUTINE SICI(SI,CI,X)
88 C COMPUTATION OF SINF & COSINE INTEGRALS
89 C
90 C

```

```

71 C=IN X : INGURENT
72 C=OUT SI : VALUE OF SINE INTEGRAL
73 C=OUT CI : VALUE OF COSINE INTEGRAL
74 C
75 Z=ADS(1)
76 IF(Z<=4.0) 100,100,400
77 100 Y=(4.0-Z)*(4.0+Z)
78 SI=-1.370797E0
79 IF(Z) 300,200,300
80 200 C1=-1.0E58
81 RETURN
82 300 SI=X*((((1.753141F-5*Y+1.5E8968E-7)*Y+1.374168E-5)*Y
83 +4.939689E-4)*Y+1.5E4682F-2)*Y+4.395509E-1+SI/X)
84 C1=((5.772156E-1+AL06(21))/Z-7*((((1.0E6045E-10*Y
85 +1.5E496E-8)*Y+1.725752F-6)*Y+1.165525E-4)*Y+4.990920E-3)*Y
86 +4.515306E-3)*Z
87 RETURN
88 400 SI=SIN(Z)
89 Y=COS(Z)
90 Z=4.0/Z
91 U=(((((4.046U69E-3*Z-2.279143E-2)*Z+5.515070E-2)*Z
92 +7.261e42E-2)*Z+4.987716E-2)*Z-3.332519E-3)*Z-2.314617E-2)*Z
93 #=1.134558E-5)*Z+6.250011E-2)*Z+2.583969E-10
94 V=((((((-5.105699E-3*Z+2.819179E-2)*Z-6.537263E-2)*Z
95 +7.902134E-2)*Z-4.400416E-2)*Z-7.945556E-3)*Z+2.604293E-2)*Z
96 #=9.76400E-4)*Z-3.122416E-2)*Z-6.646441E-7)*Z+2.500000E-1
97 CI=Z*(SI*V-Y*U)
98 SI=-Z*(SI*U+Y*V)
99 IF(X) 500,600,600
100 500 SI=-3.141593E0-SI
101 600 RETURN
102 EINI
103 C
104 C
105 C

```

REFERENCES

- [1] B.A. Munk and T.W. Kornbau, "Mono-Planar Arrays of Generalized Three-Legged Elements in a Stratified Dielectric Medium," Report 4346-6, May 1978, The Ohio State University ElectroScience Laboratory, Department of Electrical Engineering; prepared under Contract F33615-76-C-0124 for Air Force Avionics Laboratory, Wright-Patterson Air Force Base, Ohio. (AFAL-TR-78-43) (AD/B030 753L)
- [2] T.W. Kornbau, "Application of the Plane Wave Expansion Method to Periodic Arrays Having a Skewed Grid Geometry," Report 4346-3, June 1977, The Ohio State University ElectroScience Laboratory, Department of Electrical Engineering; prepared under Contract F33615-76-C-0124 for Air Force Avionics Laboratory, Wright-Patterson Air Force Base, Ohio. (AFAL-TR-77-112) (AD/A047 311)
- [3] B.A. Munk and R.D. Fulton, "Transmission Through a Bi-planar Slot Array Sandwiched Between Dielectric Layers," Report 3622-7, February 1976, The Ohio State University ElectroScience Laboratory, Department of Electrical Engineering; prepared under Contract F33615-73-C-1173 for Air Force Avionics Laboratory, Wright-Patterson Air Force Base, Ohio. (AFAL-TR-76-18) (AD/A032 160)
- [4] B.A. Munk, G.A. Burrell and T.W. Kornbau, "A General Theory of Periodic Surfaces in Stratified Dielectric Media," Report 4346-1, November 1977, The Ohio State University ElectroScience Laboratory, Department of Electrical Engineering; prepared under Contract F33615-76-C-0124 for Air Force Avionics Laboratory (AFAL/WRP), Air Force Wright Aeronautical Laboratories, Wright-Patterson Air Force Base, Ohio. (AFAL-TR-77-219) (AD/B030 544L)
- [5] B.A. Munk and R.D. Fulton, op. cit., pp. 15-17.
- [6] E.L. Pelton, "Scattering Properties of Periodic Arrays Consisting of Resonant Multi-mode Elements," Ph.D. Dissertation, The Ohio State University, 1975. Also published as Report 3622-3, June 1975, The Ohio State University ElectroScience Laboratory, Department of Electrical Engineering; prepared under Contract F33615-73-C-1173 for Air Force Avionics Laboratory, Wright-Patterson Air Force Base, Ohio. (AFAL-TR-75-98) (AD/A 016 950)

- [7] B.A. Munk and T.W. Kornbau, op. cit., p. 3.
- [8] E.C. Jordan and K.G. Balmain, Electromagnetic Waves and Radiating Systems, Prentice-Hall, Inc., 1968, pp. 517-519.
- [9] B.A. Munk and T.W. Kornbau, op. cit., p. 10.
- [10] B.A. Munk, G.A. Burrell and T.W. Kornbau, op. cit., p. 17.
- [11] Ibid., p. 36.
- [12] Ibid., p. 61.
- [13] T.W. Kornbau, op.cit., p. 11.
- [14] S.A. Schelkunoff and H.T. Friis, Antennas, Theory and Practice, John Wiley and Sons, 1952, pp. 407-420.
- [15] B.A. Munk, G.A. Burrell and T.W. Kornbau, op.cit., pp. 68,34.
- [16] Ibid., p. 54.
- [17] S.A. Schelkunoff and H.T. Früs, op.cit., pp. 241-243.
- [18] B.A. Munk, R.J. Luebbers and T.L. Oliver, "Reflection Properties of a Periodic Array of Dipoles in a Dielectric Slab," Report 2989-6, December 1972, The Ohio State University ElectroScience Laboratory, Department of Electrical Engineering; prepared under Contract F33615-67-C-1439 for Air Force Avionics Laboratory, Wright-Patterson Air Force Base, Ohio. (AFAL-TR-72-381) (AD 906 372L)
- [19] B.A. Munk, G.A. Burrell and T.W. Kornbau, op.cit., p. 35.
- [20] Ibid., p. 25.
- [21] Ibid., p. 27.
- [22] Ibid., p. 25.
- [23] Ibid., pp. 61-80.
- [24] B.A. Munk and T.W. Kornbau, op.cit., p. 20.
- [25] Ibid., p. 21.
- [26] B.A. Munk and R.D. Fulton, op.cit.
- [27] Ibid., p. 44.
- [28] B.A. Munk and T.W. Kornbau, op. cit., pp. 34-37.

- [29] B.A. Munk and R.D. Fulton, op.cit., p. 44.
- [30] T.W. Kornbau, B.A. Munk, and C.J. Larson, "Design of a Metallized Radome for the C-140 Aircraft," Report 4346-4, May 1979, The Ohio State University ElectroScience Laboratory, Department of Electrical Engineering; prepared under Contract F33615-76-C-1024 for Air Force Avionics Laboratory, Wright-Patterson Air Force Base, Ohio. (AFAL-TR-79-1103)
- [31] S.A. Schelkunoff and H.T. Friis, op. cit., p. 242.
- [32] B.A. Munk and R.D. Fulton, op.cit., pp. 11-13.
- [33] Ibid., pp. 12.
- [34] B.A. Munk, G.A. Burrell and T.W. Kornbau, op.cit., p. 55.
- [35] Ibid., pp. 58-60.
- [36] B.A. Munk and T.W. Kornbau, op.cit., p. 55.
- [37] Ibid., p. 59.
- [38] Ibid., p. 59.
- [39] Ibid., pp. 65-68.
- [40] Ibid., p. 66.
- [41] Ibid., p. 66.
- [42] Ibid., p. 67
- [43] Ibid., p. 70.
- [44] Ibid., p. 68.

